

## **Chapter 3. Komatiite-hosted nickel sulfide deposits: geology, geochemistry and genesis**

Stephen J. Barnes

CSIRO Exploration and Mining

Australian Resources Research Centre

26 Dick Perry Ave., Kensington 6151

(PO Box 1130 Bentley 6102)

Western Australia

steve.barnes@csiro.au

### **Abstract**

Most of the komatiite-hosted sulfide deposits in the Yilgarn craton exemplify the two major types: type 1, sulfide-rich accumulations at the base of magma pathways, and type 2, disseminated sulfides in the centre of very olivine rich cumulate bodies. The Yilgarn komatiite resource consists of small, high grade type 1 deposits, along with a number of much larger but lower grade type 1 and type 2 deposits. The largest deposits, Perseverance and Mt Keith, and the Kambalda Camp as a whole, are genuinely world-class deposits comparable in metal content to giant deposits elsewhere in the world.

Type 1 deposits are almost exclusively hosted by bodies of olivine cumulate at least several tens of metres thick, and in some cases hundred of metres thick. Immediately adjacent host rocks range from olivine orthocumulates to olivine adcumulates. Spinifex textured rocks are only rarely found in contact with ores, but are more common in flanking rocks tens to hundreds of metres away. There is a close association between mineralisation and the compound cumulate-rich flow facies.

Komatiite-hosted ores in general have high Ni tenors and low Cu tenors, bulk ore compositions being controlled largely by parent magma compositions and magma channel dynamics. Superimposed variations are due to internal magmatic differentiation and hydrothermal effects.

The ores of the Black Swan area illustrate primary magmatic features including partially molten footwall inclusions in ores and host rocks. The Kambalda deposits show a wide spectrum of superimposed effects due to deformation, and there is an unresolved controversy surrounding the origin of linear troughs which evidently host the ores. Orebodies at Perseverance, Honeymoon Well and elsewhere also demonstrate substantial structural modification but retain important magmatic signatures.

The body of evidence supports the substrate erosion model, whereby sulfide is derived by thermo-mechanical erosion of sulfidic rocks in the floors of major magma pathways or channels. To some degree the geochemistry of the host rocks reflects this process, but the signal varies greatly according to the immediate environment.

All the deposits are invariably deformed to some degree, and massive sulfide orebodies have had a profound influence on localising the deformation. There is wide spectrum from almost intact deposits to those which have undergone intense deformation and remobilisation into entirely shear-hosted “type 5” deposits.

### **3.1. Introduction**

This chapter is an overview of the major types of komatiite-hosted nickel sulfide deposit, with an emphasis on sulfur-rich, contact-related “type 1” deposits. The review covers the stratigraphic context, the facies relationships in the host komatiites, the imprint of metamorphism and deformation and essential features of the geochemistry of the host rocks and ores. It discusses the evidence for and against the prevalent substrate erosion model for the origin of this class of deposits, and applies the recent volcanological advances described in the last chapter to interpretation of ore genesis.

The nickel sulfide deposits of Western Australia were comprehensively reviewed by Marston (1984), and the komatiite-hosted deposit class as a whole has been the subject of reviews by Leshner and co-workers (Leshner, 1989; Leshner and Keays, 2002) and Naldrett (2004). In many cases the geological descriptions in these references remain valid and current, and additional descriptions in this chapter are concerned only with those deposits which have either been discovered since 1984, or with those where substantial advances in knowledge and understanding of the geology have been made since then.

### ***3.1.1. Classification***

Two types of komatiite-hosted deposit were initially recognised following the discovery of the Kambalda camp. They were classified as "Volcanic Peridotite" and "Intrusive Dunite" associated deposits (Marston et al., 1981; Marston, 1984) based on the mode of occurrence of sulfide and the host rock lithology. Subsequently, the classification was revised to type 1 and type 2 ores, to remove the element of intrusive or extrusive emplacement. This classification is based purely on host rock lithology and distribution of mineralisation (Leshner, 1989; Hill and Gole, 1990). Type 1 ores are accumulations of massive and net-textured or matrix ores (in which sulfide forms a continuous matrix between about 40-60 modal percent original olivine) at the base of komatiite lava flows, whereas type 2 ores are centrally disposed low-grade disseminations of sulfide within thick olivine cumulate bodies, regardless of intrusive or extrusive origin.

Subsequently, Leshner and Keays (2002) have proposed a more complex subdivision, of which a brief summary is given in Table 1. This classification refers to mineralisation styles rather than entire deposits, and many deposits contain more than one style. Deposits are classified according to the predominant style. Among the deposits described in this chapter, Rocky's Reward and Emily Ann are type 5 deposits, that is, structurally remobilised and detached from original host rocks. The bulk of this chapter is taken up with type 1 deposits.

Type 4 mineralisation is defined as sediment-hosted stratiform sulfides with significant nickel content associated with "normal" type 1 mineralisation. A large proportion of the ore in the world's largest komatiite-associated deposit at Thompson, Manitoba (Bleeker, 1990) is of type 4. This style is rare in Yilgarn deposits, but examples of type 4 ore are known within the dominantly type 1 orebodies at Perseverance, Windarra, Jan and McMahon Shoots (Kambalda) and Wannaway.

type 1 ores were first thought to be the result of gravitational settling and accumulation of mantle-derived sulfide melt transported from great depths to the surface by komatiitic magma (Naldrett and Cabri, 1976; Naldrett and Turner, 1977). Detailed studies in the early 1980s at Kambalda led to the suggestion that the sulfides were derived by thermal erosion or "ground melting" of sulfidic sediments in the immediate substrate to the lava, and that these sulfides were deposited in linear

thermal erosion troughs (Huppert et al., 1984; Leshner et al., 1984; Huppert and Sparks, 1985). This model has received widespread acceptance and application in the exploration industry, but the model, at least in its initial formulation, has been challenged repeatedly since it was first proposed (Foster et al., 1996; Cas et al., 1999; Cas and Beresford, 2001; Rice and Moore, 2001; Stone and Archibald, 2004) and debate continues on its validity.

### ***3.1.2. Distribution and tectonic setting***

The komatiite-hosted deposits of the Yilgarn Craton, with the exception of a small number of isolated deposits, occur within a number of relatively restricted areas, within two major greenstone belts of different age (Map 1, Map 2): the Kambalda-Tramways-St Ives-Widgiemooltha area of the Kalgoorlie Terrain, and the Agnew-Wiluna section of the 2.7 Ga Norseman-Wiluna Greenstone Belt; and the Eastern and Western komatiite trends of the 2.9 Ga Forrestania Greenstone Belt. The more important isolated deposits include the Maggie Hays and Emily Ann deposits of the Lake Johnston Greenstone Belt, which are probably correlative with the Forrestania sequence; the Windarra deposits of the eastern Norseman-Wiluna Belt; and the Black Swan group of deposits in the Boorara Domain in the central Norseman-Wiluna Belt. Smaller sub-economic deposits, Trough Well, Koolyanobbing and Bullfinch, are found in the Southern Cross province north of the Forrestania Belt.

The deposits of the Norseman-Wiluna Greenstone Belt are contained within a very extensive and nearly continuous belt of komatiites falling within a very narrow age span at 2705 Ma (Nelson, 1997), part of a global komatiite “event” within 10-15 million years of this date. Extensive outpourings of magnesian lava within a very short time span is a hallmark of magmatism related to the first arrival of mantle plumes at crustal levels (Campbell et al., 1989).

Other than a broad association with linear belts of submarine volcanic and volcanoclastic rocks, it is difficult to find any tectonic or stratigraphic characteristics which are common to all the Yilgarn deposits. For historical reasons, the Kambalda deposits have been generally regarded as the type example, and they display many important features common to most type 1 deposits. However, they are distinct from most of the other deposits in the Yilgarn Craton in that the komatiites of the Kambalda-Tramways-Widgiemooltha area were erupted on to a basaltic substrate,

whereas komatiites elsewhere in the Norseman-Wiluna Belt and in the Forrestania and Lake Johnston belts were erupted onto (or simultaneously with) felsic volcanic rocks or sedimentary units. The majority of individual deposits in the craton as a whole are associated with essentially bimodal komatiite-felsite volcanism.

The 2.9 Ga Eastern Forrestania komatiite trend, incorporating the Digger Rocks to Mt Hope group of deposits in the Forrestania Greenstone Belt, is associated with extensive horizons of oxide-facies banded iron formation in the immediate substrate, as are Emily Ann and Maggie Hays, and the 2.7 Ga Windarra deposits. The Flying Fox and New Morning Deposits in the Western trend of the Forrestania Belt have felsic substrates free of iron formation. Komatiites of the Agnew-Wiluna trend have almost exclusively felsic to intermediate substrates, although in many cases the detailed relationships are obscured by tectonism.

Groves and Batt (1984) proposed a division of greenstone belts into two tectonic styles, “platform-phase” and “rift-phase” greenstones, defined largely by the presence of banded iron formations and coherent, correlatable volcanic stratigraphy in the former, and deep-water sediments and chaotic volcanic stratigraphy in the latter. Within this framework, the Eastern Forrestania komatiite trend, the Lake Johnston Belt and the Windarra area of the eastern Norseman-Wiluna Belt are the only known examples of mineralised “platform-phase” associations. All of the other economic komatiite hosted deposits of the Yilgarn fall within sequences which would be classified as “rift-phase” in the Groves and Batt terminology.

### ***3.1.3. Grade and tonnage distribution***

Data on grade and tonnage for the deposits of interest are compiled in Table 2 and plotted on Figure 1. Data are compiled from a variety of sources, primarily the Western Australian Dept. of Industry and Resources Minedex database, the on-line Intierra-Ozmine database and various company sources, and in all case represent the best estimate of the pre-mining resource.

The main source of variance in the grade figures is the relative proportion of high-grade massive ore to low-grade disseminated ore included in the resource figure. This is reflected in the comparison between data for individual shoots and for aggregates from the Black Swan and Perseverance Camps in particular. The Perseverance Camp figure shows up as a very high tonnage at low grade owing to the inclusion of large

tonnages of low-grade disseminated sulfides, but includes a significant resource of high-grade massive and matrix ore. The figures for Mt. Keith are a true reflection of a very large homogenous orebody.

Much of the Yilgarn komatiite resource consists of small, high grade deposits, which are very attractive but difficult exploration targets. The largest deposits, Perseverance and Mt Keith, and the Kambalda Camp as a whole, are genuinely world-class deposits comparable in metal content to giant deposits elsewhere in the world such as Pechenga, Thompson and Voisey's Bay (Fig. 1). The total pre-mining resource of Ni metal in the Yilgarn Craton deposits is estimated at 12.3 million tonnes (Hronsky and Schodde, this volume), compared with an estimate of 15 million tonnes for the Sudbury camp (Farrow and Lightfoot, 2002).

An important factor to consider is the orientation and shape of the orebodies. Several of the deposits listed in Table 1, including Perseverance and Silver Swan, have steep plunges, and are open at depth. The Kambalda shoots have typically shallow plunges and in most cases are drilled out. If Perseverance had a similar structural setting to Kambalda and a consequent shallow plunge, there is no reason to suppose that it could not be ten times as big, making it one of the largest nickel sulfide deposits in the world. Komatiite hosted orebodies are typically small, but can also be giants.

## **3.2. General Features of Type 1 Deposits**

### ***3.2.1. Distribution of sulfides***

Type 1 deposits are accumulations of immiscible magmatic sulfide liquid at the basal contacts of olivine-enriched komatiite flows or subvolcanic intrusions. They are relatively sulfide-rich, commonly containing either massive (75-100%) sulfides, or "matrix" ore ("net-textured" in North American usage), or both. Matrix ore consists of between 30 and 70% olivine grains (or serpentine pseudomorphs) within a continuous framework of sulfides (Fig. 2). Where both occur undeformed, matrix ore characteristically overlies massive ore at discontinuous sharp contacts, and is itself typically overlain and flanked by a halo of low-grade disseminated sulfides. This relationship is common enough to be regarded as the standard configuration; in a sampling of over 600 massive ore intercepts around the less-deformed eastern side of the Kambalda dome, 44% had massive ore overlain by matrix ore.

The standard massive-matrix configuration was first identified and interpreted in the small but well-preserved Alexo deposit in the Abitibi Belt, Ontario (Naldrett 1973). According to Naldrett's "Billiard Ball" model (Fig. 2), the configuration is the result of buoyancy relationships between dense sulfide liquid (specific gravity of about 4), lighter komatiite melt (s.g. about 2.7) and a column of close-packed olivine crystals of intermediate density (s.g. about 3.3), analogous to "mercury", "water" and "billiard balls" in the model. The Archimedes principle dictates that the mercury should form a basal layer, in which the billiard balls should float; however the opposing tendency of the billiard balls to sink in the water and float in the mercury forces some proportion of the billiard ball column to push down into the mercury layer, creating the analogy to net-textured ore. The relative thickness of the net-textured ore to the basal massive layer, by analogy, is a function of the height of the billiard ball column relative to the thickness of the two liquid layers.

As Groves and others pointed out (Groves et al., 1979), the column of olivine in many natural deposits is such that no massive ore should have been preserved; this criticism was addressed by conductive thermal modelling calculations (Usselman et al., 1979) which allowed for freezing of the massive sulfide liquid pool upward from the floor at the same time as olivine accumulated in the overlying komatiite flow. Subsequently, it has become clear that type 1 ore systems are not static accumulations as implied by the simple billiard ball model, and that ore accumulation, olivine settling and other mechanical processes take place during flow of magma through magma pathways (Leshner, 1989). Variations in the standard configuration, such as repetitions of net-textured and massive ore, or complete absence of net-textured ore, can be explained by fluctuations in rate of supply and crystallisation of the three components in active flow pathways. The configuration is also very commonly modified by deformation.

### ***3.2.2. Nature of host rocks and controls on disposition of ores***

Type 1 deposits are almost exclusively hosted by bodies of olivine cumulate at least several tens of metres thick, and in some cases hundred of metres thick. Immediately adjacent host rocks range from olivine orthocumulates to olivine adcumulates. Spinifex textured rocks are only rarely found in contact with ores, but are more common in flanking rocks tens to hundreds of metres away. There is a close association between mineralisation and the compound cumulate-rich flow facies, and

on a finer scale between orebodies and pathway subfacies or dunite lens subfacies (see figures 4 and 16 of previous chapter).

Sulfide bodies in relatively undeformed settings typically form elongate, ribbon- or tube-shaped masses commonly called “shoots”. These are localised in some but by no means all cases in some form of topographic irregularity at the base of the host komatiite unit. This may take the form of a ten to two hundred meter wide linear trough, as in the case of many of the Kambalda deposits, or an irregular topographic footwall “notch” within a broader, shallow linear trough at Silver Swan. In other cases, such as most of the Widgiemooltha deposits, Durkin at Kambalda, and Cosmos, sulfides sit on a planar surface with no evidence of primary irregularity. In most of the deposits of the Kambalda Dome, and on a larger scale at Perseverance and Digger Rocks, the orebodies lie beneath the thickest part of the host unit, which thins by at least a factor of two away from the ore environment (Fig. 3), but this relationship is not universal, and tends not to be observed where orebodies lie on planar contacts.

### ***3.2.3. Sulfide mineralogy***

The bulk compositions of komatiite-hosted Ni-Fe sulfide ores are one of the prime pieces of evidence for their magmatic origin. Sulfide liquids in equilibrium with magmas have their metal to sulfur ratios buffered by the oxygen and sulfur fugacities of the parent silicate magmas, and these are constrained within narrow bounds (Naldrett, 1969). In consequence, magmatic sulfide liquids have bulk metal:sulfur ratios close to unity, and this determines their mineralogy on solidification.

Sulfide mineralogy of unaltered massive and matrix ores consists almost universally of pyrrhotite (hexagonal or monoclinic), pentlandite and chalcopyrite with or without lesser proportions of pyrite and magnetite, the typical assemblage derived by solidification and cooling of primary magmatic sulfide liquid, as represented by the Ni-S-Fe system (Fig. 4) (Kullerud et al., 1969; Hill, 1984). Pentlandite exsolves from a high-temperature nickel-rich pyrrhotite phase, monosulfide solid solution (MSS), at temperatures below about 600C, and exsolution continues down to very low temperatures (Farrell and Fleet, 2002; Etschmann et al., 2004) giving rise to fine-grained “flames” of pentlandite within pyrrhotite (Fig. 5). Depending on the initial bulk composition, pyrite may also be a significant component of the primary mineralogy.

Disseminated sulfide may be modified during serpentinisation of coexisting olivine, giving rise to pentlandite-magnetite assemblages and development of heazlewoodite and millerite in rarer cases (Barnes and Hill, 2000), as discussed in more detail in the following chapter. Vaesite, millerite and polydimite are developed within disseminated sulfide ores hosted within low-temperature talc carbonates, such as those at Black Swan (Groves et al., 1974; Barnes and Hill, 2000). Violarite and mackinawite commonly form as minor replacement of pyrrhotite and pentlandite during serpentinisation of host rocks. Trace platinum group elements occur as a large number of discrete mineral phases, of which sperrylite, stibiopalladinite, moncheite, michenerite and palladoarsenide are the most abundant (Hudson and Donaldson, 1984). A wide variety of Bi, Te, As, Bi, Zn and Sn-bearing minerals are present as accessories (Leshner and Keays, 2002).

Pyrite is a common component, forming partly in response to the shrinking of the pyrrhotite solid solution field with falling temperature, but also reflecting hydrothermal redistribution of S. Many massive orebodies contain irregular patches or layers of pyrite rich material on a scale of tens of centimetres, which has the effect of lowering the local Ni assay, and introducing short-range variance in ore composition within shoots (Stone et al., 2004).

Chalcopyrite is usually evenly distributed through the ore, but can be enriched in remobilised footwall stringers.

#### ***3.2.4. Oxide mineralogy***

Magmatic sulfide ores typically contain a small proportion of primary oxide minerals, reflecting the fact that magmatic sulfide liquid in equilibrium with terrestrial mafic or ultramafic lavas contains substantial proportions of oxygen (Naldrett, 1969; Hill, 1984; Doyle and Naldrett, 1987).

Massive ores commonly contain small amounts of primary magnetite, usually disseminated through the ore body in low abundances, and sometimes forming a narrow mm-scale rind at basal contacts. Primary upper contacts between massive sulfide and overlying sulfide poor komatiite are commonly marked by the presence of a few-mm wide rind rich in distinctive skeletal ferrian chromite, low in Al and Mg (Fig. 6, Fig 7) (Groves et al., 1977; Frost and Groves, 1989a; Dowling et al., 2004). These chromites are consistent in composition across a wide range of metamorphic

grades, and are therefore extremely unlikely to be metamorphic in origin; in any case, they can occur at low metamorphic grades under conditions where ferrian chromite is not a stable phase, and therefore can only be interpreted as relict igneous phases (Kullerud et al., 1969; Naldrett, 1969; Hill, 1984; Doyle and Naldrett, 1987). They occupy an unusual compositional field distinct from all other terrestrial spinels (Fig. 7).

This chromite rind is thought to be the result of expulsion of oxygen from the solidifying sulfide liquid pool and reaction with komatiite melt. Oxygen diffusing into adjacent silicate melt triggers nucleation of spinel at the interface (Dowling et al., 2004). Skeletal ferrian chromite rinds are therefore reliable markers for primary igneous contacts.

### ***3.2.5. Compositions of type 1 ores***

Komatiite-hosted ores in general have high Ni tenors and low Cu tenors (tenor being defined as the concentration of the metal normalised to 100% sulfides) compared with other classes of magmatic sulfide deposit (Fig. 8), a consequence of the high Ni and low Cu content of the very primitive komatiite parent magmas compared with mafic host magmas. Ore tenors are highly variable, sometimes between adjacent ore shoots within the same camp, as at Kambalda. The composition of the sulfide fraction in type 1 ores varies considerably, reflecting the superimposition of several independent controls, as follows.

*Parent magma composition.* The relationship of ore composition to host rock type is one of the key pieces of evidence for a magmatic origin of Ni-Cu-PGE sulfide ores. The elements Ni, Cu and the platinum group elements (PGEs), which have been shown experimentally to be concentrated strongly in sulfide liquid relative to coexisting silicate liquid, are exactly those which are concentrated in these ores, relative to komatiite magmas. This tendency to favour the sulfide liquid is described by an important variable, the partition coefficient  $D_i^{\text{sul}}$ , which measures the ratio of the element  $i$  in the sulfide liquid to that in coexisting silicate liquid at equilibrium.  $D_i^{\text{sul}}$  values for Ni and Cu (Table 1) fall within the range 100-1000, and the PGEs range from thousands to tens of thousands (see review by Barnes and Maier, 2002). Elements such as Pb and Zn have  $D_i^{\text{sul}}$  values close to 1, and have concentrations in nickel sulfide ores in the low ppm range, similar to those in magmas.

Nickel becomes depleted during fractional crystallisation of olivine, while Cu becomes enriched, and this is reflected in ore compositions. Ores associated with komatiitic basalt magmas, such as those of the Cape Smith Belt, have higher Cu/Ni ratios than those in true komatiites. Platinum and palladium (Pt, Pd) are incompatible elements, whereas osmium and iridium (Os, Ir) are compatible, with ruthenium and rhodium (Ru, Rh) in between; hence more evolved, lower Mg magmas give rise to sulfide deposits enriched in Pt and Pd over the IPGEs (Ir, Os, Ru). However, the overall concentration of the PGEs is dominantly controlled by other factors.

*Mass balance and the “R Factor”*. Plots of Ni vs PGE tenors of type 1 ores (Fig. 9) show two important features: first, a weak positive correlation; and second, a very wide variability in PGE relative to Ni far beyond what can be explained by fractionation of the parent silicate magma. This is a consequence of the very high partition coefficients ( $D_i^{\text{sul}}$ ) for the PGEs relative to those for both Ni and Cu.

Formation of magmatic sulfides is best modelled as a batch equilibrium process: a batch of sulfide liquid forms from a given volume of silicate melt, and segregates as an orebody. The relative proportion of silicate liquid to sulfide liquid involved in this equilibrium is defined as the “R factor”, denoted R from here on (Campbell and Naldrett, 1979). Where R is very high, the total mass of any chalcophile element (say Ni) which ends up in the sulfide liquid is small, so there is relatively little impact on the Ni content of the host silicate melt. Since the partition coefficient  $D_i^{\text{sul}}$  must always be satisfied, this means that the sulfide melt will have a high Ni content. On the other hand, if R is low (that is, the proportion of sulfide to silicate melt is high), the opposite applies: most of the Ni in the system goes into the sulfide melt, the silicate melt therefore becomes highly depleted, and the  $D_i^{\text{sul}}$  value dictates that both silicate and sulfide melt end up with low Ni contents. This relationship is expressed in the equation

$$Y_i^{\text{sul}} = [X_i^{\text{sil}} \cdot D_i^{\text{sul}} \cdot (1+R)] / (R + D_i^{\text{sul}})$$

where  $Y_i^{\text{sul}}$  is the final concentration of element i in the sulfide liquid, and  $X_i^{\text{sil}}$  the initial concentration in the silicate liquid.

The much higher values of  $D_i^{\text{sul}}$  explains the much greater variability of PGEs in magmatic sulfides compared with Ni (Fig. 10). The broad trend of PGE vs Ni in

different deposits is consistent with formation from similar parent magmas, but at widely variable R.

This R factor control was invoked by Lesher and Campbell (1993) to explain the wide variability in Ni and PGE tenor between adjacent shoots at Kambalda. Different shoots represent different lava pathways with their own characteristic flow regime and proportion of transported sulfide. In practise, the R factor is a combination of two components: the relative volume of the two liquids in the system; and the extent of mechanical stirring and equilibration between them. If a body of sulfide liquid is poorly mixed with the silicate magma, or solidifies before having time to equilibrate, then the effective R factor may be low regardless of relative volumes. Lesher and Campbell argued that R factors would be relatively lower in a situation where sulfide liquid was entrained a separate layer along the bottom of the flow channel, and higher where the sulfide was transported as suspended droplets prior to coalescence and settling. Ore compositions are a function of physics as much as chemistry.

Other mechanisms have been proposed to account for tenor variations between ore shoots, the most widely cited being the proposal of Cowden and Woolrich (1987) that partition coefficients are strongly dependent on oxidation state. In fact the relationship given by these authors in the original paper proved not to be experimentally reproducible. The experimental data of Doyle and Naldrett (1987) shows a dependence in the opposite sense to that suggested by Cowden and Woolrich, but much smaller in magnitude, and not large enough to explain the observed variations. In any case, there is no viable mechanism to produce large variations in oxidation state in lavas from essentially the same eruption, and the Cowden and Woolrich model should be discarded. The observed PGE-Ni trends are good evidence that variation in average Ni tenor between shoots is predominantly controlled by R-factor, which in turn is a function of the flow dynamics within a particular pathway. However, there are a number of superimposed effects which can cause wide within-shoot variability.

*Fractionation of sulfide liquid, and compositions of massive, matrix and disseminated ores.* Compositional variability within individual orebodies and between adjacent massive, matrix and disseminated ores has been recognised from early studies by Keays and coworkers (Ross and Keays, 1979; Keays et al., 1981; Keays, 1982; Lesher and Keays, 1984) at Kambalda, and particularly from a detailed study of the Alexo

deposit by Barnes and Naldrett (1986). The standard method of making this comparison involves recasting whole-rock analyses to concentrations of chalcophile elements in 100% sulfide, using a simple sulfide norm calculation (Naldrett, 1981) based on assumptions of stoichiometric mineral compositions, and plotting the data relative to abundances in primitive mantle, using data compiled by Barnes et al. (1988). The resulting plots are analogous to the rare earth element plots described in the previous chapter, except the other way around – the more compatible elements are to the left.

In most of the deposits studied in detail, there are systematic differences between adjacent massive and matrix ores. Massive ores are typically enriched in the IPGEs (Os, Ir, Ru) and Rh relative to Pt and Pd, and have negative Pt anomalies. Matrix and disseminated ores show the opposite relationship, being enriched in Pd and Pt over the IPGEs (Fig. 11).

Various explanations have been advanced for this phenomenon, the most plausible being that it is due to fractional crystallisation of the sulfide liquid itself (Barnes and Naldrett, 1986). The first phase to crystallise from the sulfide liquid at about 1150°C is a nickel-rich pyrrhotite (Fe-Ni-S phase diagram) or monosulfide solid solution (MSS) which has been shown experimentally (Barnes et al., 1997) to concentrate the IPGEs by a factor of about 5, but to almost completely exclude Pt and Pd. The early-solidified material cooling against the cold floor is enriched in accumulated MSS – forming massive ores which are essentially MSS orthocumulates. This solidified material prevents the overlying cumulus olivine pile from displacing sulfide liquid (see discussion above of the “billiard ball model”), while fractionated IPGE-depleted, Pt-Pd enriched sulfide liquid becomes progressively concentrated within overlying matrix ore. Hence, most massive sulfides are effectively MSS cumulates.

Strong support for this model comes from the Silver Swan deposit, which shows strong internal PGE fractionation within the massive orebody itself (Barnes, 2004). The massive sulfide in this case is strongly enriched in IPGEs towards the middle and top, and strongly depleted towards the base. These trends can be closely matched by a simple fractionation model using the measured experimental partition coefficients for these elements between MSS and sulfide liquid.

The compositional contrast between adjacent massive and matrix ores has very important implications for their primary magmatic origin. The suggestion that massive ores could be formed by structural upgrading of original matrix ores was first raised by Barrett et al. (1977), on the grounds of location of massive sulfides within low-strain zones in highly deformed deposits. The PGE data indicate that this cannot be the case. Simple mechanical deformation should result in “tectonic” massive ores having the same composition as matrix ores, or possibly being relatively enriched in Pd and Au owing to the greater hydrothermal mobility. There is no plausible mechanism which could concentrate IPGEs in remobilised massive sulfides. The PGE data imply that, whereas massive ores may well be subject to tectonic mobilisation, they cannot be formed from precursor matrix ores.

*Metamorphic effects.* Wide variations in ore composition within individual shoots have been reported in the Kambalda and Widgiemooltha areas (Buck et al., 1998; Frost et al., 1998; Heath et al., 2001), and attributed to metamorphic overprinting, through two distinct mechanisms: differential competence and structural mobilisation of Ni-rich and Ni-poor sulfides (Stone et al., 2004); and oxidation, with or without sulfidation, during hydrothermal fluid influx (Keays et al., 1981; Seccombe et al., 1981; Cowden and Archibald, 1987; Frost et al., 1998).

Phase relations in nickel sulfide ores (Fig. 5) are important in understanding their behaviour during metamorphism and deformation. A typical Ni-rich ore composition, “M” in Figure 5, forms an assemblage pyrrhotite, pentlandite and minor pyrite below about 500°C, but reverts to homogenous MSS at temperatures corresponding to lower amphibolite facies metamorphism. Subsequent MSS breakdown during cooling of metamorphosed ores within a stress field typically gives rise to strongly banded ores with pentlandite and pyrrhotite-rich layers on a centimetre scale (McQueen, 1987). Cowden and Archibald (1987) cited experimental data of McQueen (1987) to argue that MSS splits into Ni-poor and Ni-rich fields at 550-600°C, and this enables the survival of compositional heterogeneities and modal layering in ores deformed under these conditions. Differentiation of orebodies into pyrrhotite and pentlandite rich zones by differential deformation of mineralogically heterogeneous ores has been suggested (McQueen, 1979; Cowden and Archibald, 1987; Seat et al., 2004).

Slightly more S-rich ore compositions than composition “M” in Figure 4 form MSS-pyrite assemblages under amphibolite facies conditions. Mobility of S and formation

of secondary pyrite under metamorphic conditions has been invoked to account for local tenor variations and formation of pyrite bands and selvages (Keays et al., 1981; Seccombe et al., 1981; Cowden and Archibald, 1987; Stone et al., 2004). Deformation of S-rich ores under the typical metamorphic conditions of the Kambalda ores could give rise to differential tectonic mobilisation of pyrite-rich and pyrite-poor ores, giving rise to the pyritic bands and lenses common in these orebodies.

Hydrothermal processes can also result in mobilisation of the elements Pd, Au and Cu, and to lesser extent Pt. In many Kambalda deposits, these elements are mobilised into late-stage discordant veins within the immediate footwall (Leshner and Keays, 1984), resulting in further depletion of the more mobile elements in massive ores (Ross and Keays, 1979). The process is enhanced where As-bearing fluids are involved, as is commonly the case in talc-carbonate alteration.

Hydrothermal alteration has undoubtedly had an impact on the composition of some massive and matrix ores, and a very strong impact on the composition of disseminated sulfides, as discussed in detail for Mt Keith in the following chapter. Stone et al. (2004) contend that the bulk Ni contents of individual sulfide-rich ore shoots are substantially affected by post-magmatic processes. The relative magnitude of within-shoot versus between-shoot variability is a matter of sample size and density; studies which have used long-term, representative bulk sampling on orebody scale (Ross and Keays, 1979; Cowden et al., 1986; Leshner and Campbell, 1993) have emphasized significant, consistent differences between shoots, whereas more detailed studies within shoots based on analysis of large numbers of hand samples have tended to emphasize the internal variability (Heath et al., 2001; Seat et al., 2004). To date there has not been the rigorous statistical analysis necessary to discriminate primary magmatic from secondary variability, and further research is needed.

### **3.3. Examples of Yilgarn Craton Type 1 Deposits**

This section describes or updates descriptions of some of the major deposits of the Yilgarn Craton, particularly those which are not covered by (or were discovered since) Marston (1984), or where significant developments have occurred since 1984. The Kambalda deposits are also covered, in view of their iconic status, and also to emphasize current controversies about their origin.

Deformation and metamorphism have played an important role in all known Yilgarn Craton deposits, and have modified primary igneous features to a greatly variable degree. Some important deposits have been deformed to the point where the dominant controls on ore distribution are tectonic rather than magmatic (Stone and Archibald, 2004), but some primary magmatic features are recognisable in almost all cases. The emerging picture is one of a continuum from relatively pristine to extensively tectonised deposits.

### ***3.3.1. Weakly deformed deposits of the Black Swan area***

The Black Swan succession is a particularly well-preserved example of bimodal komatiitic and calc-alkaline dacitic volcanism. The complex komatiite stratigraphy hosts a number of orebodies, including the Silver Swan massive ore shoot and the larger disseminated Black Swan and Cygnet Orebodies. The following account is summarised from Hill and co-workers (Barnes et al., 2004a; Dowling et al., 2004; Hill et al., 2004).

*Stratigraphy and host rocks.* The komatiite stratigraphy can be divided broadly into two units (Fig. 12 of Chapter 2, this volume). The lower unit extends for about 2 km along strike, has a maximum thickness of at least 300m, and overlies plagioclase-phyric dacitic breccias at an irregular, locally non-tectonised contact. Internally, it consists of two thick pathways occupied by olivine mesocumulates, separated along strike by a broad central zone dominated by less magnesian olivine orthocumulates. The planar spinifex-textured top of the lower ultramafic unit is overlain by an upper sequence of quartz-plagioclase phyric dacite breccias and tuffs, and an upper komatiite sequence complexly intercalated with these dacites.

The upper komatiite sequence has a central pathway, which hosts the Black Swan disseminated orebody, and which rests directly on the lower komatiite unit. To the north, dacites are complexly intercalated with irregular komatiite units with spinifex-textured upper zones and highly irregular bases, interpreted as flow lobes by Hill et al. (2004), ranging in thickness from 30cm to 50m and in width from 10 to 100m. To the south, the Black Swan pathway is flanked by a sequence of differentiated flows with abundant spinifex textured upper zones, intercalated with dacitic lithic tuffs in the upper part. Some of these tuff units contain abundant pyrite-rich clasts. The upper komatiite unit and upper dacitic unit have relationships broadly similar to that

between the lava pathway and flanking environments at Kambalda (Leshner et al., 1984), except that the intervening volcanoclastic units are much thicker and more irregular in geometry than the Kambalda interflow sediments. This complexity is interpreted by Hill et al. (2004) as the result of the simultaneous eruption of komatiite and dacite lavas during continuous lava flow through the Back Swan pathway.

*The Silver Swan orebody.* The Silver Swan orebody is a vertically plunging ribbon-shaped orebody up to 20m thick, 20 to 75m wide, and at least 1 km long and open at depth (Fig. 12). It lies at the base of the lower ultramafic unit, close to the northern limit of the southern pathway, and locally separated from the mesocumulate rocks by thin discontinuous layer of fine-grained quenched orthocumulates. The orebody itself has a convex-up morphology, with a relatively flat basal contact, and a primary upper contact with essentially barren olivine orthocumulate. This contact is commonly marked by a narrow zone rich in distinctive skeletal ferric chromite (Fig. 6).

The most remarkable feature is the presence of abundant xenolithic inclusions of dacite in the ores (Dowling et al., 2004). These inclusions show clear evidence of partial melting at their margins, and in the interior of the orebody are disaggregated into irregular sinuous blobs and plumes (Fig. 13). The morphology, internal textures and compositions of the inclusions leave no doubt that they are partially molten fragments of the immediate dacite footwall. They extend throughout the lower 5m of the massive ore shoot; where the total thickness of the shoot is less than 5m they extend right the way through, and in places accumulate to form a layer of “xenomelt” separating the top of the massive ore from overlying ultramafic rock. Where the ore zone is thicker than 5m, the plume-bearing zone is overlain by pure inclusion-free massive ore, a feature which Barnes (2004) attributed to breaking away of ascending plumes from a three-dimensional network connected to the floor. The major and trace element geochemistry of the plumes indicates that they range from pure dacite to hybrid compositions with up to 30% komatiite melt component.

The massive sulfide orebody shows strong internal differentiation with respect to the platinum group elements (Barnes 2004), being enriched in the iridium-group PGEs (IPGEs) in the middle and upper part, and depleted in IPGEs and enriched in Pt and Pd at the base. As discussed above, this zonation is attributed to magmatic fractionation of MSS from the sulfide liquid pool. The accumulation of Pt and Pd enriched, Ir-depleted fractionated sulfide liquid at the base of the massive sulfide

layer is difficult to explain, but may be suggestive of crystallisation of the sulfide liquid pool from the top down. The bulk composition of the massive ore is enriched in but depleted in Pt and Pd relative to typical bulk ore compositions of comparable Ni tenor, implying that the ores may be enriched in cumulus MSS relative to the original sulfide liquid composition.

The basal contact of the lower ultramafic unit north and south of the orebody is highly irregular, distinctly non-planar, and marked by a zone several metres thick of distinctively hybridised rocks (Fig. 14), showing evidence for localised assimilation and back veining.

*The Cygnet disseminated to matrix sulfide orebody.* The Black Swan komatiite succession also hosts two separate disseminated sulfide orebodies: Cygnet, adjacent to Silver Swan; and the Black Swan disseminated orebody hosted with the Eastern ultramafic unit. The Black Swan sulfides are discussed further below in the context of type 2 ores, but the Cygnet orebody contains higher sulfide abundances and is better classified as a type 1 deposit.

The Cygnet shoot is a broad, steeply-plunging lenticular zone of heavily disseminated and locally matrix (net-textured) sulfide, predominantly olivine-sulfide mesocumulate, occupying a broad linear trough in the basal Western Ultramafic Unit contact (Dowling et al., 2004). The highest grade mineralisation (>1.5% Ni) is heavily disseminated grading to matrix ore, occupying the lower central portions of the mineralised zone, flanked and overlain by an envelope of progressively lower grade mineralisation. The mineralisation is separated from the footwall contact (and from Silver Swan massive ores) by a roughly 10m thick basal zone of barren olivine orthocumulate, and the basal rind of highly contaminated hybridised mixed material described above. The sulfide mineralogy shows strong evidence of modification during talc-carbonate alteration.

The host rocks of the Cygnet Orebody are a series of equigranular-, and bimodal-textured olivine orthocumulates and mesocumulates, altered to talc-carbonate and quartz-carbonate assemblages with intermittent preservation of primary igneous textures. The irregularly-distributed sulfide occurs as fine disseminations, coarse-grained patches, and lobate blobs scattered throughout all varieties of cumulate, some of which contain carbonate pseudomorphs after amygdals.

Cygnets is distinctive in containing a variety of felsic and ultramafic xenoliths. Partly resorbed and disaggregated sulfidic felsic inclusions are present throughout the high-grade zone ranging in size to tens of centimetres. The most distinctive feature of the ore is the presence of abundant, roughly golf-ball-sized spherical or near-spherical inclusions of net-textured olivine-sulfide cumulate developed within more sparsely disseminated ore and rare inclusions of spinifex-textured ore. The distinctive textures of the Cygnets ores are interpreted by Dowling et al. (2004) as evidence for reworking and redeposition of pre-existing massive and matrix sulfides up-channel.

*Geochemistry of host rocks.* Detailed sampling of the entire komatiite complex reveals that the Black Swan komatiites are pervasively contaminated by crustal material. Contamination signatures (high LREE:HREE ratio, Zr/Ti, Th/Yb, Th/Nb etc) are observed both at flow margins and in internal olivine orthocumulate zones in lava pathways, and in talc carbonate rocks as well as in serpentinites (Barnes et al., 2004a). Komatiites are contaminated with as much as 50% dacite in obviously hybridised basal zone rocks, and up to 20% in komatiites with no obvious textural features of contamination. A suite of samples from throughout the succession shows no evidence of PGE depletion, implying that the magmas were undersaturated in sulfur on emplacement.

### ***3.3.2. Deposits of the Kambalda to Tramways Corridor***

The Kambalda deposits were the first-discovered, and for many years the most closely studied, of all the Yilgarn Craton sulfide deposits. Much of the conventional view of komatiite-hosted deposits is extrapolated from some of the landmark early publications on Kambalda (Ewers and Hudson, 1972; Ross 1974; Ross and Hopkins, 1975; Marston and Kay, 1980; Gresham and Loftus-Hills, 1981). The deposits occur within a 30km long, 10 km wide corridor between the Kambalda Dome and the Tramways Dome (Fig. 15, Fig. 16), and are localised at, or very close to, the contact between the Lunnon Basalt and the overlying Kambalda Komatiite Formation. The deposit of the Widgiemooltha Dome further to the south west (Fig. 15) occur within the same stratigraphy and show broadly similar features. This section gives a general description of common elements, with emphasis on the deposits of the Kambalda Dome itself, and highlights recent areas of controversy.

The Kambalda Dome is a doubly-plunging D3 anticline on the crest of the major regional D2 Kambalda Anticline, the D2 episode being accompanied by extensive parasitic folding and thrusting. Much of this thrusting was localised along the zone of competency contrast between the komatiite-basalt contact, particularly where massive sulfide shoots are developed at this contact, to the point where undeformed magmatic contacts on massive ores are rare. This relationship accounts for much of the observed diversity in ore geometry (Stone and Archibald, 2004).

The conceptual 3D block model in Figure 17 (Stone and Masterman, 1998) is a reconstruction of the inferred geometry of stereotypical Kambalda Dome ore environment. It shows a number of common features: the antipathy between contact ore and sediment at the contact between Silver Lake Member komatiite and footwall Lunnon Basalt; the linear nature of ore shoots; the occasional presence of ores in successive flows within the corridors above contact ore; and the localisation of massive contact ores within footwall trough structures. Much of the controversy around the Kambalda deposits relates to the origin of these trough features.

A number of broadly similar ore shoots have been delineated in the last few years, at the same stratigraphic position away from the Kambalda Dome itself, which diverge significantly from the typical Kambalda picture (Stone and Masterman, 1998). The massive ores in the Helmut deposit (in the Tramways camp, Fig. 15) are separated from the footwall basalts by unmineralised olivine orthocumulate rocks, and the ores at Carnilya Hill are separated from the footwall basalts by a 20m thick unit of relatively low MgO "picrite". At the Blair deposit the massive sulfide orebody is underlain by pelitic sediment, a relationship which is also found at Coronet (Beresford et al., 2005), Wannaway on the Widgiemooltha Dome (Seat et al., 2004), Windarra (Leshner, 1989) and Alexo (Houlé et al., 2002).

*Host komatiites.* The facies architecture of the Silver Lake Member has been described in the previous chapter. This unit consists primarily of thick cumulate-rich flows 40-100m thick, although thinner intercalated units are present and there may be as many as 20 distinct cooling units in the vertical section (Stone et al., 2005). Mineralisation is mainly (but not exclusively) restricted to the basal flow, which can be up to 100m thick and is commonly the thickest, and contains the highest proportion of forsteritic olivine meso-to orthocumulates with MgO contents in excess of 45% (anhydrous). The pathway subfacies is defined by a thickening of the flow unit

associated with linear troughs in the underlying Lunnon Basalt, and by absence of an underlying sedimentary layer, and is typically traceable over up to 15km in length and 500m in width (Stone and Masterman, 1998). The host komatiites are typically extensively reconstituted to talc carbonate assemblages with no preservation of original texture in cumulates and local preservation in spinifex zones. Serpentinites are preserved in rare pockets, such as at Victor and Durkin Shoots (Beresford et al., 2002; Lesher, 1983).

*Mineralisation.* Over eighty percent of the resources are contained within contact ore, defined as massive or matrix ore located at the basal contact of the Silver Lake Member. Roughly half the ore shoots consist of massive ore overlain by matrix ore; some have massive and disseminated ore only, some have matrix without massive ore, and most have a halo of low-grade disseminated ore which in some cases displays spherical, buckshot or blebby textures described further below. Orebodies typically have strongly linear, ribbon-like geometries, up to 3 km long, 300m wide, usually less than 5m thick and ranging from less than 0.5 Mt to 10 Mt in mass (Stone and Masterman, 1998). Detailed descriptions of vertical variations within ore shoots are given in some of the early papers on the Kambalda ores (Ewers and Hudson, 1972; Ross and Hopkins, 1975; Groves et al., 1977; Groves et al., 1979; Marston and Kay, 1980; Gresham and Loftus-Hills, 1981).

Nickel and PGE tenors (concentration in 100% sulfide) vary considerably both between and within shoots, as discussed above. Neighbouring ore shoots, for example Victor and Long Shoots, have markedly contrasting tenor. As discussed above, the likely explanation for such grade variation is variable fluid dynamic conditions, determining the extent of equilibration between the komatiite lava and the entrained sulfide ore magma. The wide variability within shoots on a hand-sample scale is attributable to metamorphic effects (Keays et al., 1981; Stone et al., 2004).

A small proportion of the ores of the Kambalda Dome occur at the basal contact of the flow immediately overlying the basal flow, notably at Lunnon and at Coronet West (Beresford et al., 2005). In this setting, interflow sediment is missing beneath the ore but is present in the flanking position. The hanging-wall ore at Lunnon displays some remarkable textural relationships which are described below in the context of evidence for the substrate erosion model.

*Troughs, ore geometries and deformation.* Most of the ore shoots of the Kambalda – Tramways corridor are completely or partially confined within linear trough-like features in the upper contact of the Lunnon Basalt (Figs. 18, 19, 20). All of these trough features are substantially overprinted by, and in some cases defined by, tectonic deformation, giving rise to a long-standing controversy as to their origin.

Troughs were first recognised on the Kambalda Dome itself. The larger orebodies on the regional scale are associated with the best development of trough structures. There is a general trend from the Kambalda Dome through St. Ives and Tramways to Widgiemooltha of smaller deposits and more planar basalt-komatiite contacts.

The troughs have been classified by Gresham and Loftus-Hills (1981) and by Stone and Archibald (2004) into re-entrant and open varieties. Re-entrant troughs, such as the type example at Lunnon Shoot (Fig. 18) are typically wider at the bottom than at the top, and show a marked tectonic asymmetry depending on their position relative to the axis of the Kambalda Dome. They are highly elongate, up to 3 km in strike extent and up to 100m deep, with relatively flat floors which in at least some cases can be shown to be shear zones. Massive ore commonly occurs in “pinchout” structures (Fig. 19) where ore is developed entirely within Lunnon Basalt. In most cases these are primarily the result of D2 thrusting, but Leshner (1983, 1989) provides textural evidence (e.g., undeformed contacts decorated with skeletal ferrochromites) for a primary origin in some cases.

Open troughs are broad, low amplitude linear depressions in the footwall contact which are also typically modified by faulting (Fig. 20), typically tens of metres deep, and lacking pinchout structures. Some orebodies, notably Coronet (Beresford et al., 2005), appear to occupy planar basal contacts with no evidence of troughs at all.

In a number of documented cases, there is an association between troughs, ore and the petrographically and geochemically distinct pathway subfacies of the overlying flow (Leshner and Groves, 1984, Leshner, 1989, Leshner and Arndt, 1995, Leshner et al., 2001). In some other cases, such as Ken and Gellatly on the generally more tectonised north-west segment of the Kambalda Dome, evidence for primary volcanological controls are lacking.

*Origin of trough structures.* The origin of the Kambalda trough structures remains one of the most contentious issues in the study of these deposits, and centres on whether they are primary or tectonic in origin.

There have been a number of hypotheses for generating the troughs: thermal erosion of underlying basalt (Huppert and Sparks, 1985); topographic sea-floor depressions between linear parallel basalt flows modified by deformation (Leshner et al., 1984; Leshner, 1989); syn-volcanic grabens (Ross and Hopkins, 1975; Brown et al., 1999); eruptive fissures (Gresham and Loftus-Hills, 1981); and combinations of various primary topographic features unrelated to thermal erosion, enhanced by deformation (Squire et al., 1998). Drained lava tubes or channels within the uppermost flows of the Lunnon Basalt is another possibility. All researchers who have worked in detail on the basalt-komatiite contact agree that there is no direct outcrop-scale field evidence known for thermal erosion of basalt along this contact, consistent with fluid dynamic modelling (Williams et al., 2001)

The alternative to primary hypotheses of origin, as initially proposed by Cowden and co-workers (Cowden, 1985; 1988; Cowden and Archibald, 1987) and strongly propounded recently by Stone and Archibald (2004), is that the troughs are entirely structural in origin. Stone and Archibald argue that the competency contrast between talc-carbonate altered komatiites and basalt, with the additional effect of lubrication by incompetent sulfide orebodies, resulted in the troughs being localised by the orebodies rather than the other way round. The main arguments of Stone and Archibald are summarised as follows.

- 1) The orientation of the troughs corresponds to the axis of shortening of the dome, and other linear tectonic elements making up the structural grain of the area.
- 2) The present shape and disposition of the troughs is consistent with, and can be entirely explained by, asymmetric thrusting on either side of the dome. Stone and Archibald suggest that the troughs develop initially as open synclines, localised initially by the presence of the orebodies, and modified by subsequent box folding, overturning and shearing.
- 3) In several shoots, for example Ken and Fisher, there is a small but significant discordance of ten or twenty degrees between the axis of the orebody and the axis of the trough, and the trough structure evidently truncates the orebody.

In opposition to this view, several lines of evidence argue in favour of a primary component to at least some of the troughs.

1) As discussed elsewhere, troughs are restricted to linear zones where sediment is absent from the basal komatiite/basalt contact.

2) In areas of relatively mild regional deformation, such as the Lunnon/Hunt section to the south of the Dome, the troughs correspond to thickening of the basal flow unit and are overlain by relatively planar flow tops. The host pathway-filling rocks that have been studied in detail (e.g., Lunnon, Victor) differ considerably from the flanking units in terms of their more primitive major element geochemistry and textures (Leshner and Groves, 1986; Leshner, 1989; Woolrich et al., 1981), trace element and Nd isotope geochemistry (Leshner and Arndt, 1995) and PGE geochemistry (Leshner et al., 2001b), inconsistent with their being simple structural equivalents.

3) Detailed mapping of contact relationships around less-deformed troughs including Ken, Durkin, Lunnon and Juan (Leshner, 1989; Evans et al, 1989) has identified evidence for primary, pre-structural embayments and discordances, identifiable from facies variations and primary flow tops in the basalt. Evidence includes primary “pinchout” relationships where massive ore is developed within footwall pillow basalts in zones of low deformation (Leshner, 1989, fig 5.24).

4) Not all troughs contain mineralisation (e.g. the Fletcher Trough near Hunt Shoot), and not all mineralisation is in troughs. Massive ore in many cases does not completely occupy the floor of the trough. This is difficult to reconcile with a model whereby the troughs are entirely a consequence of the ductility contrast of the sulfide bodies. Also, the very flat floors (except as disrupted by superimposed faulting) are incompatible with an origin involving folding.

This controversy is likely to remain unresolved, given the general intensity of deformation and limited opportunities for detailed study of contact relationships underground. The most likely resolution is that, as concluded by Leshner (1989), some primary topographic relief must have existed, but that it has been modified and enhanced as the result of deformation. Orebodies have exerted a profound influence on strain partitioning in the rocks, and consequently on the geometry of thrusts and

shear zones, and these have exerted a corresponding influence on the geometry of the ores.

To conclude this section on the Kambalda region, the deposits of the Kambalda Dome remain in many respects the iconic example of this style of mineralisation, but in detail the individual deposits are much more variable than the stereotyped picture suggests. Elucidation of the structural style, and the role of structure and metamorphism in modifying and localising orebodies, is one of the major advances of the last few years of research. Debate is likely to continue on the origin of troughs, hanging wall ores and other critical features. The Kambalda deposits represent a subset of a wide variety of styles of mineralisation, not a universal template.

### ***3.3.3. Deposits of the Honeymoon Well area***

The Honeymoon Well area contains a large tonnage of low-grade disseminated sulfides, with some minor massive ore, and at the time of writing represents the largest unexploited accumulation of sulfide ore within the Yilgarn Craton (Fig. 1). The deposits show an unusual combination of intense deformation and sub-greenschist metamorphic grade.

The geology of the area is dominated by a very large lenticular dunite body, with spinifex-textured flows preserved on both flanks, and five distinct sulfide deposits – Harrier, Hannibals, Corella, Wedgetail and Harakka located along its contacts with country rocks (Fig. 21). The following summarises the detailed account given by Gole et al. (1998)

Deposits range from relatively high-grade massive ore (Wedgetail) to large low-tonnage, low-grade disseminated sulfide accumulations, representing a range of settings. The sequence represents a large, complex D1 thrust duplex, with extensive duplication and overturning of stratigraphy, making reconstruction of the original volcanology an extremely challenging task.

The Honeymoon Well dunite itself is an extremely pure, very coarse grained olivine adcumulate, completely serpentinitised. Both flanks are marked by discontinuous sequences of thin spinifex-textured flows and minor intercalated sedimentary units, associated with all of the contact-related mineralisation, and in all cases evidently younging to the west. Gole et al. interpret this package along the western margin as being a tectonically repeated thrust slice of the eastern contact rocks. Spinifex-

textured rocks along the eastern margin near Corella contain very distinctive bent and crushed spinifex plates associated with high-temperature melting and slow recrystallisation of the original groundmass. This feature was interpreted by Gole et al. (1990) as the result of high-temperature metamorphism in a “thermal sandwich” between two thick cumulate flow units, driven by conductive relaxation of the original sinusoidal thermal profile. This interpretation implies very rapid accumulation of the entire sequence, on a scale of hundreds of years.

*Disseminated sulfide deposits.* In the three significant disseminated deposits, Harrier, Corella (Fig. 21) and Hannibals, mineralisation consists of trace to 5 modal percent interstitial sulfides within olivine meso- to adcumulates, within extensively faulted sequences close to the margin of the dunite. Host rocks appear to be contiguous with the main dunite lens. The Hannibals deposit is flanked by orthocumulate and spinifex textured units suggesting an origin in a primary pathway about 30-80m deep and 150m wide. Spinifex textured rocks also occur in close proximity to ore at Corella and Harrier, although the juxtaposition is almost certainly tectonic. The Harrier ore zone is about 100m thick, overturned and dipping to the east along the eastern contact of the dunite body. Corella, also along the east side of the dunite, contains ore over widths up to 100m, but is intensely tectonised, and comprises a stack of shear-bounded, vertically dipping boudins of various sizes. Reconstruction of primary volcanological features is essentially impossible, but the general setting appears similar to Perseverance and Digger Rocks.

An unusual feature of the Hannibals deposit is the presence of a zone of extremely low Cu mineralisation, within which most samples contain less than 5 ppm Cu, and where the sulfide assemblage consists of nickel-rich pentlandite and heazlewoodite (Gole, pers. comm., 2004). The host serpentinite is a largely magnetite-free lizardite serpentinite. Evidently large volumes of Cu and Fe were mobilised out of the ultramafic host during serpentinisation, which also caused the characteristic upgrading of the disseminated sulfides in Ni.

*Massive sulfides – Wedgetail.* Wedgetail (Fig. 21) is unique among the Honeymoon Well deposits in containing massive sulfides, which define a distinct resource of 2.5 Mt at 3.4% Ni within a larger low-grade resource. Massive sulfides occur along the western contact between the dunite and a felsic volcanic footwall, and appear to show the typical features of contact massive ores, except that the spinifex-textured flows

which immediately overlie them show evidence for overturning and westward-younging; i.e. the sulfides appear to occupy an upper, not lower contact. The explanation is almost certainly structural, and the orebody probably occupies the bounding shear of the overturned limb of a nappe.

*Interpretation.* Gole et al. (1998) interpret all of the Honeymoon Well deposits to have formed in the lowermost of two distinct komatiite units, the upper being the dunite lens. The lower unit, originally up to 250m thick, is interpreted as a compound flow facies sequence with disseminated sulfides localised in pathways, and capped by spinifex-textured flow lobes. The upper unit formed almost immediately afterwards, in a massive lava channel 6km long by as much as 1 km thick, with extensive thermal erosion along its base resulting in juxtaposition of basal dunite with earlier-formed orebodies. Subsequent deformation was greatly influenced by the competency of this large dunite unit, and resulted in extensive duplication and thrust ramping of the basal contact sequence onto the original top contact of the dunite.

### ***3.3.4. Deposits of the Perseverance Area***

*The Perseverance Deposit.* The Perseverance deposit is the largest known type 1 deposit in the Yilgarn Craton, and the largest in the world in Archaean terranes. In excess of 40 million tonnes of massive and matrix ore are associated with the largest of the lenticular dunite bodies of the Agnew-Wiluna trend (Chapter 2, Figure 8), and a further 10 million tonnes comprise the satellite Rocky's Reward and Harmony deposits to the north.

The Perseverance Ultramafic Complex occupies the overturned eastern limb of the regional Leinster anticline, and is bounded on its eastern margin by a major shear zone, the Keith-Kilkenny lineament. The sequence is overturned, and dips at about 80° to the west. It lies within a zone of high strain and low to mid amphibolite facies metamorphism, and shows a metamorphic zonation from enstatite through anthophyllite to talc-bearing assemblages attributed to equilibration with CO<sub>2</sub> rich fluids during breakdown of early serpentine and talc-carbonate assemblages (Gole et al., 1987). Unstrained, unserpentinised olivine adcumulate occupies the core of the dunite lens, and primary spinifex textures are preserved in the flanking sequence to the south of the lens, but most if not all contacts between ultramafic rocks and country rocks are intensely tectonised. Original differentiated flows and olivine-poor marginal

rocks are converted to tremolite-chlorite-olivine schists (Fig. 2.21), referred to here as “metakomatiite”. The detailed geology of the ore deposit is shown as level plans in Figure 22.

Tremolite-chlorite schists corresponding to komatiite liquid and olivine orthocumulate compositions (Barnes et al., 1988a) are present in the flanking rocks to either side of the lens, within a zone of near-mylonites on the eastern margin, and closely associated with the main orebody. Libby et al. (1998) reinterpreted the tremolite chlorite rocks of the ore zone as products of metasomatism along shear zones, a process which has clearly taken place and which is evident from the presence of tourmaline along ultramafic-felsic contacts. An origin of the tremolite-chlorite schists as metakomatiites (i.e., modified original chilled margins) and not as metasomatized peridotites (i.e., metasomatized fault contacts) is strongly indicated on the basis of their high Al and Ti contents coupled with a very strong correlation between Al and Ti, and the correspondence of the Al/Ti ratio in these rocks to the mantle ratio diagnostic of komatiites (Fig. 23). However, some of the facing directions inferred from these rocks by Barnes et al. (1988a) are unreliable, as no spinifex textures are preserved, and relatively liquid-rich rocks could just as easily have formed at chilled lower margins as at flow tops.

Massive ores are of two mutually gradational types: “primary” ores in contact with metakomatiite and matrix ore, at or close to the margins of the dunite lens itself, and remobilised breccia ores developed in shear zones within the felsic country rock, principally with the main 1A ore shoot (Fig. 22). This is a major fault zone containing an assemblage of remobilised massive ores and tectonic slices of isoclinally folded ultramafic and felsic rock, enclosed within felsic mylonite.

At depth, the portion of the 1A shoot adjoining the main dunite body widens out into a 50m-wide zone of metakomatiite and matrix ores, linking with the main matrix orebody. Barnes et al. (1988a) interpreted tremolite-chlorite rocks on the eastern contact of this unit as an original flow top, and concluded that the 1A shoot was an early flow, emplaced before the immediately overlying felsic sequence and pre-dating the dunite body. The evidence on which this interpretation was made is ambiguous, and the Barnes et al. interpretation is inconsistent with more recent structural work indicating a dextral shear sense on the 1A zone (Libby et al., 1998). The 1A shoot is more likely to be a tectonic slice from the base of the originally dunite-hosted deposit.

“Primary” ores were identified by Barnes et al (1988b) on the basis of skeletal chromite development at apparently unshered contacts with metakomatiite. They are relatively rare, and are indistinguishable chemically from the tectonised sulfides of the 1A shoot.

The bulk of the ore tonnage is composed of a continuous zone of matrix ore up to 80m thick, plunging at approximately 70° to the south, extending from the surface and open at the current limit of exploration drilling at 1100 m depth. Within about 20-40m of the original basal contact, the matrix ore shows spectacular development of bladed metamorphic olivine or “triangular” textures, consisting of elongate metamorphic olivine grains up to 5cm in size within a continuous matrix of about 30-40% sulfide (a typical pyrrhotite, pentlandite and chalcopyrite assemblage) (Fig. 24).

Compositionally these rocks are extremely pure olivine-sulfide adcumulates, with essentially no trapped komatiite liquid component. Some of the coarser olivine blades retain the ghost morphology of the original magmatic olivines (Fig. 24). Further into the body of the dunite, the bladed metamorphic textures gradually give way to primary matrix ores, showing evidence for dynamic recrystallisation textures in the form of microgranular aggregates of clear neoblastic olivine surrounding brown-tinged relict igneous olivine cores, a texture which persists into sulfide-free rocks in the core of the dunite. The marginal distribution of the bladed ore marks the limit of an original episode of serpentinisation, the bladed olivines being regenerated by dehydration during prograde metamorphism. These olivines have been subjected to a subsequent episode of post-metamorphic retrograde serpentinisation, which decreases in extent and intensity with depth below the present-day erosion surface.

The matrix ore is surrounded by an extensive halo or “cloud” of low-grade disseminated sulfide, defining up to three distinct layers or zone towards the southern end of the dunite lens (Fig. 25). Disseminated ores are typically fresh and unserpentinised, and consist of up to about 5% sulfides interstitial to olivine grains within a very pure olivine-sulfide adcumulate. Layering is evident on a scale from centimetres to tens of meters; at the finest scale, it consists of alternations of coarse-grained olivine with no sulfide to much finer-grained olivine with nearly continuous interstitial sulfide. This texture is inconsistent with mechanical accumulation of olivine and sulfide liquid by crystal settling, and implies that olivine grains were growing by in situ accretion of the floor of the magma pathway in the presence of

fluctuating proportions of sulfide liquid, which, when present, wetted olivine grains and inhibited further growth.

The stratigraphic footwall to the Perseverance Ultramafic Complex from Perseverance itself north to Harmony is made up of a complex sequence of highly deformed porphyritic dacites, garnet-biotite metapelites, mafic amphibolites, sulfidic cherts and other minor components. Within the immediate Perseverance mine area, there is also a distinctive pyrrhotite-rich actinolite-quartz-feldspar schist which extends at consistent width for a kilometre or more north of the main ore body roughly parallel with the 1A shoot, and shows evidence for complex isoclinal folding in the immediate vicinity of the orebody. Barnes et al. regarded this unit as a stratigraphic marker bed truncated by the base of the main dunite lens. (Trofimovs et al., 2003) regard the entire footwall sequence as being a tectonised pseudo-stratigraphy, but the evidence for a primary pre-tectonic origin of the actinolite-quartz-feldspar schist is strong. Detailed structural studies are clearly necessary to resolve this and many other issues, but either way it is evident that the intensity of the deformation obscures much crucial evidence on the origin of this deposit and its country rocks.

Barnes et al. (1988c) proposed that the PUC occupied a broad (1-3 km wide), concave submarine channel, at least (~100-150m deep) formed by a high-volume komatiite eruption, and that the channel was formed by thermal erosion. Subsequent modelling showed that formation of deep erosional channels is favoured by the presence of a low-melting point substrate, especially if the substrate was unconsolidated at the time (Williams et al., 2001). The initial basis for this interpretation was the geometry of the komatiite sequence, particularly the great thickness of the dunite lens as compared with the flanking orthocumulate sequences, and the truncation of footwall marker horizons by the basal contact of the dunite lens.

The Barnes et al. model depended heavily on the identification of facing directions in metakomatiites. Subsequent structural studies (Libby et al., 1998) and more detailed studies of the country rock lithologies (Trofimovs et al., 2003) are inconsistent with the original Barnes et al. reconstruction, which was revised by Williams et al. (2001). It is entirely possible that the apparently discordant relationships between the base of the dunite and the footwall stratigraphy are entirely tectonic in origin, and it would be impossible to conclusively prove otherwise. A mechanism is still required to explain

the evidently primary thickening of the sequence and the relationship to flanking spinifex rocks, however.

*Rocky's Reward.* The Rocky's Reward deposit is one of the most intensely tectonised massive sulfide deposits known anywhere, and corresponds to type 5 mineralisation of Lesher and Keays (2002, table 1). A resource of approximately 10 Mt at around 2.5% Ni is associated with tightly folded, poly-deformed komatiitic rocks within the same felsic country rock sequence which hosts the main Perseverance orebody (Fig. 26), and which contains numerous sedimentary sulfidic layers.

The deposit lies within a narrow high-strain "corridor" about 100m wide which is contiguous with the Perseverance 1A shoot 2km to the south, extends to the Harmony deposit 5km to the north, and which is intermittently mineralised along its length. Mineralisation lies within intensely deformed ultramafic layers, folded about an upright axis and forming two subhorizontal surfaces which plunge gently to the north (De-Vitry et al., 1998). The sequence is truncated to the west by a steeply dipping shear zone which contains abundant massive sulfide. Massive sulfides generally occupy fold closures and form a matrix to extensively boudinaged slivers of felsic and ultramafic rocks, including "triangular-textured" metamorphosed matrix ore similar to that in the main Perseverance orebody.

The complex structure of the deposit is attributed to early thrusting and isoclinal folding of a single mineralised ultramafic unit, with subsequent refolding about the vertical F2 axis. The critical unsolved problem remains the relationship of Rocky's Reward, and the broadly similar Harmony deposit, to the main Perseverance deposit. The dextral displacement along the Perseverance 1A shear zone, and the very high strain intensity, is consistent with a model whereby both Rocky's Reward and Harmony are tectonic slices of the Perseverance orebody (De-Vitry et al., 1998). This contradicts the earlier interpretation of Barnes et al. (1988b) that Rocky's Reward represents a discrete flow, older than the main Perseverance dunite body. Further detailed structural analysis is required to evaluate these alternatives.

*Compositions of ores and host rocks.* The massive and matrix ores of both Perseverance and Rocky's Reward have relatively low Ni tenors, and low PGE contents, falling at the low end of the trend defined by the Kambalda ore shoots (Fig. 10) and interpreted above as the result of R-factor variations. Accompanying this

feature is evidence for depletion of Ni in olivine, by a factor of two or more below model concentrations for sulfide-free fractionation. In part this is due to low-temperature re-equilibration between olivine and sulfide liquid, which tends to redistribute Ni out of olivine and into sulfide through the mechanism of Fe-Ni exchange (Binns and Groves, 1976; Barnes et al., 1988c). However, this cannot explain the low Ni content of olivines in sulfide-poor rocks of the disseminated ore zone, and the slightly Ni-depleted character of the entire Perseverance komatiite suite (see below). This depletion of both ores and olivines can be modelled by equilibration of olivine, sulfide and komatiite liquid during bulk equilibration at low R values (Barnes et al., 1995).

Wholesale Ni depletion of this type is a rare feature, not seen in most komatiite sequence whether mineralised or not. It may be a distinctive characteristic of very large ore systems on the Perseverance scale, and hence a valuable exploration guide, as discussed further below.

The Perseverance dunite body is also notably depleted in chromite. This is expected in the more primitive, Mg-rich cumulates, which would have crystallised from chromite-undersaturated melts (Barnes, 1998), but not in the more Fe-rich cumulates associated with the matrix ores. There appears to be an antipathetic relationship between sulfide and chromite deposition even in magmas which would be expected to be chromite-saturated (Barnes and Brand, 1999).

### ***3.3.5. The Forrestania and Lake Johnston Belt Deposits***

The nickel deposits of the Forrestania Greenstone Belt are relatively small, but disproportionately significant for two reasons: they are the only examples of economic mineralisation associated with Al-depleted komatiites, and at 2920 Ma (Wang et al., 1996) also the oldest known deposits of this type. They represent a spectrum from dunitic sheet to compound flow facies environments, with country rocks ranging from pure felsic volcanics to mixtures of felsic volcanics and oxide-facies banded iron formation (Perring et al., 1995). The degree of deformation varies widely; deposits of the western komatiite belt (Flying Fox and New Morning) are relatively well preserved, whereas the eastern belt has undergone pervasive penetrative deformation and probable isoclinal folding. This summary is based on the

work of Perring and co-workers, earlier work by Porter and McKay (1981) and a general description of the major deposits by Frost et al. (1998).

*Digger Rocks.* The host ultramafic unit at Digger Rocks is a sheet-like body of olivine adcumulates and mesocumulates, retaining relict igneous olivine and primary magmatic textures in the core, and metamorphosed to spectacular bladed olivine-anthophyllite rocks, rare olivine-talc-enstatite schists and “jackstraw” olivine talc rocks towards the margins. The orebody itself occupies the basal contact of the upper of two thick adcumulate-dominated units, sandwiched between disseminated sulfide-bearing olivine adcumulate above, and an unusual xenolith-bearing altered orthopyroxene cumulate (now tremolite amphibolite) below, interpreted as a basal layer to the upper unit (Fig. 3, Fig. 27). Beneath the orebody, the pyroxenite lies directly on top of the underlying unit; flanking the orebody, it is separated from the underlying unit by an oxide-facies banded iron formation layer up to 10m thick. The pyroxenite contains abundant inclusions of oxide facies banded iron formation (BIF) and quartz-mica-schist showing varying degrees of disaggregation. The clasts range from angular and coherent to wispy, diffuse magnetite-rich bands developed within the amphibolite matrix. The unit as a whole has strongly contaminated trace element chemistry indicating assimilation of at least 10% dacite component as well as BIF (Perring et al., 1996) (Fig. 28); the contaminant is inferred to be similar in composition to the quartz mica schist which underlies the lower flow unit, and which is intermittently developed between the two units.

*Flying Fox.* The Flying Fox deposits represents a contrasting environment, in the Western Belt on the opposite side of the synformal Forresteria Greenstone Belt. Here, BIFs are absent, and the komatiite sequence overlies a thick quartz biotite schist (QBS) unit of roughly dacitic composition, with minor cherty units. The Flying Fox deposit occupies the base of a broad olivine mesocumulate-filled pathway, the basal contact of which truncates a chert unit developed at the QBS-komatiite contact on either side (Fig. 3). The Flying Fox pathway is occupied by a mixture of igneous textured cumulates and olivine-talc “jackstraw” rocks. It is flanked by thinner spinifex-textured units, interpreted by Perring et al. (1995) as flow lobes, in a similar relationship to that at Kambalda, but is distinctive in one respect. The adcumulate pathway-fill is overlain by a laterally restricted unit of pyroxenite and gabbro interpreted as the result of stagnation and fractionation of lava in the temporarily

blocked tube. The orebody occupies a more or less planar contact, and is offset by a pair of planar granite sheets occupying original subhorizontal faults.

The geochemical contrast between komatiites of the Flying Fox area and those of the eastern Belt, including Digger Rocks and the host rocks to the Cosmic Boy and Liquid Acrobat deposits further north, is illustrated in Figure 28. The three Eastern Belt deposits and the entire eastern komatiite sequence are intimately intercalated with BIF layers as well as felsic volcanics; the geochemical trends show a marked and highly distinctive enrichment in Fe, with a minor signature of LREE and Zr enrichment related to felsic contamination (Perring et al., 1996). This Fe enrichment is completely absent in the Western Belt komatiites, which show felsic contamination signatures. These trends are indicative of supracrustal contamination by the immediate substrate lithologies, on a regional scale.

*Cosmic Boy.* The Cosmic Boy deposit also occupies a roughly planar contact, in this case between banded iron formation and a homogenous 40-60m thick metamorphosed olivine mesocumulate unit, lacking in spinifex textures. Mineralisation is dominated by matrix ore, much of it recrystallised to ‘triangular ore’ textures like those at Perseverance (Fig. 24), with no accompanying massive ore. The komatiitic cumulates are almost entirely metamorphosed to jackstraw-textured olivine-talc rocks (see Chapter 2), implying a period of pervasive talc carbonate alteration prior to the metamorphic peak. The morphology of the ultramafic bodies may therefore be entirely controlled by deformation. There is no clear evidence for a relationship to a pathway. The deposit lies close to a prominent convergence and thickening of multiple banded iron formation units in what is almost certainly a regional isoclinal fold closure, probably the nose of a regional nappe structure (Frost et al., 1998). In section, the Cosmic Boy deposit is separated by a basalt interval from a second mineralised unit carrying heavily disseminated sulfide ore on its structural hanging wall contact, the whole sequence dipping at 50° to the west. The two units are probably on opposite sides of an isoclinal overturned syncline. Despite this evidence for intense deformation, also evident from tight parasitic folding within the BIF, there is little evidence for formation of sulfide pinchouts, and the ores exactly occupy the komatiite-BIF contacts.

*Maggie Hays and Emily Ann Deposits.* The Maggie Hays and Emily Ann deposits lie within the small greenstone enclave called the Lake Johnston greenstone belt (Map 2)

(Buck et al., 1998). This is very similar in general stratigraphy, particularly the association between thick cumulate komatiite units and BIFs, in tectonic style, metamorphic grade and age to the Forresteria Belt and is almost certainly correlative with it and the smaller Ravensthorpe greenstone enclave further to the south (Map 2).

The Maggie Hays deposit is a basal accumulation of massive, matrix and disseminated ore within the mesocumulate-dominated “Central Ultramafic Unit”. The massive orebody in part occupies the basal contact with a porphyritic meta-dacite containing lapilli tuff units, and to the north occupies an extensively developed “pinchout” within the felsic unit extending some 300 m north of the limit of the ultramafic host (Fig. 29). The whole sequence is overturned and dips at 60 to 80 degrees to the east. The host ultramafic unit attains a maximum thickness of 400m, and consists of a basal orthocumulate layer about 50m thick, intercalated with units of orthopyroxene orthocumulate, overlain by a central core of olivine mesocumulate and adcumulate, metamorphosed to olivine-anthophyllite and olivine-talc assemblages with abundant fresh olivine in the core. Rare diffuse iron-rich xenoliths interpreted as partially assimilated banded iron formation clasts, similar to those observed at Digger Rocks, have been observed within these basal pyroxenite units. Limited drill information implies the existence of a fractionated cap of pyroxene cumulates and gabbros above the mesocumulate. The sequence is extensively disrupted by at least two generations of faults including an early set of thrusts.

The orebody is a planar tabular body about 1400m long by 200-400m wide, divided into two zones. The southern zone, comprising the northern 500m strike extent of the orebody, consists of a basal massive sulfide up to 7m thick, overlain by net textured ore up to about 10m thick and low-grade disseminated sulfides to total of 40m thickness, overlain by barren olivine mesocumulate. The massive ore section is continuous into the northern zone, which consists of a tectonised sheet of multiple massive sulfide layers up to 3m thick containing abundant deformed felsic clasts.

The contiguous nature of the remobilised and ultramafic-hosted ores at Maggie Hays is reminiscent of the situation at Perseverance, and on a smaller scale the relationship between “pinchouts” and primary ores at Kambalda. This is clearly a widespread feature of deformed type 1 deposits.

The Emily Ann deposit, like Rocky's Reward, is an example of a highly tectonised deposit which has been almost entirely detached from its original komatiite host (Fig. 30), and is designated as a "type 5" deposit according to the Lesher and Keays classification (Table 1). The deposit occupies a prominent NW-trending shear zone, which may represent a strike extent of the shear zone which hosts the off-contact portion of Maggie Hays on the opposite side of the Jimberlana Dyke. The deposit consists of a number of roughly planar en echelon massive sulfide sheets, with abundant inclusions of various lithologies including BIF and olivine cumulate, within a complexly sheared sequence consisting primarily of a similar porphyritic metadacite to that seen at Maggie Hays. The sequence also contains several tectonised units of komatiitic olivine cumulates with no primary contacts.

*Distinctive features of the Forrestania and Lake Johnston Deposits.* The Digger Rocks and Maggie Hays deposits show strong similarities to Perseverance: massive, matrix and disseminated ores at the base of a thick dunite body, probably of the dunite lens subfacies, with structural mobilisation of massive sulfides into planar shear zones at Perseverance and Maggie Hays. However, there are some distinctive features which distinguish them from deposits in the Norseman-Wiluna Belt. The main one is the association with banded iron formation. The correspondence between komatiites and BIFs is remarkable strong, particularly in the eastern belt where one rarely occurs without the other within a few tens of metres of section. (This is not true in the Western Belt where BIF is absent). One possible explanation is that the Forrestania komatiites are intrusive sills, and are localised by the sedimentary layers. The problem with this interpretation is that the clearly extrusive multiple spinifex-textured flow lobes of the Liquid Acrobat-Seagull-Ratbat area (Perring et al., 1995) are also closely associated with BIF. The Forrestania east belt in general is an example of correlation of thick dunite bodies with stratigraphically equivalent flows.

The other distinctive feature at Digger Rocks and Maggie Hays is the presence of orthopyroxenites associated with the mineralised basal margins of the dunite bodies, and with disaggregated BIF xenoliths, an association which has also been described from the Hunters Road deposit in Zimbabwe (Prendergast, 2001). These rocks are interpreted by Perring et al. as the result of crystallisation of orthopyroxene in place of olivine due to increased silica introduced by contamination. However, in other areas where extensive contamination has taken place, particularly Black Swan,

orthopyroxenites are extremely rare. Assimilation of BIF may be the crucial factor, with pyroxene saturation being triggered by the addition of substantial amounts of Fe as well as Si.

### **3.4. The Substrate Erosion Model for Type 1 deposits**

#### ***3.4.1 History and background***

The idea that komatiite lava-hosted Ni sulfide deposits could have formed by assimilation of sulfidic substrates was initially proposed by Huppert, Sparks and co-workers (Huppert et al., 1984; Huppert and Sparks, 1985), and the concept was developed and applied to the Kambalda deposits by Leshner and others (Leshner et al., 1984; Leshner, 1985; Leshner and Arndt, 1990). The initial impetus for the interpretation was the observation of the distinctive linear host units, trough features and sediment free contacts at Kambalda, and the recognition that the host units represented lava channels (Leshner et al., 1984; Leshner, 1989). The essence of the model is that komatiite lavas were erupted undersaturated with immiscible sulfide liquid, and that S-saturation was achieved on a local scale as a result of thermal or thermo-mechanical erosion of the sulfidic substrate and bulk assimilation of S into the magma (Fig. 31). Sulfide liquid may then have exsolved subsequently from the magma with olivine crystallisation, or may have formed a basal “xenomelt” layer of sulfide entrained beneath komatiite lava and equilibrating to varying degrees with it (Leshner and Campbell, 1993). Sulfur in the orebody is derived from the assimilated sediment, whereas Ni, PGE and Cu are derived from the komatiite lava as a result of their high partition coefficients into sulfide liquid.

The premise for the initial Huppert et al. model was that komatiite lavas were emplaced rapidly as large, high volume, turbulent floods of lava, and that erosion and flow emplacement happened essentially instantaneously and simultaneously. Cas and co-workers (Cas et al., 1999; Cas and Beresford, 2001) have criticised the model on the grounds that these assumptions are unrealistic, and specifically that turbulent flow is unlikely (or only found close to the vent), and Rice and Moore (2001) have argued that thermal erosion beneath lava flows is impossible and has never been demonstrated. The substrate erosion model needs to be reviewed in the light of the

volcanological concepts of inflation and endogenous growth discussed in the previous chapter.

### ***3.4.2. Thermo-mechanical substrate erosion in modern basalts***

Evidence for substrate erosion by normal tholeiitic basalts has been established for some decades, and is reviewed by Greeley et al. (1998). Evidence is of two types: geological evidence for erosional features at the base of lava tubes, and direct observations of flowing lava.

Greeley and Hyde (1972) describe erosional features at the base of the Cave Basalt, Mount St. Helens, where there is field evidence for erosion by lava of an underlying lahar containing dacite blocks. Field relationships indicate minimum amounts of downcutting of 5 to 15.5 m, the maximum extent of erosion corresponding to the maximum palaeoslope. The presence of xenoliths of dacite in the basalt, and the presence of partially molten dacite blocks dribbling down tube walls (Greeley et al., 1998), indicate that the erosion process was both thermal and mechanical. Greeley et al. further describe a number of other localities including the Ainahu Ranch and Earthquake lava tubes on Kilauea, where lava tubes cut down through underlying palaeosols into earlier flows.

The first direct observation of downcutting and entrenchment in Hawaiian lava tubes was made by Swanson (1973), and downcutting has also been observed directly in a modern carbonatite flow on Oldoinyo Lengai volcano, Tanzania (Challis and Greeley, 1997; Pinkerton et al., 1990). More recently, and most significantly, observations of active lava tubes on Kilauea by Kauahikaua et al. (1998) have revealed that the continuous passage of lava over months to years in well-insulated tubes results in substantial thermo-mechanical erosion of basalt at the base of the tubes. Kauahikaua measured average down-cutting rates of up to 10cm per day, by direct measurement of the distance between the top crust of a partially filled tube to the base of the flowing lava, over a period of months. The lava appears to have been undergoing laminar flow throughout; turbulent flow is apparently not necessary for the process, in line with recent theoretical modelling (Kerr, 2001).

Rice and Moore (2001) rejected the validity of these observations, under an incorrect impression that the measurements were made to the top of the flowing lava, and therefore reflect merely the fall in lava level due to declining flow rate. In fact the

measurements were made to the base of the flowing lava using a measuring rod pushed down through a skylight into the lava. The tube in question was partially drained, such that the crust was not being inflated, and the increasing distance between the top of the crust and the base of the flowing lava could only be due to erosional downcutting. These observations invalidate the theoretical and experimental arguments of Rice and Moore for the impossibility of erosion beneath lavas.

Rice and Moore also point out that basaltic flow lobes commonly propagate across low-melting substrates such as asphalt roads without melting them. This is indeed the case for the initial phase of lobe emplacement, where lava typically quenches against the cold substrate. As can be seen from the Kilauea observations of Hon, Kauahikaua and others, and discussed in Chapter 2, erosion takes place at a much later stage where flow has become concentrated in tubes, lava pathways have become well established and the original basal quenched contact has been reheated to its melting point. This accounts for only a very small proportion of the total area of the flow field.

The substrate erosion process appears to involve several stages: firstly, the establishment of a well-insulated lava tube by the processes of inflation and radial cooling discussed above; secondly, prolonged lava flow through the tube, raising the temperature of the floor basalt to its liquidus; and finally mechanical plucking and entrainment of blobs and fragments of plastic, partially molten floor material into the eroding lava. The process is more accurately referred to as thermo-mechanical, rather than thermal erosion. The critical observation is that erosion is strictly limited to the major long lived lava pathways. No erosion of any description takes place at the base of newly propagating pahoehoe lobes.

*Implications for komatiites.* Field observations confirm the reality of rapid rates of thermo-mechanical erosion of basalt by basalt, but the process is limited to one very specific environment: large, long lived and continuously active lava tubes or pathways. We have argued that such tubes or pathways are likely to have existed in komatiite flow fields, and that these can be identified by their association with thick, homogeneous bodies of close-packed olivine cumulates. By analogy with basalts, we would expect that thermal erosion by komatiite lavas would be restricted to major lava pathways.

The low viscosity of komatiite lavas, given much prominence in early versions of the model, is doubtless a contributing factor, but perhaps not a crucial one. It comes into play only when lava is flowing freely through established pathways in long-lived lobes, and consequently may extend to distances of many kilometres away from eruption sites.

If basalt can erode basalt in Kilauea lava tubes, then komatiite should erode dacite or rhyolite, where the melting temperature may be as much as 800°C below the lava temperature, at a considerably greater rate. The rate would be highest where the substrate was unconsolidated (Williams et al., 2001). Large komatiite lava pathways would be expected to produce deep, broad troughs on felsic substrates, relative to much smaller features on basaltic substrates, and erosion could happen in principal at the base of well-insulated tubes at great distances from the original source. In this section, we review the available field evidence, some of which has been presented elsewhere in this chapter, for operation of the process in komatiite sequences.

### ***3.4.3. Evaluation of geological evidence in komatiites and ores***

*Evidence from Kambalda.* For historical reasons, the deposits of Kambalda Dome have been taken as the type example of type 1 orebodies. Consequently, discussion of evidence or lack thereof for thermal or thermo-mechanical substrate erosion has centred on Kambalda, and particularly on the footwall “trough features”. As pointed out by Stone and Archibald, the intensity of deformation of some of the Kambalda deposits makes them a less than ideal testing ground, but crucial primary relationships do exist.

The critical distinction between ore-bearing and barren environments in the Kambalda sequence is the distribution of “contact” sediment between the base of the lowermost Silver Lake member komatiite flow and the top of the underlying Lunnon Basalt. This contact sediment is widely developed beneath flanking sheet flows, but almost universally absent beneath the lava pathways (Fig. 32), regardless of the presence or absence of ore at the contact. Non-deposition of sediment within the subsequent site of lava pathways and ore deposition would require an implausible coincidence. They must have been removed by some erosional process prior to solidification of komatiite and sulfide ores.

Cas and Beresford (2001) argued for a purely physical process of mechanical scouring by the fronts of propagating komatiite flows, with dispersion of sediment to the water column. A thermomechanical assimilation process is more plausible, and more consistent with the subsequent deposition of sulfide ores above the former site of erosion, which would otherwise require a remarkable coincidence. However, direct evidence for its operation at Kambalda is scarce.

Direct observations of discordant relationships at the basal komatiite contact are rare, and typically obscured by deformation. Evans et al (1989) describe such a relationship in the Foster Shoot, where the base of an ore bearing embayment transgresses an estimated 5m of footwall stratigraphy, cutting through sediment into underlying massive basalt. As everywhere at Kambalda, however, this interpretation is complicated by structure and not universally accepted. Beresford et al. (2005) document thinning of sediment beneath the ore zone at McCloy, and attribute this to incomplete erosion of sediment.

Hanging Wall ores at Lunnon are developed immediately above the spinifex flow top of the basal flow which hosts the underlying contact ore. Groves et al. (1986) describe a remarkably well preserved sequence of textures which they interpreted as thermal erosion of the underlying komatiite flow top by the overlying sulfide liquid pool (Fig. 33). The interflow sediment and the upper A1 and A2 zones of the underlying flow are missing, and the A3 zone is occupied by remarkable "spinifex ore" in which the space between the original olivine spinifex plates is occupied by sulfide. The spinifex plates are curved, bent and slightly crumpled, indicative of high temperature deformation. At the top of this zone, at the interface with the massive sulfide, small blebs and plumes of quenched silicate melt about 5-10cm in size are enclosed within the lower few cm of the sulfide pool. Each bleb has a narrow rim of fine, wiry skeletal spinel, a hallmark of primary contacts between massive sulfide ores and komatiite melt. Heat from the sulfide has clearly caused interstitial komatiitic material to melt and ascend, and be replaced by dense, downward percolating sulfide liquid. Several tens of centimetre at least of quenched komatiite flow top must have been removed altogether. Neither a metamorphic replacement process as favoured by Cas and Beresford (2001), nor a tectonic origin as proposed by Stone and Archibald (2004), can account for the observed crumpling and bending of the spinifex plates, the typically magmatic sulfide mineralogy of the spinifex ore, the absence of A1 and A2 zones

between the spinifex ore and the massive sulfide, or the extremely delicate balloon-like morphology of the komatiite plumes within sulfide.

Groves et al. (1986) concluded from this evidence that erosion is possible only where massive sulfide is present, and that the high thermal conductivity of the sulfide is an essential condition. Arndt (1986) refuted this argument, showing that the presence of a high conductivity layer is irrelevant, as the essential condition is only that heat be conducted from the base of the flowing lava to the floor.

The identification of silicate “plumes” in sulfides here and at Silver Swan depends in part on the ease of their recognition. Inclusions of footwall rocks within komatiite hosts are much harder to see, particularly underground.

Frost and Groves (1989b) describe an unusual unit which overlies the top of the mineralised flow on the immediate flank of lava pathways at Foster, Fisher, Hunt and Lunnon Shoots. This unit has the bulk composition identical to the underlying contact sediment outside the pathway, and has ocellar textures indicative of liquid immiscibility. Frost et al. conclude that this is a “xenomelt” derived by complete melting of contact sediment, which subsequently split into two immiscible liquids on eventually cooling again. They suggest that this xenomelt ascended buoyantly through a thick komatiite flow without mixing; it is also possible that the unit formed at an early stage when the komatiite flow was much thinner, and was elevated into its present position by subsequent inflation of the komatiite flow pathway, as discussed in the previous chapter.

*Evidence from type 1 ores with felsic/intermediate substrates.* Outside the Kambalda-St Ives region, most of the known nickel sulfide deposits in the Norseman-Wiluna Greenstone Belt are associated with bimodal komatiitic-felsic/intermediate volcanism, and have felsic volcanic, sedimentary or epiclastic substrates. This category includes the deposits of the Silver Swan-Black Swan camp; Perseverance, Cosmos and Cliffs-Mt Keith in the Agnew-Wiluna trend; and the Digger Rocks, Cosmic Boy, Flying Fox and New Morning deposits in the Forresteria greenstone belt.

Theory predicts that large komatiite lava pathways would be expected to produce deep, broad troughs on felsic substrates, relative to much smaller features on basaltic substrates. This appears to be broadly true if the morphology of the larger dunite lenses is considered to be primary. This must be tempered with recognition that many

deposits have their relationships obscured by deformation, and also that at least some of the dunites are intrusive.

Mine-scale transgressive relationships between ore and felsic footwall are rare. The basal contact of the Windarra deposit, as described by Marston (1984, fig 78), transgresses footwall stratigraphy, and primary erosional features on a metre scale are evident beneath the Silver Swan deposit (Dowling et al., 2004).

A prediction of the thermal erosion model is that xenoliths of ores and host rocks, in varying degrees of melting and disaggregation should be found within type 1 ores and their immediate host rocks. A number of examples have been identified.

1. The disaggregated felsic inclusions or “plumes” in the Silver Swan and associated massive ores at Black Swan; also disaggregated xenoliths in the Cygnet disseminated ores, and hybridisation textures and xenoliths in its immediate footwall contact.
2. Disaggregated and partially resorbed banded iron formation xenoliths within evidently contaminated pyroxenites associated with the Digger Rocks ores; similar examples have been noted at Maggie Hays.
4. Xenolithic blocks of banded iron formation substrate have been identified in the Hunters Road deposit, Zimbabwe, within the basal contact zone of a thick ore-bearing olivine adcumulate unit (Prendergast, 2001; Prendergast, 2003).
5. Complex primary embayment structures at a range of scales and variably melted xenoliths are reported in well-exposed ore-bearing footwall contacts at Alexo and Sothman in the Abitibi Belt (Houlé et al 2002a,b, 2003).

*The rarity of geological evidence for erosion by lavas.* The case against the substrate erosion model is largely one of shortage of evidence. Despite the discussion so far, it must be conceded that direct geological observations of demonstrably erosional contacts are rare in type 1 deposits. The main reason for this, as we have seen, is that these deposits are commonly deformed, and what evidence remains is often obscured to the point of being equivocal. Even in weakly deformed, well preserved deposits (with a few notable exceptions such as Black Swan), the evidence is not overwhelming.

This is not surprising, in the light of the volcanological mechanisms discussed in the previous chapter. Lava flow fields are dynamic entities, preserved in outcrop as two-

dimensional snapshots. Lava at the propagating edge of a flow field quenches against cold substrate, and cold contacts probably account for at least 95% of the basal contact area of a flow field. Only that very small proportion of the contact area which is intersected by subsequently developed flow pathways is subject to erosional processes. Furthermore, erosion is likely to be a characteristic of the phase of lava emplacement where flow rates are high and little or no crystallisation is taking place in situ. By their very nature, all of the contacts which are observed now represent cooling and solidification of magma, and hence are depositional.

There is no reason why there should be exact spatial correspondence between sulfide deposition sites and former erosion sites, any more than there is in a meandering river. It is essential to the model that sediment is eroded in one place and the products of the process transported downstream to another, and deposition may well be expected to occur in response to conditions which do not favour erosion, such as at the termination of major pathways. It is more surprising that the antipathy between contact sediment and ore illustrated in Figure 32 is as strong as it is.

*Thermal aureoles.* The lack of obvious thermal metamorphic aureoles beneath Kambalda ores is cited by Stone and Archibald (2004) and Seat et al. (2004) as evidence against thermal erosion. In fact aureoles would not be expected to extend for more than a few tens of centimetres owing to the low thermal conductivity of rocks. On the time scale of a lava flow, thermal effects in the footwall would be restricted to an extremely narrow boundary layer with very steep thermal gradients immediately at the floor (Gole et al., 1990), and temperatures would be at the ambient level within less than a metre. Pronounced thermal aureoles have in fact been observed beneath the Katinniq deposit in the Cape Smith belt (Gillies, 1993; 1999) and beneath the Alexo deposit (Houlé et al., 2002a,b).

#### **3.4.4. Geochemical evidence**

*Trace element evidence.* The geochemical evidence for crustal contamination within komatiite sequences has been reviewed by Barnes et al. (2004b) and Leshner et al. (2001b). These workers emphasize the use of ratios of relatively “immobile” elements which are incompatible in olivine, and hence insensitive to fractionation or accumulation of olivine, and which are concentrated to varying degrees in potential crustal contaminants. Commonly used elements are Th, Nb, the rare earth elements,

(REE), Zr, Ti and Y. Contamination can be indicated by the presence of “enriched” signatures – that is, having highly incompatible, lithophile elements such as Th and light REE, enriched over those elements which are less concentrated in crustal rocks, such as Ti, Y and heavy REE. On this basis, there is a significant association between mineralised komatiite sequences and mineralisation on a global basis. The most extensively contaminated komatiites, where contamination can be identified on geological as well as purely geochemical evidence, have been found in association with komatiites erupted on felsic or sedimentary substrates, notably Black Swan and Digger Rocks, and possibly at Perseverance (Fig. 34). The complicating factor, as discussed in detail by Barnes et al. is the problem of discriminating effects of alteration from the signal of contamination. Evidence for disruption of trace element signatures can be seen where samples of olivine-rich rocks, with low original concentrations of all incompatible elements, have more “enriched” signatures than olivine-poor rocks from the same locality. In applying trace element ratio to exploration, it is therefore important to use samples of spinifex-textured rocks wherever possible, or at least rocks with as high a proportion of interstitial liquid to cumulus olivine as possible, and to compare data on ratio:ratio plots such as those in Figure 34 with appropriate model mixing trends. In some cases, it is likely that pathway subfacies rocks may well be more contaminated than flanking sheet flow subfacies equivalents (Leshner et al., 2001b), but finding samples not susceptible to alteration may be more difficult. Liquid-rich segregation veins such as those observed at Black Swan (Barnes et al., 2004a) may be the best material.

On a local scale, the distribution of contaminated komatiites is a function of the volcanological environment and nature of the substrate (Fig. 35). (Leshner and Stone, 1996; Leshner et al., 2001b). At Kambalda, the stratigraphic sequence as a whole, including the overlying Devon Consuls and Paringa basalts, shows a gradually increasing signature of crustal contamination reflected in lithophile incompatible elements such as LREE, and also in Nd isotopes. Within the Silver Lake Member, contamination signatures are generally absent in the lava pathways, but evident in non-cumulate rocks of the flanking sheet flow sequence (Leshner and Arndt 1995). In contrast, Black Swan and Perseverance show evidence for extensive contamination within pathways, and in direct association with ore.

Evidence of contamination is not necessarily evidence for mineralisation, if the assimilated rocks are not sulfide-bearing. Evidence for this is seen in the highly contaminated Paringa Basalt, overlying the Kambalda komatiite sequence, which like many of the samples analysed from Black Swan are evidently strongly crustally contaminated without showing any evidence for PGE depletion (Redman and Keays, 1985).

*Re-Os isotopes.* Aside from discussions of the validity or otherwise of trace element trends as indicators of contamination, the major line of geochemical evidence against sediment assimilation has been Re-Os systematics. Foster and coworkers (Foster et al., 1996; Lambert et al., 1998) demonstrated that ores from Perseverance and a number of Kambalda shoots have essentially chondritic initial Os isotope ratios. They argue that this precludes addition of more than 2% of crustal material into the ores. Foster et al. argued that this limit was inconsistent with R factors inferred independently from other observations, and therefore that sediment assimilation did not happen. A similar case has been made (Shirey and Barnes, 1995) to account for non-radiogenic Os signatures in the Katinniq ores of the Cape Smith Belt.

Foster's data have been discussed at length by Leshner and co-workers (Leshner and Stone, 1996; Leshner and Burnham, 2001), who carried out detailed modelling of trace element and isotopic fractionations during the process of assimilation and crystallisation, and demonstrated that significant decoupling of isotopic and trace element systems could occur, Os isotopes being among the least sensitive indicators of contamination. Furthermore, interpretation is very dependent on assumptions, and in the Kambalda case involves a large extrapolation from a single sample of the contaminant sediment.

Constraining the R factor of ore formation depends on reliable knowledge of the initial Os isotopic composition of the contaminant, and is also dependent on the model of ore formation. The dynamic environment of ore formation means that a batch of sulfide liquid would continue to equilibrate with potentially pristine, uncontaminated komatiite lava long after the initial assimilation episode which produced it, and much of the non-radiogenic, mantle Os present in the ore is derived from uncontaminated komatiite lava during this process. The single phase batch equilibrium process described by the use of the R factor is simply not realistic for ores formed in lava pathways

A more recent Re-Os study of komatiite-hosted Ni sulfides and host rocks in the Abitibi belt found evidence for incorporation of crustal Os (Lahaye et al., 2001). Particularly significant are observations on very fresh samples from the Alexo deposit, where enrichment in radiogenic Os correlated with mild LREE enrichment in glassy melt inclusions in fresh olivine grains. Lahaye et al. interpreted variability in  $\gamma^{Os}$  in terms of R factor variations between the deposits studied, in line with the theoretical models of Lesher and Burnham (2001). Os isotopes appear to be effective indicators of contamination in low R deposits, but are inconclusive at high R values.

*S isotopes.* Sulfur isotopes have been proposed as indicators of S source in a number of deposits. According to the compilation of Lesher (1989), S isotopes of ores closely match S isotopic compositions of associated substrate sediments at a number of localities including Kambalda, Windarra and Alexo, but the localities differ significantly from one another and (except for Kambalda) from mantle values. This could be taken as support for a local sedimentary S source, but this line of evidence must be treated with caution. It is not impossible that pervasive metasomatic fluid infiltration could have homogenised S isotope compositions on a regional scale. A similar argument can be applied to Pb isotopes (McNaughton et al., 1988).

*Origins of S saturation.* If the S in nickel sulfide ores is not locally derived, then it must be derived in one of two alternative ways: from the mantle, or from deep crustal assimilation prior to eruption.

A mantle derivation of S runs against two lines of evidence. Firstly, experimental measurement of the effect of pressure on S saturation indicates that S solubility increases with decreasing pressure (Huang and Williams, 1980; Wendlandt, 1982; Mavrogenes and O'Neill, 1999). In other words, a mantle melt which was S-saturated at source would become S-undersaturated on ascent. Given that komatiites were derived from previously melted (and hence S-depleted) source mantle, it is extremely unlikely that komatiites could be erupted saturated with mantle derived S. Secondly, geochemical evidence from a number of localities indicates komatiites are typically erupted undepleted in Ni and PGEs (Keays, 1995). The majority of S-free non-cumulate komatiite samples analysed for PGEs from Kambalda (Lesher et al., 2001b), Perseverance (Barnes et al., 1995) the Black Swan area (Barnes et al., 2004a) and the Alexo-Munro area in the Abitibi Belt (Puchtel et al., 2004) show Pt and Pd levels expected from mantle derived melts. Had these lavas been S saturated at any point,

they would have suffered significant depletion in PGEs owing to the very high partition coefficients for these elements into sulfide liquid. Wholesale pre-eruption S saturation can therefore be ruled out.

This requires that komatiite lavas become S saturated post-eruption, and in many cases only in the major lava pathways and not in the sheet flow environment. If substrate assimilation has not taken place, then the spatial correspondence of S-saturation with linear sediment-free pathways would have to be a coincidence. This makes the suggestion of mechanical erosion of S-bearing sulfide very hard to reconcile with the restriction of ores to the same pathways.

*Assimilation of sulfur by other mechanisms.* An alternative possibility is that komatiite lavas assimilate sulfur by some mechanism that does not involve wholesale melting and assimilation of substrate rocks. One possibility is through thermal decomposition of pyrite in the substrate, releasing S which is transported into the lava via the vapour phase (Barnes et al., 1997; Baker et al., 2001). This could account for addition of S without any other evidence for assimilation. However, the low thermal conductivity of rocks means that only the uppermost few tens of cm of the footwall are likely to reach the temperatures required on the time scale of an active lava flow; the direct contact may reach its melting temperature, but the thermal gradient away from the contact is likely to be extremely steep, and the volume of rock within which pyrite might dissociate is not much bigger than the volume which might melt. This leaves wholesale assimilation as the most viable mechanism.

### ***3.4.5. Summary***

Most of the objections which have been raised to the substrate erosion model have been dealt with in the foregoing discussion, and the case against the model is more from shortage of evidence than from any counter-evidence. Fluid dynamic or theoretical objections can be dismissed on the grounds that the process has been observed in real time beneath modern basaltic lava tubes. To date, opponents of the model have not come up with a viable alternative hypothesis, or compelling evidence to dismiss the substrate erosion mechanism, but debate is likely to continue.

## **3.5. Type 2 Disseminated ores**

Type 2 ores are defined as accumulations of low grade disseminated sulfides located internally within cumulate-rich komatiite units, typically lenticular dunite bodies. The type example is the Mount Keith MKD5 deposit within the Eastern Ultramafic Unit at Mt Keith, and is described in detail in the next chapter. In this section we summarise some key features and some important variants, and address the issue of whether type 1 and type 2 deposits are genetically distinct, or part of a continuum.

### ***3.5.1. General features***

Type 2 ores are defined as large, homogenous bodies of olivine-sulfide accumulates to mesocumulates, centrally disposed within dunite lens sub-facies units. There are two distinct varieties, defined by the textural relationship of sulfide blebs to olivine (or olivine pseudomorphs): interstitial sulfides (type 2b) moulded around olivine grains, as illustrated in Figure 2 of Chapter 2, or subspherical or globular sulfide aggregates (type 2a).

### ***3.5.2. Type 2b “Interstitial Ores”***

The two largest deposits (in overall tonnage, and tonnes of contained Ni) in the Yilgarn Craton, and rivalling Thompson as the largest individual komatiite-related deposits, are Yakabindie, and the Mt Keith MKD5 orebody, both of which are typical type 2b deposits. General features of type 2b deposits are: pentlandite-rich sulfide assemblages resulting from addition of Ni originally in olivine during subsolidus equilibration, and from mineralogical modification during low-grade hydration; a general homogeneity of grade; and presence of cm-scale layering defined by variations in sulfide proportion and olivine grain size. The MKD5, Yakabindie and Goliath North orebodies are described in detail in Chapter 3.

### ***3.5.3. Type 2a “Globular Ores”***

Globular ores are a variety of disseminated sulfide deposit, in some cases forming a halo around type 1 basal accumulations and in others being centrally disposed within thick cumulate units. The definitive characteristic is the presence of spherical or subspherical sulfide “blebs” several mm to 2 cm in size, as distinct from the typical interstitial texture whereby sulfides are moulded around original olivines. They have

sometimes been referred to as “buckshot” or “globular” ores; here, the term “globular” is preferred to “blebby”, and the term “bleb” is applied to sulfide aggregates regardless of their shape. Examples include the Marriott’s deposit in the Mt Clifford area; and numerous occurrences around the Kambalda dome, including the Otter and Durkin Shoots (Beresford et al., 2000); and the Black Swan disseminated sulfide ore body, taken as the type example here.

*Black Swan disseminated sulfides.* The Black Swan disseminated orebody occupies the lower central part of a 500m thick pile of very coarse grained olivine ortho- and mesocumulates forming the central pathway of the eastern Ultramafic Unit at Black Swan (Chapter 2 Fig. 12) (Dowling et al., 2004; Hill et al., 2004). The orebody is a roughly cigar-shaped elongate accumulation of disseminated sulfides, amounting to about 8 mt at 0.8% Ni, comprising a thick sequence of disseminated sulfide-bearing, coarse-grained olivine orthocumulates with distinctive vesicular textures (Fig. 36). The host rocks have distinctive hopper-textured and harrisitic olivines, commonly over 2 cm in size; even coarser branching and chevron-textured olivine harrisites are developed within segregation veins.

The orebody is characterised by very distinctive globular-textured sulfide blebs (Fig. 36). Many of these blebs are interpreted as partially filling original segregation vesicles, following the interpretation of similar textures at Otter Shoot, Kambalda by Beresford et al. (2000). The Black Swan globular blebs are rounded to subspherical, with a clear meniscus developed against segregated komatiite melt which itself shows rarely-preserved microspinfex textures. Not all sulfide blebs show this relationship; some are diffuse sub-spherical globules, probably with similar origin but obscured by alteration. Amorphous sulfide blebs are also found in irregular segregation patches up to 5 cm across, interpreted as coalesced vesicles developed interstitial to cumulus olivine grains, and also within segregation veins. Typical interstitial disseminated sulfide blebs are also widespread, and account for most of the tonnage of the orebody. Rare coarse dendritic chromites, possibly derived from eroded and re-transported massive ore, have been identified.

Sulfide blebs are commonly finely intergrown with fine grained carbonate. The present sulfide mineralogy of Black Swan depends on the metamorphic mineralogy (Groves et al. 1974). Pyrite-millerite-polydimite±chalcopyrite assemblages are intergrown with magnetite and carbonate (ferroan magnesite) in serpentinised host

rocks. In talc-carbonate rocks, vaesite accompanies millerite, polydymite and pyrite. Spherical sulfide globules commonly contain relict primary pentlandite in addition to violarite and millerite. Like Cygnet, the bulk composition of the sulfide fraction has been substantially modified by redistribution of Ni and Fe between original olivine and the final sulfide-silicate-carbonate-oxide assemblage, with redistribution of Fe into siderite and haematite playing an important role (Eckstrand, 1975; Donaldson, 1981). Nickel tenors in 100% sulfide are hard to estimate reliably, owing to the low sulfide abundance; projection to 38% S gives Ni tenors around 35%. Such high values are unlikely to be primary.

*The Marriott's Deposit.* A similar association of globular, spherical sulfide blebs with coarse skeletal and harrisitic olivines is found in the small Marriott's deposit in the Mt Clifford area (Map 1) and at the nearby Mt. Newman prospect 9 km to the ESE. The Marriott's deposit has another curious attribute, in that the sulfide blebs are unusually metal rich and sulfur-deficient, containing phases such as awaruite (Fe-Ni alloy), heazlewoodite and trevorite ( $\text{NiFe}_2\text{O}_4$ ) (Hudson and Travis, 1981). It is possible that this unusual mineralogy, distinct from that typically found in serpentinites, may be a primary feature related to S-loss during vesiculation.

#### ***3.5.4. Are type 2 ores genetically distinct from type 1?***

Hill and Gole (1990) quoting Duke (1986), contend that type 2 ores are distinctive in having highly consistent grades, and that this is the result of cotectic simultaneous precipitation of sulfide liquid and olivine from cooling, fractionating komatiite melt. According to this model, type 2 ores are fundamentally distinct from type 1, in that sulfide liquid is transported to the deposition site in the type 1 case, whereas sulfide liquation (that is, the nucleation and growth of new droplets of sulfide liquid) and deposition happen simultaneously in situ in type 2 ores.

Grades of type 2 deposits are indeed consistent, typically falling in the range 0.55 to 0.8% Ni, but this is largely determined by economic factors and choice of cut-off grades in resource calculations. In fact within type 2 deposits there are typically wide fluctuations in the abundance of sulfide on a decimetre scale.

If type 2 deposits have a distinct origin by cotectic precipitation of olivine and sulfide, then there should be a strong peak in the histogram of whole rock S content corresponding to the cotectic ratio, and they should have distinct S distributions

compared with disseminated sulfide haloes around type 1 deposits, where sulfides are held to be mechanically deposited. The latter population, dominated by Perseverance, Maggie Hays and Digger Rocks, show textural relationships very similar to those at Mt Keith and Six Mile. Consistent with the two-type hypothesis, there is indeed a distinct difference in S distribution between type 1 haloes and type 2 deposits, as exemplified by Mt Keith and Six Mile (Fig. 37).

The “halo” disseminated sulfides show a roughly log-linear distribution of sulfide abundance, while Six Mile and Mt Keith both show a prominent shoulder. These trends are mixtures of log-linear distributions similar to “halo” sulfides with log-normal distributions centred on a median S abundance around 0.8-0.9% S, corresponding to around 2-3 modal percent sulfide. This observation tends to support the view that there is a genetic distinction between type 1 and type 2 ore. However, the Goliath North deposit has a sulfur distribution more similar to the “halo” sulfides but a central distribution of sulfides more like Six Mile and Mt Keith, implying that a continuum of deposit types exists. This point is explored further in the following chapter.

It is likely that type 2 ores represent a mixture of sulfide liquid droplets which segregated in roughly cotectic proportions in situ, with a variably abundant component of droplets which were transported and deposited mechanically. Mechanical sulfide deposition combined with in-situ olivine and sulfide liquid accumulation explains the observation of delicate olivine grain size layering related to sulfide abundance (Fig. 24).

### **3.6. Types 4 and 5 Nickel Sulfide Mineralisation**

Numerous examples exist within the deposits of the Yilgarn Craton of other styles of mineralisation: type 5, or tectonically mobilised ores, and type 4, sediment hosted ores (Table 1). In most cases these form small components of larger type 1 orebodies, but in some cases they constitute entire orebodies in their own right.

#### ***3.6.1. Type 4 Mineralisation***

Yilgarn examples of this style all consist of nickeliferous sediment-hosted sulfide layers in direct contact with “normal” type 1 ores, in areas of fairly intense deformation and high metamorphic grade. One example is the F1A shoot at

Perseverance, where the “actinolite sulfide schist” unit is in tectonic juxtaposition with deformed primary type 1 ore, and becomes Ni enriched within a few tens of metres of the contact. Seat et al. (2004) describe a close association between massive and breccia ores and sulfidic metasediments in the Wannaway deposit of the Widgiemooltha Dome area, and report Ni tenors of up to 6% in the “sedimentary” sulfide. Large variations occur in Ni tenor both within remobilised primary massive ore and the lower-grade ore associated with metasediment, a situation broadly similar to that seen at Thompson (Bleeker, 1990).

This relationship could be interpreted in two ways: either in terms of entirely metamorphic diffusional upgrading of pre-existing sedimentary sulfide, or as evidence of a sulfide assimilation process being “caught in the act”. Low-grade ores may have formed at low R-factors in an environment where the process of sediment assimilation is frozen in place during its waning stages, resulting in sulfides mid-way in character between sedimentary and magmatic. However, such a situation has yet to be observed at low metamorphic grades where metamorphic upgrading could be ruled out. Detailed studies of the distribution of other elements such as Cr and Ir are needed to evaluate these alternatives.

### ***3.6.2. Type 5 mineralisation***

This style has already been described in the context of several highly deformed deposits. There is a spectrum of scales, from relatively minor “pinchouts” as described in the section on Kambalda (Fig. 19), to large bodies of entirely shear-hosted ore at Rocky’s Reward, Harmony and Emily Ann which probably initiated as pinchout-like structures. There is clearly a continuum from primary ores with largely primary contacts and limited remobilisation during deformation (Silver Swan), through weakly deformed ores with minor shear-related pinchouts, to completely shear-hosted type 5 orebodies. The simplest explanation in all cases is that massive sulfides have localised the initiation of early thrusting along contacts between ultramafic and country rock units of contrasting competency (Fig. 38). In some cases, the additional complexity of folding has resulted in migration of sulfide bodies into low-strain zones within fold or boudin axes (McQueen, 1987).

### **3.7. Geochemical Signatures of Mineralised Komatiites**

This topic has already been alluded to in the content of various individual orebodies, and of the discussion of evidence pro and con thermal erosion models, and is the subject of detailed discussion by Barnes et al. (2004b) and Lesher et al. (2001b). Previous discussion has centred around the incompatible trace element signatures of particular volcanic facies and sub-facies (previous chapter), and on the existence or otherwise of crustal contamination signatures (section 3.3.4 of this chapter). Two other areas are discussed here: nickel depletion and enrichment due to sulfide accumulation and extraction; and the use of Ni:Cr ratios.

#### ***3.7.1. Nickel backgrounds, enrichments and depletions***

Identifying small traces of magmatic sulfides in komatiites is not always straightforward; S can be mobile during alteration, and the background level of Ni is strongly dependent on the MgO content, as shown in the previous chapter, due to olivine fractionation and accumulation. The percentile field for unmineralised komatiites (Fig. 39), derived from the data shown in the previous chapter, is a reliable basis for the identification of subtle anomalies providing the MgO content is also known.

Figure 39 shows the 80th and 50th percentiles on data density on samples from S-poor komatiites from barren sequences (see Barnes et al., 2004b, for definitions and details), which effectively define the Ni-MgO background for unmineralised systems, based on the extensive global data compilation reported by Barnes et al. (2004b). This is compared with two datasets: all samples from mineralised komatiite sequences in the Yilgarn Craton, and data S-poor samples from Perseverance and Mt Keith. These are the only mineralised localities where there is distinct evidence for Ni depletion, presumably due to previous sulfide liquid extraction, within S-poor rocks.

Significantly, Perseverance also contains markedly nickel-depleted fresh olivine, and has generally low-Ni tenor sulfides. Ni depletion does appear to be a feature of large tonnage, low-R systems, but is not detectable in most mineralised environments.

However, the presence of Ni levels above the “barren” Ni-MgO field is good evidence for the presence of accumulated magmatic sulfide, which is the most significant geochemical indicator of all.

### ***3.7.2. Nickel-Chromium relationships***

The distribution of Ni and Cr in komatiites shows an L-shaped distribution; komatiites high in Cr are typically relatively low in Ni, and vice versa (Barnes and Brand, 1999). This relationship is the result of a number of independent factors. Firstly, both elements have a strongly skewed distribution in komatiites, with a “tail” of high Cr values due to presence of cumulate chromite, and of high Ni due to cumulate sulfide liquid, and a relatively low probability of finding both in the same rock. Secondly, mineralised flow pathways in general, and sulfide-bearing rocks within those pathways in particular, tend to be anomalously Cr-depleted; and thirdly, the most Cr-enriched rocks are typically from fractionated cumulate sequences with low potential for mineralisation. The consequence is that samples from favourable environments, whether mineralised or not, are more likely to have Ni:Cr ratios greater than 1 than other samples. However, if the comparison is restricted to low-S rocks from mineralised and barren flows in favourable environments only, the contrast largely (but not completely) disappears. The small residual difference is due to the presence of anomalously low-Cr samples in some mineralised pathways (Barnes et al., 2004b).

## **3.8. Summary and Exploration Significance**

### ***3.8.1. Exploration implications of the substrate erosion model***

The obvious main implication of the model is that mineralisation is associated with favourable stratigraphic and volcanological features. Favourable host komatiite sequences are voluminous compound flows with well-developed pathways, and the most favourable circumstances occur when these pathways are emplaced above erodable, potentially sulfidic substrates. There are three main varieties of these: felsic or felsic-to-intermediate volcanic sequences containing syngenetic, VMS-style sulfides; platform sequences containing sulfidic iron formations or other stratiform sulfidic sediments; and basaltic sequences with distal, interflow sulfidic sedimentary units as at Kambalda. The critical question from the point of view of exploration is how close these sulfide units need to be to the site of ore formation. At Kambalda, there is an immediate proximal relationship, although this may be misleading: the sulfides in the orebody may have been derived from sediment kilometres away along strike. Such a relationship possibly also exists at Perseverance in the form of the

actinolite-sulfide schist marker unit. However, at Black Swan, whereas there are primary sedimentary or volcanogenic sulfides within the bounding felsic sequence, there are none recognised in the immediate footwall. This question is closely bound up with the issue of transport and deposition mechanisms, and the degree and distance to which entrained magmatic sulfide droplets may be carried in komatiite flows remains essentially unknown.

Identification of favourable host komatiite sequences depends on identifying favourable volcanic architecture. On a regional scale, it is necessary to identify pathway-fed compound flow units (either intrusive or extrusive), whereas at a local and mine-scale it is necessary to identify the pathways themselves. In areas of intense deformation, the second objective becomes much less necessary, as ore localisation becomes a factor of tectonics as much as primary volcanology.

Lithochemistry can play a role in thumb-printing favourable volcanic facies, identifying komatiite liquids which have been extensively contaminated with substrate lithologies, and in favourable cases detecting the signature of chalcophile element depletion due to sulfide liquid extraction. In most cases, though, the presence of accumulated magmatic sulfide, marked by nickel levels above the expected background for the given MgO content of the rock, is the most indicative geochemical anomaly of all, and the only entirely reliable indicator that all the essential processes have been operating.

### ***3.8.2. Structural modification***

Deformation demonstrably plays an important role in localising economically significant bodies of massive ore, particularly in areas of intense deformation at medium and high metamorphic grade. What is less clear is whether deformation has played any role in concentrating or upgrading sulfides, or in localising medium-grade matrix ores which in many cases form the bulk of the economic resource. There is no compelling evidence that it does, and the platinum-group element chemistry of massive, matrix and disseminated ores argues strongly that tectonic upgrading is not an important process, even in areas of severe deformation such as Perseverance where it might be most likely (Barnes et al., 1988b).

The main lesson from detailed structural analysis such as that of Stone and Archibald (2004) is that the presence of sulfides exerts a substantial influence on the subsequent

deformation pattern; the extreme ductility of massive sulfides instigates planes of weakness which localise reverse faults or thrusts with extensive displacements on scales from a few metres to possibly kilometres. Sulfide orebodies influence the development of structures which in turn control the final geometry of the orebodies.

There is an important exploration implication here: if sulfides localise structures, rather than the other way around, then structural analysis is unlikely to be useful large-scale regional exploration tool. On the other hand, detailed understanding of structure is absolutely essential in understanding high-grade massive ore distribution on a local camp scale and within a known orebody.

## References Cited

- Arndt, N.T., 1986, Thermal erosion by komatiites at Kambalda: *Nature*, v. 324, p. 600.
- Baker, D.R., Barnes, S.J., Simon, G. and Bernier, F., 2001, Fluid transport of sulfur and metals between sulfide melt and basaltic melt: *Canadian Mineralogist*, v. 39, p. 537-546.
- Barnes, Sarah-J. and Naldrett, A.J., 1986, Variations in platinum group element concentrations in the Alexo mine komatiite, Abitibi greenstone belt, northern Ontario: *Geological Magazine*, v. 123, p. 515-524.
- Barnes, Sarah-J. and Maier, W.D., 2002, Platinum group element distributions in the Rustenburg Layered Suite of the Bushveld Complex, South Africa, *in* Cabri, L.J., ed., *Canadian Institute of Mining Metallurgy and Petroleum Special Volume 54*, p. 483-506.
- Barnes, Sarah-J., Boyd, R., Nilsson, L.P., Often, M., Pedersen, R.B. and Robins, B., 1988, The use of mantle normalisation and metal ratios in discriminating between the effects of partial melting, crystal fractionation and sulphide segregation on platinum group metals, gold, nickel and copper: examples from Norway, *in* Prichard, H.M., Potts, P.J., Bowles, J.F.W. and Cribbs, S.J., eds., *Elsevier Science Publishers Ltd.*, p. 113-139.
- Barnes, Sarah-J., Makovicky, E., Makovicky, M., Rose-Hansen, J. and Karupmoller, S., 1997a, Partition coefficients for Ni, Cu, Pd, Pt, Rh, and Ir between monosulfide solid solution and sulfide liquid and the formation of compositionally zoned Ni-Cu sulfide bodies by fractional crystallization of sulfide liquid: *Canadian Journal of Earth Sciences*, v. 34, p. 366-374.
- Barnes, Sarah-J., Zientek, M.L. and Severson, M.J., 1997b, Ni, Cu, Au, and Platinum-Group Element contents of sulphides associated with intraplate magmatism - A synthesis: *Canadian Journal of Earth Sciences*, v. 34, p. 337-351.
- Barnes, Stephen J., 1998, Chromite in komatiites, 1. Magmatic controls on crystallization and composition: *Journal of Petrology*, v. 39, p. 1689-1720.

Barnes, Stephen J., 2004, Komatiites and nickel sulfide ores of the Black Swan area, Yilgarn Block, Western Australia. 4. Platinum Group Element distribution in the ores, and genetic implications: *Mineralium Deposita*, v. 39, p. 752-765.

Barnes, Stephen J. and Brand, N.W., 1999, The distribution of Cr, Ni, and chromite in komatiites, and application to exploration for komatiite-hosted nickel sulfide deposits: *Economic Geology*, v. 94, p. 129-132.

Barnes, Stephen J. and Hill, R.E.T., 2000, Metamorphism of komatiite hosted nickel sulfide deposits, *in* Spry, P.G., Marshall, B. and Vokes, F.M., eds., *Society of Economic Geologists*, v. 11, p. 203-216.

Barnes, Stephen J. and Roeder, P.L., 2001, The range of spinel compositions in terrestrial mafic and ultramafic rocks: *Journal of Petrology*, v. 42, p. 2279-2302.

Barnes, Stephen J., Gole, M.J. and Hill, R.E.T., 1988a, The Agnew nickel deposit, Western Australia: part I. Stratigraphy and structure: *Economic Geology*, v. 83, p. 524-536.

Barnes, Stephen J., Gole, M.J. and Hill, R.E.T., 1988b, The Agnew Nickel Deposit, Western Australia: part II. Sulfide geochemistry, with emphasis on the platinum-group elements: *Economic Geology*, v. 83, p. 537-550.

Barnes, Stephen J., Hill, R.E.T. and Gole, M.J., 1988c, The Perseverance ultramafic complex, Western Australia: product of a komatiite lava river: *Journal of Petrology*, v. 29, p. 305-331.

Barnes, Stephen J., Leshner, C.M. and Keays, R.R., 1995, Geochemistry of mineralised and barren komatiites from the Perseverance Nickel Deposit, Western Australia: *Lithos*, v. 34, p. 209-234.

Barnes, Stephen J., Hill, R.E.T. and Evans, N.J., 2004a, Komatiites and nickel sulfide ores of the Black Swan area, Yilgarn Block, Western Australia. 3. Komatiite geochemistry, and implications for ore forming processes: *Mineralium Deposita*, v. 39, p. 729-751.

Barnes, Stephen J., Hill, R.E.T., Perring, C.S. and Dowling, S.E., 2004b, Lithochemical exploration for komatiite-associated Ni-sulfide deposits: strategies and limitations: *Mineralogy and Petrology*, v. 82, p. 259-293.

Barrett, F.M., Binns, R.A. and Groves, D.I., 1977, Structural history and metamorphic modification of Archaean volcanic-type nickel deposits: *Economic Geology*, v. 72, p. 1195-1223.

Beresford, S., Cas, R., Lahaye, Y. and Jane, M., 2002, Facies architecture of an Archean komatiite-hosted Ni-sulphide ore deposit, Victor, Kambalda, Western Australia: implications for komatiite lava emplacement: *Journal of Volcanology and Geothermal Research*, v. 118, p. 57-75.

Beresford, S.W., Cas, R.A.F., Lambert, D.D. and Stone, W.E., 2000, Vesicles in thick komatiite lava flows, Kambalda, Western Australia: *Journal of the Geological Society*, v. 157, p. 11-14.

Beresford, S.W., Stone, W.E., Cas, R.A.F., Lahaye, Y. and Jane, M., 2005, Volcanological controls on the localization of the komatiite-hosted Ni-Cu-(PGE) Coronet deposit, Kambalda, Western Australia: *Economic Geology*, in press.

Binns, R.A. and Groves, D.I., 1976, Iron-nickel partition in metamorphosed olivine-sulphide assemblages from Perseverance, Western Australia: *American Mineralogist*, v. 61, p. 782-787.

Bleeker, W., 1990, New structural-metamorphic constraints on Early Proterozoic oblique collision along the Thompson Nickel Belt, northern Manitoba, Canada, *in* Lewry, J.F. and Stauffer, M.R., eds., *Geological Association of Canada*, v. 37, p. 57-73.

Brown, M.A.N., Jolly, R.J.H., Stone, W. and Coward, M.P., 1999, Nickel ore troughs in Archaean volcanic rocks, Kambalda, Western Australia: indicators of early extension: *Geological Society Special Publication*, v. 155, p. 197-221.

Buck, P.S., Vallance, S.A., Perring, C.S., Hill, R.E. and Barnes, S.J., 1998, Maggie Hays nickel deposit, *in* Berkman, D.A. and Mackenzie, D.H., eds., *Geology of Australian and Papua New Guinean Mineral Deposits: Australian Institute of Mining and Metallurgy*, p. 357-364.

Campbell, I.H., Griffiths, R.W. and Hill, R.I., 1989, Melting in an Archaean mantle plume: heads it's basalts, tails it's komatiites: *Nature*, v. 339, p. 697-699.

Campbell, I.H. and Naldrett, A.J., 1979, The influence of silicate:sulphide ratios on the geochemistry of magmatic sulphides: *Economic Geology*, v. 74, p. 503-505.

Cas, R., Self, S. and Beresford, S., 1999, The behaviour of the fronts of komatiite lavas in medial to distal settings: *Earth and Planetary Science Letters*, v. 172, p. 127-139.

Cas, R.A.F. and Beresford, S.W., 2001, Field characteristics and erosional processes associated with komatiitic lavas: Implications for flow behavior: *Canadian Mineralogist*, v. 39, p. 505-524.

Challis, D.M. and Greeley, R., 1997, Theoretical and experimental modeling of erosion by lava: *Abstracts with Programs - Geological Society of America*, v. 29, p. 419.

Cowden, A., 1985, The effects of metamorphism upon the mineralogy, textures and geochemistry of the Kambalda nickel ores: *Canadian Mineralogist*, v. 23, p. 325.

———, 1988, Emplacement of komatiite lava flows and associated nickel sulphides at Kambalda, Western Australia: *Economic Geology*, v. 83, p. 436-442.

Cowden, A. and Archibald, N.J., 1987, Massive-sulfide fabrics at Kambalda and their relevance to the inferred stability of monosulfide solid-solution: *Canadian Mineralogist*, v. 25, p. 37-50.

Cowden, A., Donaldson, M.J., Naldrett, A.J. and Campbell, I.H., 1986, Platinum group elements and gold in the komatiite-hosted Fe-Ni-Cu sulphide deposits at Kambalda, Western Australia: *Economic Geology*, v. 81, p. 1226-1235.

Cowden, A. and Woolrich, P., 1987, Geochemistry of the Kambalda iron-nickel sulfides: Implications for models of sulfide-silicate partitioning: *Canadian Mineralogist*, v. 25, p. 21-36.

De-Vitry, C., Libby, J.W. and Langworthy, P.J., 1998, Rocky's Reward nickel deposit, *in* Berkman, D.A. and Mackenzie, D.H., eds., *Australian Institute of Mining and Metallurgy*, v. 22, p. 315-320.

Donaldson, M.J., 1981, Redistribution of ore elements during serpentinisation and talc-carbonate alteration of some Archaean dunites, Western Australia: *Economic Geology*, v. 76, p. 1698-1713.

Dowling, S.E., Barnes, S.J., Hill, R.E.T. and Hicks, J., 2004, Komatiites and nickel sulfide ores of the Black Swan area, Yilgarn Block, Western Australia. 2. Geology and genesis of the orebodies: *Mineralium Deposita*, v. 39, p. 707-728.

Doyle, C.D. and Naldrett, A.J., 1987, The oxygen content of 'sulphide' magma and its effect on the partitioning of nickel between coexisting olivine and molten ores: *Economic Geology*, v. 82, p. 208-211.

Duke, J.M., 1986, The Dumont nickel deposit: a genetic model for disseminated magmatic sulphide deposits of komatiitic affinity, *in* Gallacher, M.J., Ixer, R.A., Neary, C.R. and Prichard, H.M., eds., *The Institute of Mining and Metallurgy*, p. 151-160.

Eckstrand, O.R., 1975, The Dumont serpentinite: a model for control of nickeliferous opaque assemblages by alteration products in ultramafic rocks: *Economic Geology*, v. 70, p. 83-201.

Etschmann, B., Pring, A., Putnis, A., Grguric, B.A. and Studer, A., 2004, A kinetic study of the exsolution of pentlandite (Ni,Fe)<sub>9</sub>S<sub>8</sub> from the monosulfide solid solution (Fe,Ni)S: *American Mineralogist*, v. 89, p. 39-50.

Evans, D.M., Cowden, A. and Barrett, R.M., 1989, Deformation and thermal erosion at the Foster nickel deposit, Kambalda St. Ives, Western Australia, *in* Prendergast, M.D. and Jones, M.J., eds., *Institute of Mining and Metallurgy*, p. 215-219.

Ewers, W.E. and Hudson, D.R., 1972, An interpretive study of a nickel-iron sulfide ore intersection, Lunnon Shoot, Kambalda: *Economic Geology*, v. 67, p. 1075-1092.

Farrell, S.P. and Fleet, M.E., 2002, Phase separation in (Fe, Co)<sub>(sub1-x)</sub> S monosulfide solid-solution below 450 degrees C, with consequences for coexisting pyrrhotite and pentlandite in magmatic sulfide deposits: *Canadian Mineralogist*, v. 40, p. 33-46.

Farrow, C.E.G. and Lightfoot, P.C., 2002, Sudbury PGE revisited: towards an integrated model, *in* Cabri, L.J., ed., *Canadian Institute of Mining Metallurgy and Petroleum Special Volume 54*, p. 273-298.

Foster, J.G., Lambert, D.D., Frick, L.R. and Maas, R., 1996, Re-Os isotopic evidence for genesis of Archaean nickel ores from uncontaminated komatiites: *Nature*, v. 382, p. 703-705.

Frost, K.M. and Groves, D.I., 1989a, Magmatic contacts between immiscible sulfide and komatiitic melts; implications for genesis of Kambalda sulfide ores: *Economic Geology*, v. 84, p. 1697-1704.

——, 1989b, Ocellar units at Kambalda: evidence for sediment assimilation by komatiite lavas, *in* Prendergast, M.D. and Jones, M.J., eds., *Institute of Mining and Metallurgy*, p. 207-214.

Frost, K.M., Woodhouse, M. and Pitkajarvi, J.T., 1998, Forrestania nickel deposits, *in* Berkman, D.A. and Mackenzie, D.H., eds., *Australian Institute of Mining and Metallurgy*, v. 22, p. 365-370.

Gillies, S.L., 1993, Physical volcanology of the Katinniq peridotite complex and associated Fe-Ni-Cu-(PGE) mineralization, Cape Smith Belt, Northern Quebec: University of Alabama, Tuscaloosa.

Gole, M.J., Andrews, D.L., Drew, G.J. and Woodhouse, M., 1998, Honeymoon Well nickel deposits, *in* Berkman, D.A. and Mackenzie, D.H., eds., *Geology of Australian and Papua New Guinean Mineral Deposits: Australian Institute of Mining and Metallurgy*, p. 297-306.

Gole, M.J., Barnes, S.J. and Hill, R.E.T., 1987, The role of fluids in the metamorphism of komatiites, Agnew nickel deposit, Western Australia: *Contributions to Mineralogy and Petrology*, v. 96, p. 151-162.

——, 1990, Partial melting and recrystallization of Archaean komatiites by residual heat from rapidly accumulated flows: *Contributions to Mineralogy and Petrology*, v. 105, p. 704-714.

Greeley, R., Fagents, S.A., Harris, R.S., Kadel, S.D., Williams, D.A. and Guest, J.E., 1998, Erosion by flowing lava - field evidence: *Journal of Geophysical Research Solid Earth*, v. 103, p. 27325-27345.

Greeley, R. and Hyde, J.H., 1972, Lava tubes of the Cave Basalt, Mount St. Helens, Washington: *Geological Society of America Bulletin*, v. 83, p. 2397-2418.

Gresham, J.J. and Loftus-Hills, G.D., 1981, The geology of the Kambalda nickel field, Western Australia: *Economic Geology*, v. 76, p. 1373-1416.

Groves, D.I., Barrett, F.M., Binns, R.A. and McQueen, K.G., 1977, Spinel phases associated with metamorphosed volcanic-type iron-nickel sulfide ores from Western Australia: *Economic Geology*, v. 72, p. 1224-1244.

Groves, D.I., Barrett, F.M. and McQueen, K.G., 1979, The relative roles of magmatic segregation, volcanic exhalation and regional metamorphism in the generation of

volcanic-associated nickel ores of Western Australia: *Canadian Mineralogist*, v. 17, p. 319-336.

Groves, D.I. and Batt, W.D., 1984, Spatial and temporal variations of Archaean metallogenic associations in terms of evolution of granitoid-greenstone terrains with particular emphasis on the Western Australian Shield, *in* Kroner, A., Hanson, G.N. and Goodwin, A.M., eds., Springer Verlag, p. 73-98.

Groves, D.I., Hudson, D.R. and Hack, T.B.C., 1974, Modification of iron-nickel sulphides during serpentinisation and talc-carbonate alteration at Black Swan, Western Australia: *Economic Geology*, v. 69, p. 1265-1281.

Groves, D.I., Korhonen, E.A., McNaughton, N.J., Leshner, C.M. and Cowden, A., 1986, Thermal erosion by komatiites at Kambalda, Western Australia and the genesis of nickel ores: *Nature*, v. 319, p. 136-139.

Heath, C., Lahaye, Y., Stone, W.E. and Lambert, D.D., 2001, Origin of variations in nickel tenor along the strike of the Edwards lode nickel sulfide orebody, Kambalda, Western Australia: *Canadian Mineralogist*, v. 39, p. 655-671.

Hill, R.E.T., 1984, Experimental study of phase relations at 600°C in a portion of the Fe-Ni-Cu-S system and its application to natural sulphide assemblages, *in* Buchanan, D.L. and Jones, M.J., eds., Institute of Mining and Metallurgy, p. 14-21.

———, 2001, Komatiite volcanology, volcanological setting and primary geochemical properties of komatiite-associated nickel deposits., *in* Butt, C.R.M., ed., Geological Society, v. 1, p. 365-381.

Hill, R.E.T., Barnes, S.J., Dowling, S.E. and Thordarson, T., 2004, Komatiites and nickel sulfide orebodies of the Black Swan area, Yilgarn Block, Western Australia. 1. Petrology and volcanology of host rocks: *Mineralium Deposita*, v. 39, p. 684-706.

Hill, R.E.T. and Gole, M.J., 1990, Nickel sulphide deposits of the Yilgarn Block, *in* Hughes, F.E., ed., Australian Institute of Mining and Metallurgy, p. 557-559.

Houlé, M.G., Leshner, C.M. and Davis, P.C., 2003, Alexo and Sothman Ni-Cu-(PGE) deposits in the Abitibi Greenstone Belt, Canada: thermochemical erosion and multiple mineralization events. (Abstract). CIM Annual meeting, Montreal Canada, Abstracts, 188-199.

Houlé, M.G., Leshner, C.M., Gibson, H.L. and Sproule, R.A., 2002a, Recent advances in komatiite volcanology in the Abitibi Greenstone Belt, Ontario: Summary of fieldwork and other activities 2002: Ontario Geological Survey Open File Report, v. 6100-7, p. 1-19.

Houlé, M.G., Leshner, C.M., Davis, P.C., Sproule, R.A. , and Montgomery, J.K., 2002b, Thermomechanical Erosion of Footwall Andesites by Komatiites at the Alexo Ni-Cu-(PGE) Deposit, Abitibi Greenston Belt, Canada. (Abstract). 9th International Platinum Symposium, Billings, Montana.

Huang, W.L. and Williams, R.J., 1980, Melting relations of the system Fe-S-Si-O to 32 kb with implications as to the nature of the mantle-core boundary: Lunar and Planetary Science Conference XI, p. 486-488.

Hudson, D.R. and Donaldson, M.J., 1984, Mineralogy of platinum group elements in the Kambalda nickel deposits, Western Australia, *in* Buchanan, D.L. and Jones, M.J., eds., Institute of Mining and Metallurgy, p. 55-61.

Hudson, D.R. and Travis, G.A., 1981, A native nickel - heazlewoodite - ferroan trevorite assemblage from Mount Clifford, Western Australia: *Economic Geology*, v. 76, p. 1686-1697.

Huppert, H.E. and Sparks, R.S.J., 1985, Komatiites I: Eruption and flow: *Journal of Petrology*, v. 26, p. 694-725.

Huppert, H.E., Sparks, R.S.J., Turner, J.S. and Arndt, N.T., 1984, Emplacement and cooling of komatiite lavas: *Nature*, v. 309, p. 19-22.

Kauahikaua, J., Cashman, K.V., Mattox, T.N., Heliker, C.C., Hon, K.A., Mangan, M.T. and Thornber, C.R., 1998, Observations on basaltic lava streams in tubes from Kilauea Volcano, Island of Hawaii: *Journal of Geophysical Research - Solid Earth*, v. 103, p. 27303-27323.

Keays, R.R., 1982, Palladium and iridium in komatiites and associated rocks: application to petrogenetic problems., *in* Arndt, N.T. and Nisbet, E.G., eds., George Allen and Unwin, p. 435-458

———, 1995, The role of komatiitic and picritic magmatism and S-saturation in the formation of ore deposits: *Lithos*, v. 34, p. 1-18.

- Keays, R.R., Ross, J.R. and Woolrich, P., 1981, Precious metals in volcanic peridotite-associated nickel sulfide deposits in Western Australia, II. Distribution within ores and host rocks at Kambalda: *Economic Geology*, v. 76, p. 1645-1674.
- Kerr, R.C., 2001, Thermal erosion by laminar lava flows: *Journal of Geophysical Research-Solid Earth*, v. 106, p. 26453-26465.
- Kullerud, G., Yund, R.A. and Moh, G.H., 1969, Phase relations in the Cu-Fe-S, Cu-Ni-S and Fe-Ni-S systems, *in* Wilson, H.D.B., ed., p. 323-343.
- Lahaye, Y., Barnes, S.J., Frick, L.R. and Lambert, D.D., 2001, Re-Os isotopic study of komatiitic volcanism and magmatic sulfide formation in the southern Abitibi greenstone belt, Ontario, Canada: *Canadian Mineralogist*, v. 39, p. 473-490.
- Lambert, D.D., Foster, J.G., Frick, L.R., Hoatson, D.M. and Purvis, A.C., 1998, Application of the Re-Os isotopic system to the study of Precambrian magmatic sulfide deposits of Western Australia: *Australian Journal of Earth Sciences*, v. 45, p. 265-284.
- Leshner, C.M., 1983, Localisation and genesis of komatiite-associated Fe-Ni-Cu sulfide mineralization of Kambalda, Western Australia: University of Western Australia, Nedlands, Australia. 318 pp.
- , 1985, Evidence for thermal erosion of basalt and hybridisation of komatiite at Kambalda, Western Australia: *Geological Society of America - Abstracts with Programs*, v. 17, p. 642.
- , 1989, Komatiite-associated nickel sulfide deposits, *in* Whitney, J.A. and Naldrett, A.J., eds., *Economic Geology Publishing Company*, v. 4, p. 44-101.
- (Ed.), 1999, Komatiite peridotite-hosted Fe-Ni-Cu-(PGE) sulfide deposits in the Raglan area, Cape Smith Belt, New Québec. *Guidebook Series*, v. 2, Mineral Exploration Research Centre, Laurentian University, Sudbury, 184 pp.
- Leshner, C.M. and Arndt, N.T., 1990, Geochemistry of komatiites at Kambalda, Western Australia: assimilation, crystal fractionation and lava replenishment, *in* Glover, J.E. and Ho, S.E., eds., *Geoconferences (W.A.)*, p. 149-152.

——, 1995, REE and Nd isotope geochemistry, petrogenesis and volcanic evolution of contaminated komatiites at Kambalda, Western Australia: *Lithos*, v. 34, p. 127-157.

Lesher, C.M., Arndt, N.T. and Groves, D.I., 1984, Genesis of komatiite-associated nickel sulphide deposits at Kambalda, Western Australia: a distal volcanic model, *in* Buchanan, D.L. and Jones, M.J., eds., Institute of Mining and Metallurgy, p. 70-80.

Lesher, C.M. and Burnham, O.M., 2001, Multicomponent elemental and isotopic mixing in Ni-Cu-(PGE) ores at Kambalda, Western Australia: *Canadian Mineralogist*, v. 39, p. 421-446.

Lesher, C.M., Burnham, O.M., Keays, R.R., Barnes, S.J. and Hulbert, L., 2001a, Geochemical discrimination of barren and mineralized komatiites associated with magmatic Ni-Cu-(PGE) sulphide deposits: *Canadian Mineralogist*, v. 39, p. 673-696.

——, 2001b, Trace-element geochemistry and petrogenesis of barren and ore-associated komatiites: *Canadian Mineralogist*, v. 39, p. 673-696.

Lesher, C.M. and Campbell, I.H., 1993, Geochemical and fluid dynamic modelling of compositional variations in Archean komatiite-hosted nickel sulfide ores in Western Australia: *Economic Geology*, v. 88, p. 804-816.

Lesher, C.M. and Groves, D.I., 1986, Controls on the formation of komatiite-associated nickel-copper sulfide deposits, *in* Friedrich, G.H., ed., Springer Verlag, p. 63-90.

Lesher, C.M. and Keays, R.R., 1984, Metamorphically and hydrothermally mobilized Fe-Ni-Cu sulphides at Kambalda, Western Australia, *in* Buchanan, D.L. and Jones, M.J., eds., Institute of Mining and Metallurgy, p. 62-69.

Lesher, C.M. and Keays, R.R., 2002, Komatiite-associated Ni-Cu-PGE deposits: geology, mineralogy, geochemistry and genesis, *in* Cabri, L.J., ed., Canadian Institute of Mining Metallurgy and Petroleum Special Volume 54, p. 579-617.

Lesher, C.M. and Stone, W.E., 1996, Exploration geochemistry of komatiites, *in* Wyman, D.A., ed., Geological Association of Canada, v. 12, p. 153-204.

Libby, J.W., Stockman, P.R., Cervoj, K.M., Muir, M.R.K., Whittle, M. and Langworthy, P.J., 1998, Perseverance nickel deposit, *in* Berkman, D.A. and

- Mackenzie, D.H., eds., *Geology of Australian and Papua New Guinean Mineral Deposits: Australian Institute of Mining and Metallurgy*, v. 22, p. 321-328.
- Marston, R.J., 1984, Nickel mineralization in Western Australia: *Geological Survey of Western Australia Mineral Resources Bulletin*, v. 14, p. 271.
- Marston, R.J., Groves, D.I., Hudson, D.R. and Ross, J.R., 1981, Nickel sulfide deposits in Western Australia: a review: *Economic Geology*, v. 76, p. 1330-1363.
- Marston, R.J. and Kay, B.D., 1980, The distribution, petrology and genesis of nickel ores at the Juan complex, Kambalda, Western Australia: *Economic Geology*, v. 75, p. 546-565.
- Mavrogenes, J.A. and O'Neill, H.S.C., 1999, The relative effects of pressure, temperature and oxygen fugacity on the solubility of sulfide in mafic magmas: *Geochimica et Cosmochimica Acta*, v. 63, p. 1173-1180.
- McNaughton, N.J., Frost, K.M. and Groves, D.I., 1988, Ground melting and ocellar komatiites - a lead isotopic study at Kambalda, Western Australia: *Geological Magazine*, v. 125, p. 285-295.
- McQueen, K.G., 1979, Experimental heating and diffusion effects in Fe-Ni sulphide ore from Redross, Western Australia: *Economic Geology*, v. 74, p. 140-148.
- , 1987, Deformation and remobilization in some Western Australian nickel ores: *Ore Geology Reviews*, v. 2, p. 269-286.
- Naldrett, A.J., 1969, A portion of the system Fe-S-O and its application to sulfide ore magmas: *Journal of Petrology*, v. 10, p. 171-202.
- , 1973, Nickel sulphide deposits: their classification and genesis, with special emphasis on deposits of volcanic association: *Canadian Institute of Mining and Metallurgy Bulletin*, v. 66, p. 45-63.
- , 1981, Nickel sulphide deposits - classification, composition and genesis: *Economic Geology*, 75th Anniversary Volume, p. 628-687.
- , 2004. *Magmatic sulfide deposits: Geology, Geochemistry and Exploration*, Heidelberg, Springer. 727 pp.

Naldrett, A.J. and Cabri, L.J., 1976, Ultramafic and related rocks: their classification and genesis with special reference to the concentration of nickel sulfides and platinum group elements: *Economic Geology*, v. 71, p. 1131-1158.

Naldrett, A.J. and Turner, A.R., 1977, The geology and petrogenesis of a greenstone belt and related nickel sulfide mineralisation at Yakabindie, Western Australia: *Precambrian Research*, v. 3, p. 43-103.

Nelson, D.R., 1997, Evolution of the Archaean granite-greenstone terranes of the Eastern Goldfields, Western Australia: SHRIMP U-Pb zircon constraints: *Precambrian Research*, v. 83, p. 57-81.

Perring, C.S., Barnes, S.J. and Hill, R.E.T., 1995, The physical volcanology of komatiite sequences from Forrestania, Southern Cross Province, Western Australia: *Lithos*, v. 34, p. 189-207.

———, 1996, Geochemistry of Archaean komatiites from the Forrestania Greenstone Belt, Western Australia: evidence for supracrustal contamination: *Lithos*, v. 37, p. 181-197.

Pinkerton, H.L., Wilson, L. and Norton, G., 1990, Thermal erosion - observations on terrestrial lava flows and implications for planetary volcanism: *Proceedings of Lunar and Planetary Science Conference*, v. 21, p. 964-965.

Porter, D.J. and McKay, K.G., 1981, The nickel sulphide mineralization and metamorphic setting of the Forrestania area, Western Australia: *Economic Geology*, v. 76, p. 1524-1549.

Prendergast, M.D., 2001, Komatiite-hosted Hunters Road nickel deposit, central Zimbabwe - physical volcanology and sulfide genesis: *Australian Journal of Earth Sciences*, v. 48, p. 681-694.

———, 2003, The nickeliferous Late Archean Reliance komatiitic event in the Zimbabwe craton-magmatic architecture, physical volcanology, and ore genesis: *Economic Geology and the Bulletin of the Society of Economic Geologists*, v. 98, p. 865-891.

Puchtel, I.S., Humayun, M., Campbell, A.J., Sproule, R.A. and Lesher, C.M., 2004, Platinum group element geochemistry of komatiites from the Alexo and Pyke Hill areas, Ontario, Canada: *Geochimica et Cosmochimica Acta*, v. 68, p. 1361-1383.

Redman, B.A. and Keays, R.R., 1985, Archaean basic volcanism in the Eastern Goldfields Province, Yilgarn Block, Western Australia: *Precambrian Research*, v. 30, p. 113-152.

Rice, A. and Moore, J.M., 2001, Physical modeling of the formation of komatiite-hosted nickel deposits and a review of the thermal erosion paradigm: *Canadian Mineralogist*, v. 39, p. 491-503.

Ross, J.R., 1974, Archaean nickel sulphide mineralisation, Lunnon Shoot, Kambalda, Western Australia: University of California, Berkeley.

Ross, J.R. and Hopkins, G.M.F., 1975, Kambalda nickel sulfide deposits, *in* Knight, C.L., ed., *Australian Institute of Mining and Metallurgy*, p. 100-121.

Ross, J.R. and Keays, R.R., 1979, Precious metals in volcanic-type nickel sulphide deposits in Western Australia - I. Relationship with the composition of the ores and their host rocks: *Canadian Mineralogist*, v. 17, p. 417-435.

Seat, Z., Stone, W.E., Mapleson, D.B. and Daddow, B.C., 2004, Tenor variation within komatiite-associated nickel sulphide deposits: insights from the Wannaway Deposit, Widgiemooltha Dome, Western Australia: *Mineralogy and Petrology*, v. 82, p. 317-339.

Seccombe, P.K., Groves, D.I., Marston, R.J. and Barrett, F.M., 1981, Sulfide paragenesis and sulfur mobility in Fe-Cu-Ni sulfide ores at Lunnon and Juan Main Shoots, Kambalda: textural and sulfur isotopic evidence: *Economic Geology*, v. 76, p. 1675-1685.

Shirey, S.B. and Barnes, S.-J., 1995, Os-Nd isotope systematics of ultramafic-mafic magmatism: Cape Smith foldbelt and midcontinental rift system: IGCP Project 336, *Proceedings*, Duluth, MN, p. 175-176

Squire, R.J., Cas, R.A.F., Clout, J.M.F. and Behets, R., 1998, Volcanology of the Archaean Lunnon Basalt and its relevance to nickel sulfide-bearing trough structures at Kambalda, Western Australia: *Australian Journal of Earth Sciences*, v. 45, p. 695-715.

Stone, W.E. and Archibald, N.J., 2004, Structural controls on nickel sulphide ore shoots in Archaean komatiite, Kambalda, WA: the volcanic trough controversy revisited: *Journal of Structural Geology*, v. 26, p. 1173-1194.

Stone, W.E., Beresford, S.W. and Archibald, N.J., 2005, Towards a holistic model for Kambalda-style NiS deposits: Economic Geology, in press.

Stone, W.E., Heydari, M. and Seat, Z., 2004, Nickel tenor variations between Archaean komatiite-associated nickel sulphide deposits, Kambalda ore field, Western Australia: the metamorphic modification model revisited: Mineralogy and Petrology, v. 82, p. 295-316.

Stone, W.E. and Masterman, E.E., 1998, Kambalda nickel deposits, *in* Berkman, D.A. and Mackenzie, D.H., eds., Geology of Australian and Papua New Guinean Mineral Deposits, Australian Institute of Mining and Metallurgy Monograph 22, Carlton, p. 347-356.

Swanson, D.A., 1973, Pahoehoe flows from the 1969-1971 Mauna Ulu eruption, Kilauea Volcano, Hawaii: Geological Society of America Bulletin, v. 84, p. 615-626.

Trofimovs, J., Tait, M.A., Cas, R.A.F., McArthur, A. and Beresford, S.W., 2003, Can the role of thermal erosion in strongly deformed komatiite-Ni-Cu-(PGE) deposits be determined? Perseverance, Agnew-Wiluna Belt, Western Australia: Australian Journal of Earth Sciences, v. 50, p. 199-214.

Usselman, T.M., Hodge, D.S., Naldrett, A.J. and Campbell, I.H., 1979, Physical constraints on the characteristics of nickel-sulfide ore in ultramafic lavas: Canadian Mineralogist, v. 17, p. 361-372.

Wang, Q., Schiotte, L. and Campbell, I.H., 1996, Geochronological constraints on the age of komatiites and nickel mineralisation in the Lake Johnston Greenstone Belt, Yilgarn Craton, Western Australia: Australian Journal of Earth Sciences, v. 43, p. 381-385.

Wendlandt, R.F., 1982, Sulfide saturation of basalt and andesite melts at high pressure: American Mineralogist, v. 67, p. 877-885.

Williams, D.A., Kerr, R.C., Leshner, C.M. and Barnes, S.J., 2001, Analytical/numerical modeling of komatiite lava emplacement and thermal erosion at Perseverance, Western Australia: Journal of Volcanology and Geothermal Research, v. 110, p. 27-55.

Woolrich, P., Cowden, A. and Giorgetta, N.E., 1981, The chemical and mineralogical variations in the nickel mineralization associated with the Kambalda Dome: *Economic Geology*, v. 76, p. 1629-1644.

Origin	Magmatic			Hydrothermal/ metamorphic	Tectonic	
Type	Type 1 “Basal/footwall” or “Contact”	Type 2 “Internal”		Type 3 “Reef”	Type 4	Type 5
Subtype		2a	2b			
Description	Stratiform, sulphide-rich mineralisation at or near the basal contact of komatiite flows or subvolcanic intrusions (1a), also associated veins and stringers (1b).	Disseminated sulphides as composite spheroidal blebs, internally disposed within host unit	Disseminated sulphides interstitial to cumulus silicates, internally disposed within host unit	Stratiform disseminated sulphide-bearing layer within fractionated gabbroic or pyroxenitic cumulates	Ni-enriched metasediment layers, or veins in country rocks, associated with (usually in direct contact with) type 1 mineralisation.	Massive ores in shear zones and/or fold hinges associated with Type 1 ores.
Yilgarn examples	Many – Kambalda, Widgiemooltha camps, see elsewhere in this chapter.	Black Swan, Otter and Durkin shoots (Kambalda), Marriott’s prospect.	Mt Keith Perseverance disseminated zone Yakabindie, David, Goliath	Wiluna	Jan Shoot (Kambalda), Wannaway, Perseverance F1A shoot	Emily Anne, Harmony, Rocky’s Reward, Perseverance 1A, Nepean
Significant global examples	Katinniq (Cape Smith Belt, Quebec), Alexo		Dumont (Abitibi, Quebec)	Delta (Cape Smith), Fred’s Flow, Boston Creek (Abitibi, Ontario)	Thompson (Manitoba)	Thompson

Table 1. Classification of komatiite-hosted nickel sulphide mineralisation types, modified from Lesher and Keays (2002).

Table 2. Pre-mining resource estimates (indicated plus inferred, plus mined ore where appropriate) for Yilgarn komatiite-hosted deposits. Data from a variety of sources including WA Dept. of Industry and Resources, company reports, and the references indicated. Data from Pechenga, Raglan, Noril'sk, Voisey's Bay, Sudbury and Thompson from compilation of Naldrett (2004).

Camp, Area	Name	Tonnage kt	Ni grade %	Contained Ni kt	Ore types
Black Swan	Black Swan disseminated	7,400	0.8	296	2a
	Cygnets	3,100	1.3	40	1
	Silver Swan	400	9.4	38	1
Cosmos	Cosmos	601	7.7	46	1
	Cosmos Deeps	560	8.1	46	1, 5
	Prospero	911	6.6	61	1, 5
Forrestania East	Cosmic Boy	4,000	2.4	96	1
	Digger Rocks	2,400	1.6	39	1
	Diggers South	2,120	1.6	34	1
Forrestania West	Flying Fox	315	5.9	18	1
	New Morning/Daybreak	275	5.6	15	1
Honeymoon Well	Corella	53,500	0.6	332	1 or 2b
	Hannibals	36,100	0.7	253	1 or 2b
	Harrier	43,000	0.6	275	1 or 2b
	Wedgetail	22,900	1.1	247	1
Kambalda - St. Ives - Tramways	Blair	2,240	1.0	22	1
	Carnilya Hill	1,474	3.4	50	1
	Coronet	446	2.9	13	1
	Durkin	3,524	3.2	114	1
	Edwin	141	4.5	6	1
	Fisher	1,651	2.3	38	1
	Foster	2,375	2.6	61	1
	Helmut	203	3.8	8	1
	Hunt-Beta	1,285	2.6	33	1
	Jan	1,074	2.8	30	1, 4
	Ken	468	4.3	20	1
	Lanfranchi	1,404	2.3	32	1
	Long-Victor	5,254	3.7	195	1
	Lunnon	4,539	2.7	123	1
	McMahon	1,186	2.9	34	1
	Otter	7,500	3.5	263	1
	Schmitz	652	4.8	32	1
Skinner	254	5.2	13	1	
Lake Johnston	Emily Anne	1,597	3.8	61	5
	Maggie Hays	12,284	1.5	190	1, 5
Mount Keith	Cliffs Mount Keith	5,500	2.3	127	1
	Mount Keith MKD5	503,000	0.6	2767	2b
Perseverance	Harmony	1,500	3.2	48	5
	Perseverance 1A/matrix	31,300	1.7	516	1, 4, 5
	Eleven Mile Well	544	2.0	11	1
	Perseverance disseminated	89,900	0.6	539	1 or 2b

	Rocky's Reward	6,400	2.2	142	5
Ravensthorpe	RAV 8	206	5.5	11	1
	RAV1 to RAV5	383	1.5	6	1
Scotia	Scotia	1,130	3.1	35	1
Widgiemooltha	Mariners	1,318	2.7	36	1
	Miitel	933	4.1	39	1
	Mount Edwards	955	2.7	26	1
	Nepean	409	2.3	9	1
	North Dordie	190	2.4	5	1
	North Miitel	253	3.9	10	1
	Redross	829	3.9	33	1
	Spargoville	442	2.4	10	1
	Wannaway	4,500	1.2	55	1, 4, 5
	Widgiemooltha 3	83	2.2	2	1
	Widgiemooltha North	10,200	1.0	106	1
	Zabel	979	1.9	19	1
	Windarra	South Windarra	2,561	1.0	26
WINDARRA NICKEL		4,100	1.3	49	1, 4
Yakabindie	Six Mile Well	214,000	0.56	1198	2b
	Goliath North	75,000	0.61	458	2b
Total Yilgarn sulfide resource	(Hronsky and Schodde, this volume)	1,530,120	0.83	12,700	

## Figure captions.

Figure 1. Grade versus tonnage for komatiite-hosted sulphide deposits of the Yilgarn Craton, compared with some other significant global resources. Data from Table 1 for Yilgarn deposits, others from Naldrett (2004).

Figure 2 . Photographs of typical disseminated and matrix ores in relation to the “Billiard Ball Model” of Naldrett (1973). A: Disseminated sulfides (white) interstitial to euhedral olivine grains (serpentinised, black) showing orthocumulate texture, Black Swan deposit. B: Sulfide (pyrrhotite plus pentlandite, white) making continuous interstitial matrix to olivine (serpentinised, black), Katinniq Deposit, Canada.

Figure 3. Reconstructed stratigraphic sections through various type 1 deposits, all to the same scale, vertical scale exaggerated by factor of 2, showing localisation of ore in relation to size and geometry of the host komatiite unit and its footwall rocks.

Figure 4. Phase relations in the Fe-Ni-S system with falling temperature, modified from summary by Naldrett (2004).

Figure 5. Nickel-iron sulphide mineralogy photos. Po=pyrrhotite, pn=pentlandite. A, blocky coarse pn in po, annealed metamorphosed ore.. B, exsolution of pn around po grain boundaries; C and D, fine lamellar pn exsolution “flames” within po.

Figure 6. Skeletal sulfide associated chromite, from the Silver Swan orebody.

Figure 7. Compositions of chromites associated with massive sulphide ores, compared with chromites from interiors of komatiite flows, data from compilation of Barnes and Roeder (2001)

Figure 8. Summary plot of Ni-Cu vs MgO in magmatic sulphide ores from various data sources summarised by Naldrett (2004).

Figure 9. Plots of Ni vs Cu, PGE tenors of type 1 ores associated with various magma types, from various data sources summarised by Naldrett (2004).

Figure 10. Plots showing the theoretical effect of R factor on the composition of magmatic ores.  $Y_i^{sul}$  vs R top, R trends on Ni-Pt, bottom.

Figure 11. Chalcophile element abundances from adjacent massive, matrix and/or disseminated ores from various type 1 deposits. Mantle normalising values: Ni 2000 ppm, Os 4.2 ppb, Ir 4.4 ppb, Ru 5.6 ppb, Rh 1.6 ppb, Pt 8.3 ppb, Pd 4.4 ppb, Au 1.2 ppb, Cu 20 ppm.

Figure 12. Silver Swan orebody, detailed level plans, modified from Dowling et al. (2004).

Figure 13. A-F, Polished drill core slabs showing textures in felsic inclusions (“plumes”, “F”) in pyrrhotite-pentlandite massive sulfide (“S”) in the Silver Swan massive ore shoot. G-H, photomicrographs in transmitted light showing textures in unmelted cores and re-melted and quenched margins of plumes, after Dowling et al (2004).

Figure 14. Polished drill core slabs showing textures developed in hybrid rocks associated with the base of the Black Swan Western Ultramafic Unit. A, B: “back veins” of ocellar-textured dacite/komatiite hybrid melt cutting olivine cumulate; C: disaggregated fragments of dacite and olivine cumulate in a hybrid komatiite/dacite groundmass; D: angular fragments of sulfide (S)-bearing dacite in hybridised dacite-komatiite melt with relic feldspar phenocrysts.

Figure 15. Geology of the Kambalda-Tramways corridor, modified from Stone and Masterman (1998).

Figure 16. Geology of the Kambalda Dome showing horizontal projection of the main sulphide ore shoots, modified from Stone and Masterman (1998).

Figure 17. 3D schematic block diagram of “typical” Kambalda Dome ore shoot, modified from Stone and Masterman (1998).

Figure 18. Kambalda troughs – re-entrant troughs. Lunnon contact and hanging wall ore cross from Stone and Archibald, isometric projection of Lunnon Shoot from Gresham and Loftus-Hills (1981).

Figure 19. Detailed maps of basalt-ore-basalt pinchouts, Juan Shoot, from Stone and Archibald (2004) and Lesher (1989).

Figure 20. Kambalda troughs – minor troughs or planar contacts. Durkin Shoot cross section (above) and 3D model of Lanfranchi Shoot (below) from Stone and Archibald (2004).

Figure 21. Geological map of the Honeymoon well area, and cross sections through Corella and Wedgetail, from Gole et al. (1998)

Figure 22. Perseverance level plans, modified from Libby et al. (1998) and Barnes et al. (1988a)

Figure 23. Plot of  $\text{Al}_2\text{O}_3$  vs  $\text{TiO}_2$  in metakomatiites from the Perseverance Ultramafic Complex.

Figure 24. Perseverance sulphide textures. A, B, C – typical textures of bladed metamorphic olivine in po-pn matrix, “triangular ore”. D, thin section of heavily disseminated olivine sulphide cumulate with granular recrystallised olivine surrounding igneous olivine, scale bar 1 mm. E, polished slab of disseminated “cloud sulphide” showing finer grained olivine in area of interstitial sulphide. F, skeletal chromite near massive ore – komatiite contact. G, igneous-textured matrix ore in drill core, showing irregular patches and veinlets of semi-massive ore.

Figure 25. Distribution of matrix and disseminated ores in the Perseverance dunite, after Libby et al. (1998)

Figure 26. Rocky's Reward cross section, after De Vitry et al. (1998).

Figure 27. Digger Rocks geological plan and pre-deformation reconstruction, from Perring et al. (1995.)

Figure 28. Geochemistry of komatiites from the eastern and western komatiite belts, Forrestania from Perring et al. (1996).

Figure 29. Maggie Hays map and sections through northern and southern zones, after Buck et al. (1998).

Figure 30. Emily Ann cross section after Buck et al. (1998).

Figure 31. Substrate erosion cartoon from Hill (2001).

Figure 32. Distribution of nickel grade in last metre interval immediately above basalt contact, for drill intersections where sediment is absent, and where there is more than 50cm of sediment present at the contact, for intersections from the eastern side of the Kambalda dome, from unpublished WMC Kambalda database.

Figure 33. Stope in Lunnon Shoot Hanging Wall ore, showing massive sulfide overlying "spinifex ore". Photo by Mike Donaldson.

Figure 34. Ratio:ratio trace element plots for mineralised vs barren komatiites, after Barnes et al. (2004b).

Figure 35. The distribution of contaminated and uncontaminated komatiite as a function of flow regime and substrate type, after Lesher et al. (2001a).

Figure 36. Black Swan globular ore textures: sulphide blebs (with partial replacement by carbonate) enclosed within segregation vesicles.

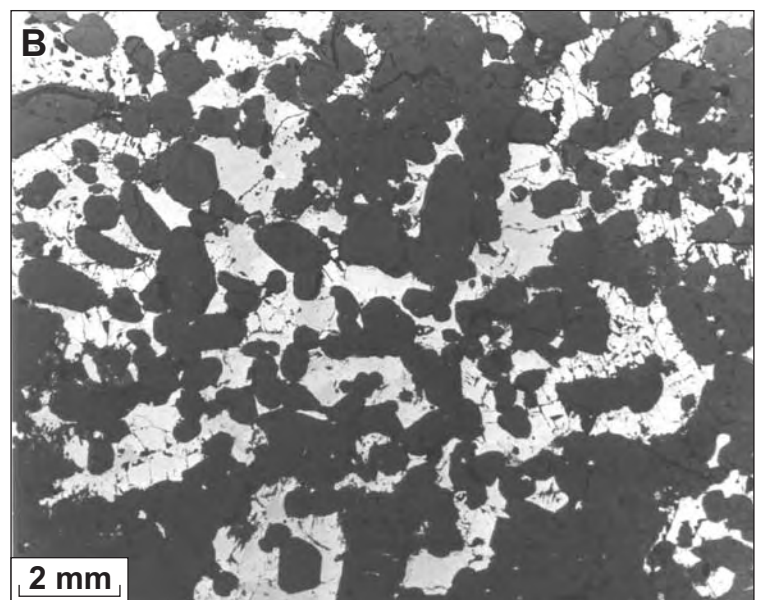
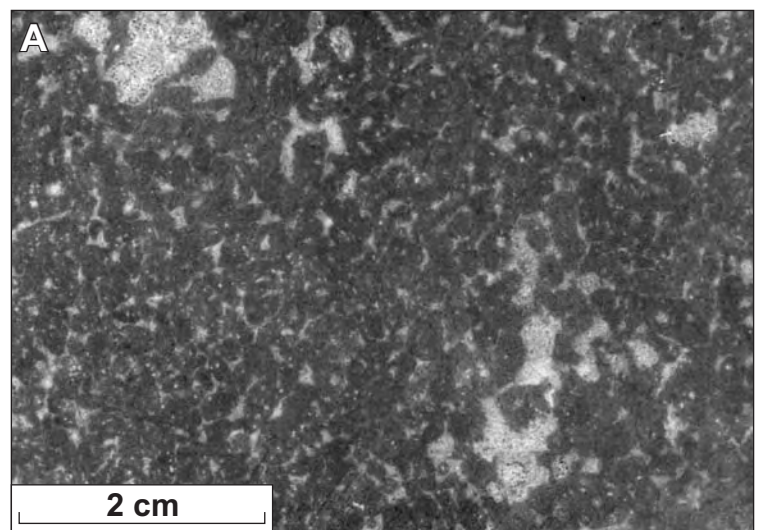
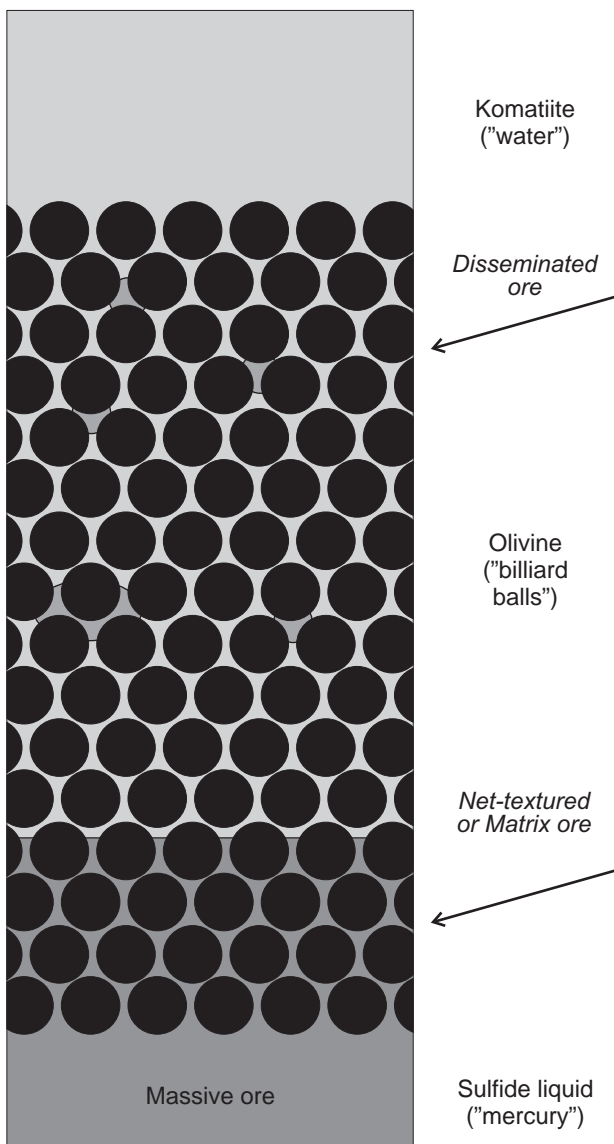
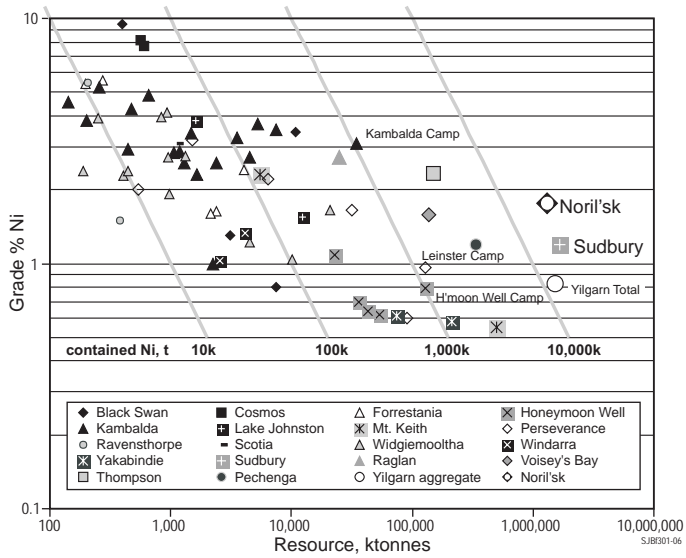
Figure 37. Histogram of S distribution (in weight %) in disseminated-sulphide bearing olivine cumulates (>40% MgO, <0.05% TiO<sub>2</sub>, >0.01% S). A: disseminated sulfide halo around basal type 1 sulfide accumulations: Perseverance, Maggie Hays, Digger Rocks. B,C,D: Six Mile deposit at Yakabindie, Mt Keith Ultramafic Complex MKD5

orebody; and Goliath North deposit at Yakabindie, data from WMC Resources assay database, with acknowledgment to Ben Grguric and WMC staff.

Figure 38. Cartoon illustrating the continuum of deformation between embayment-hosted ores through development of pinchouts to shear-hosted and totally dislocated type 5 orebodies.

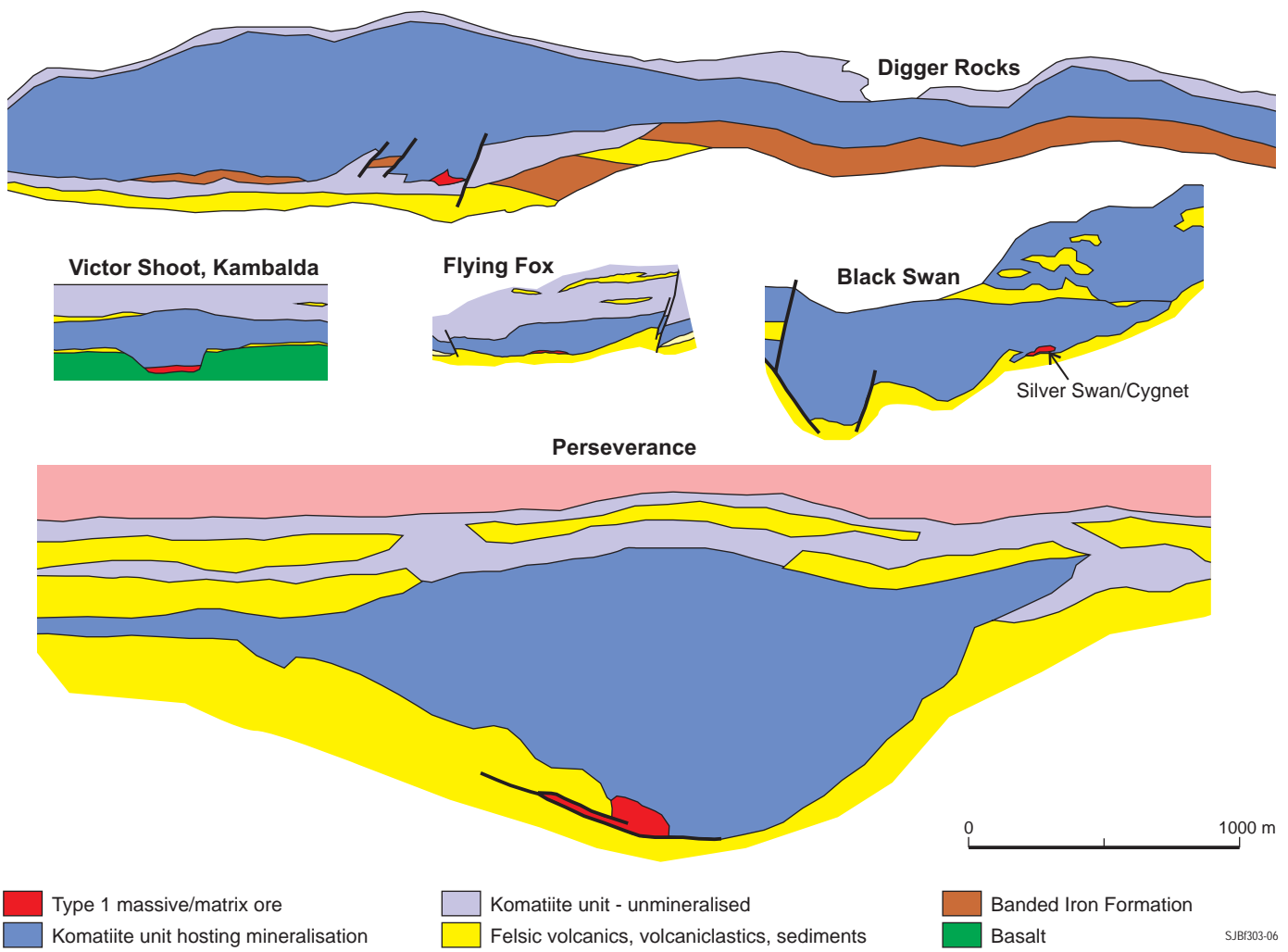
Figure 39. Ni-MgO backgrounds for unmineralised komatiites, shown as contours on data density, with data for low-S samples from Perseverance and the Mt Keith Dunite, and for all samples from other mineralised sequences.

Figure 40. Data density contour plots of Cr vs Ni in global komatiite database, from Barnes et al (2004b). Heavy outlines include densest 50% of data, lighter lines 90%. comparison of mineralised vs unmineralised sequences, all facies, including S-rich samples. B: same comparison, sulfide-free samples only, compound cumulate-rich flow facies and dunitic compound sheet facies (CCF, DCSF) only.



SJB302-06

Figure(s) 1,2



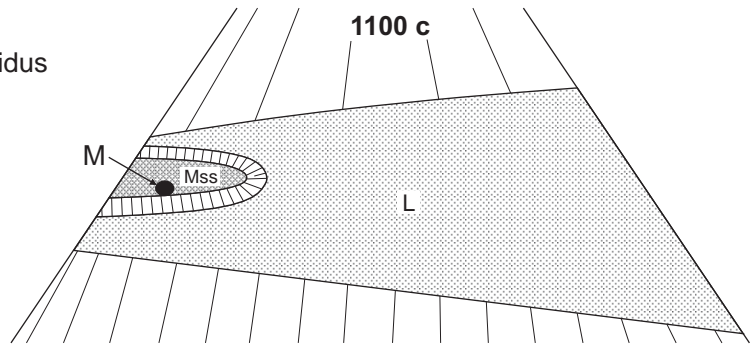
Figure(s) 3

1150°C

Initial crystallisation of MSS on sulfide liquidus

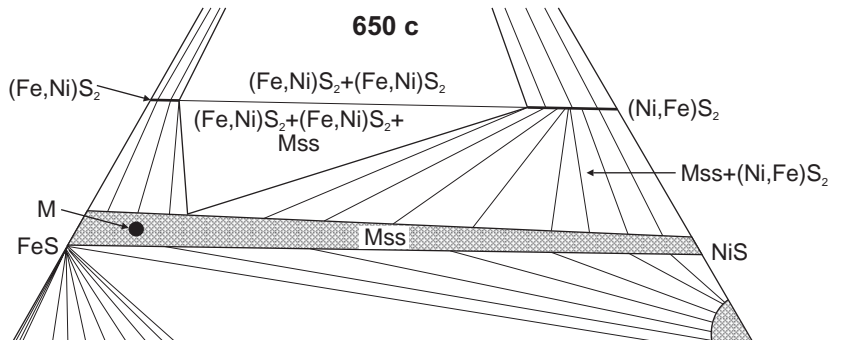
1000-1050°C

Final solidification of sulfide liquid.  
Fractionated Cu-rich residuum  
may persist to ~ 850C



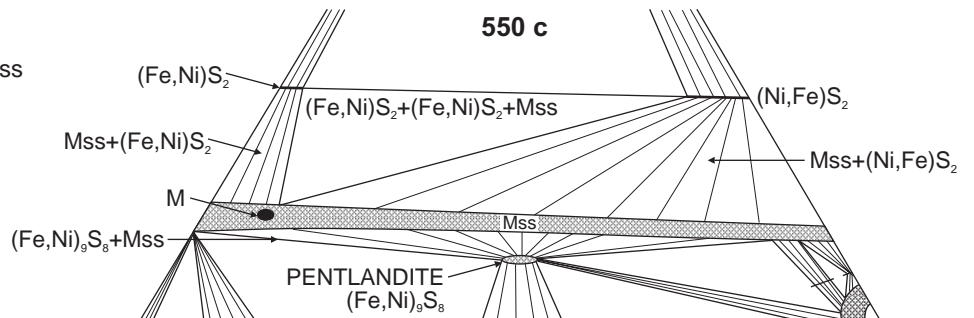
1000-600°C

Homogenous Mss  
(plus Cu-Fe-S phase)



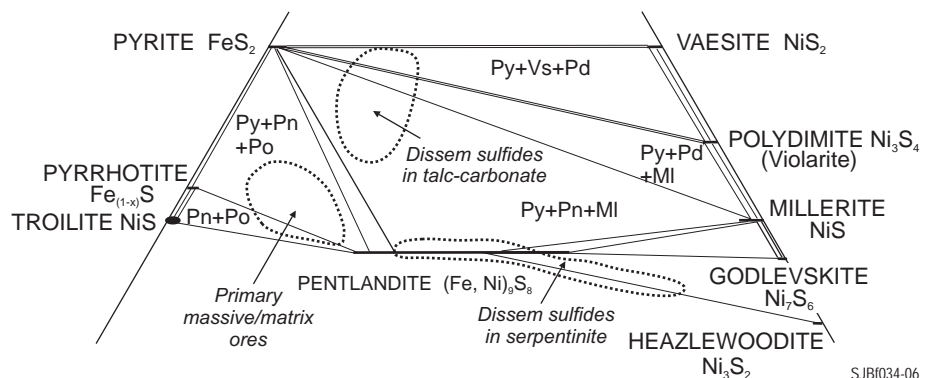
600-300°C

Pentlandite stable, exsolves from Mss  
with falling temperature.



300°C and below

Pentlandite-pyrite assemblage stable,  
secondary assemblages involving  
millerite, vaesite etc develop during  
low-T alteration.

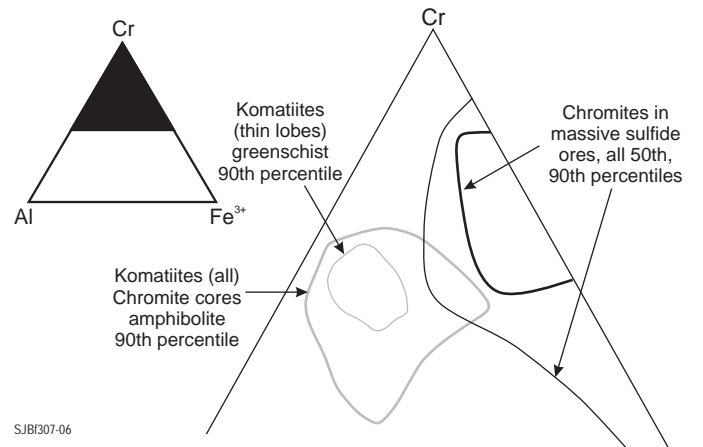
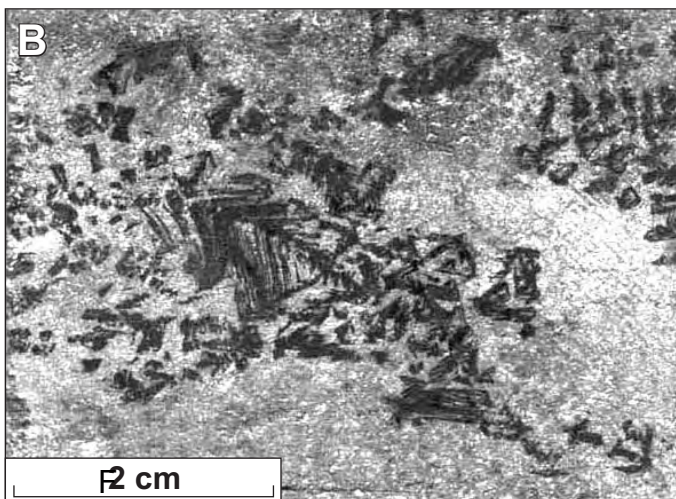
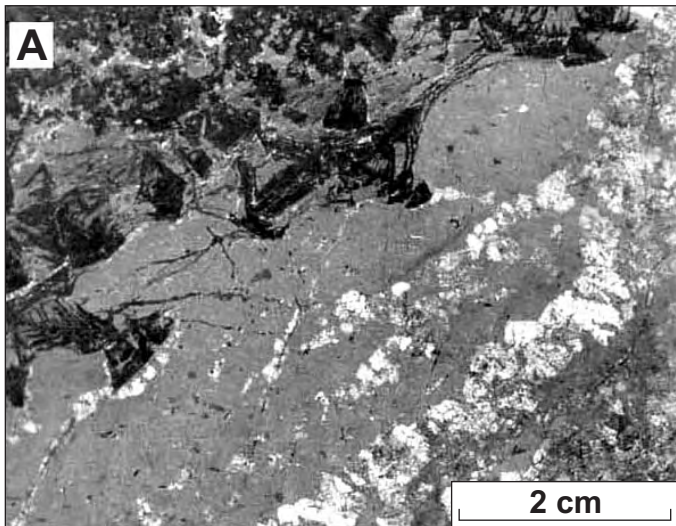
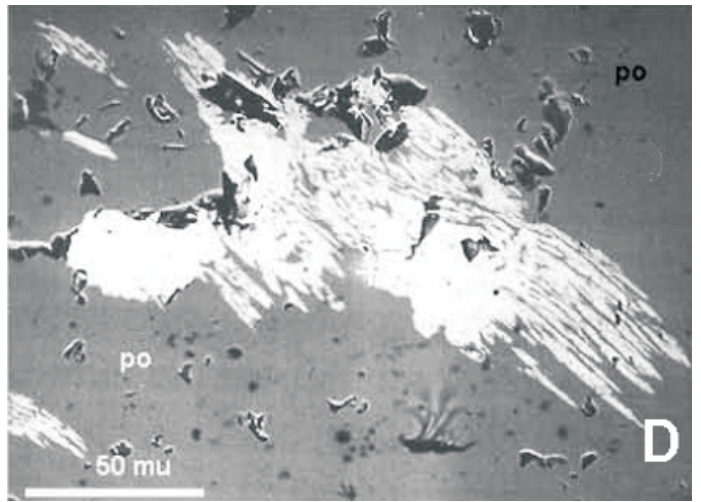
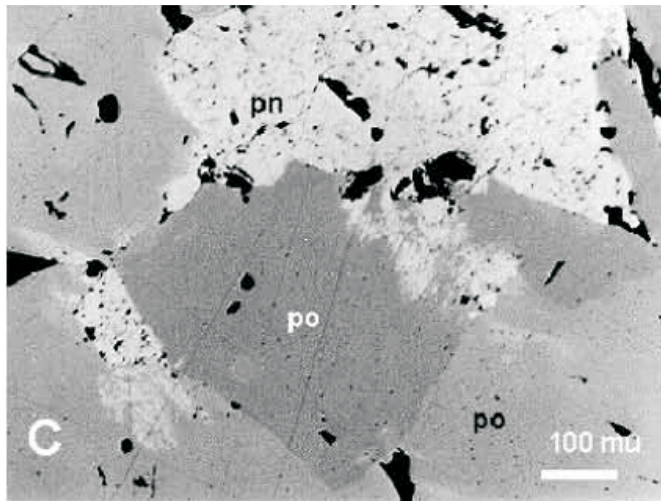
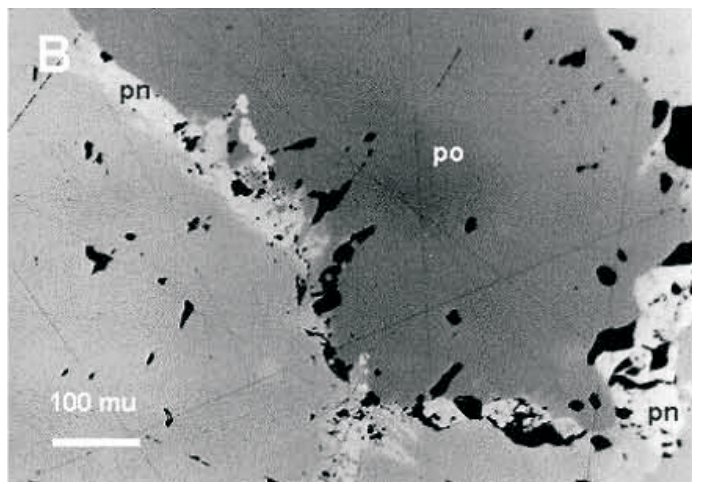
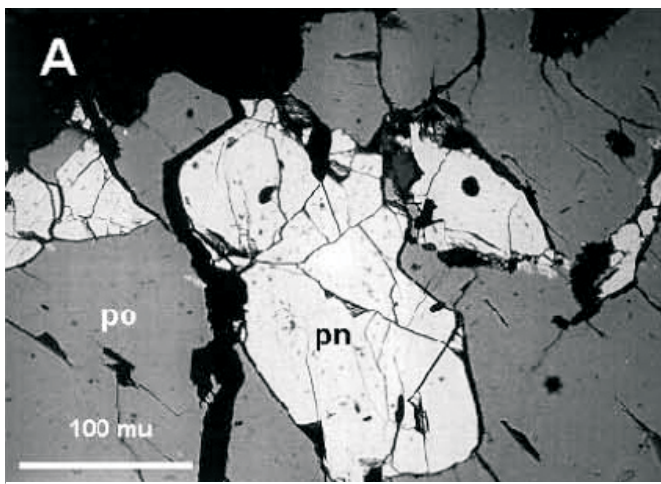


25°C and below

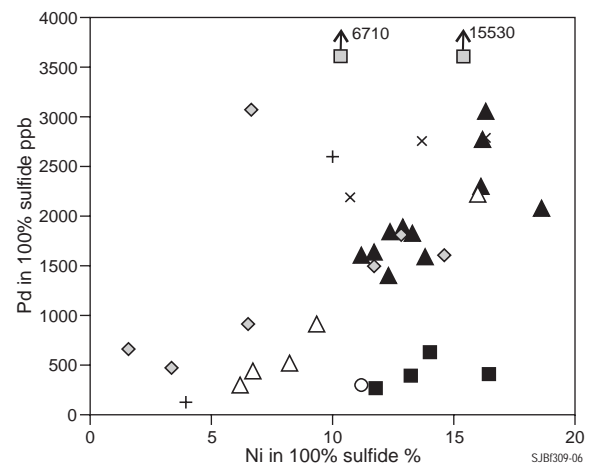
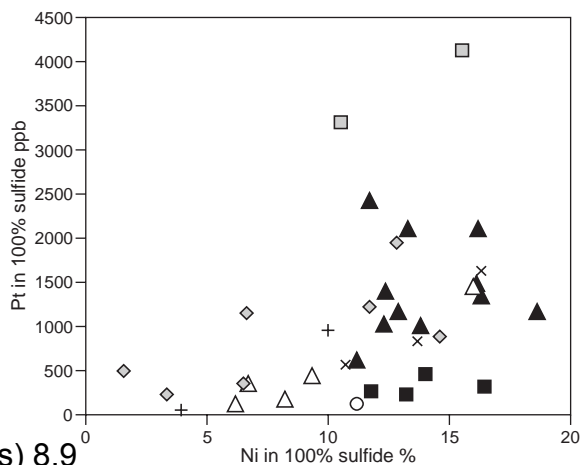
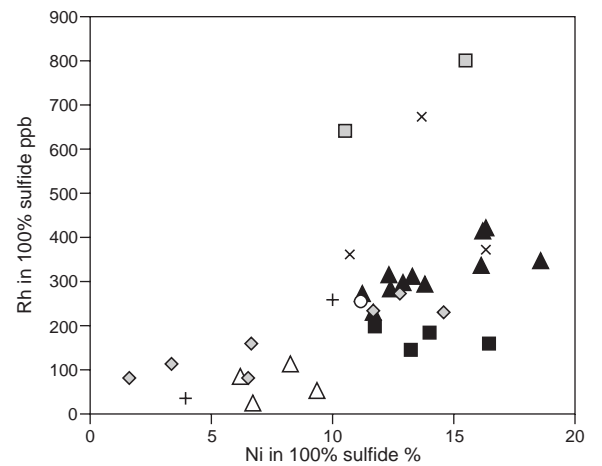
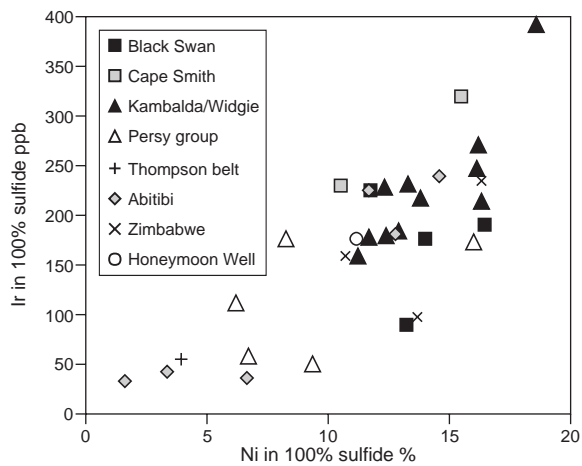
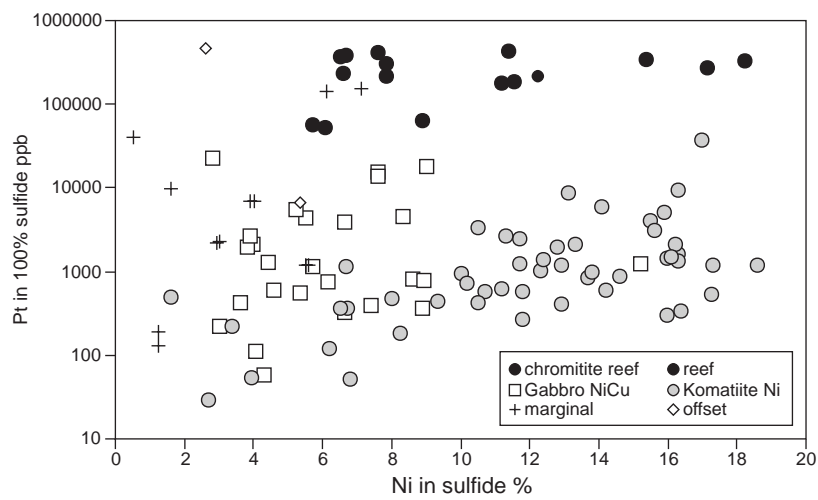
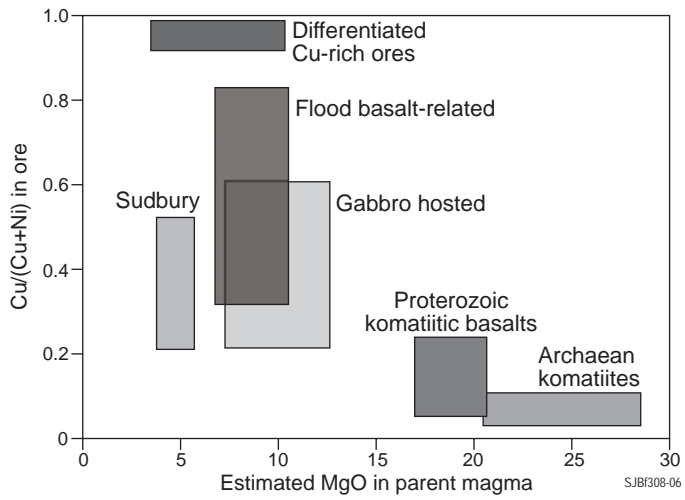
Supergene violarite-pyrite assemblage  
develops during deep weathering

SJB1034-06

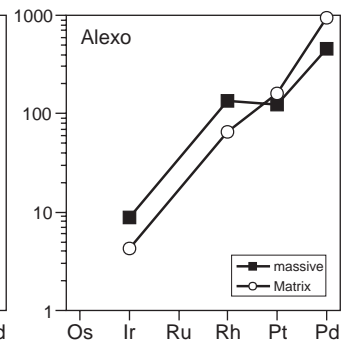
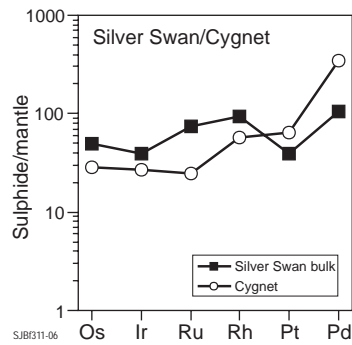
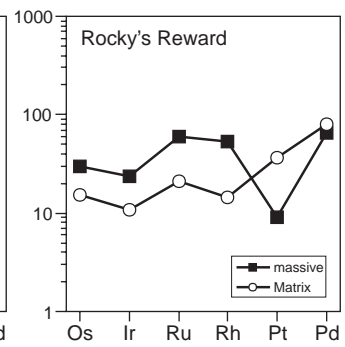
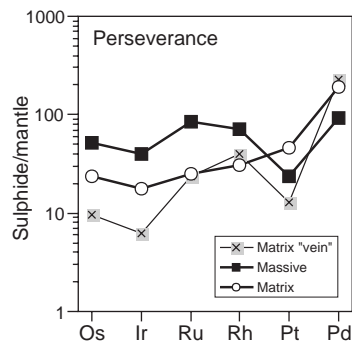
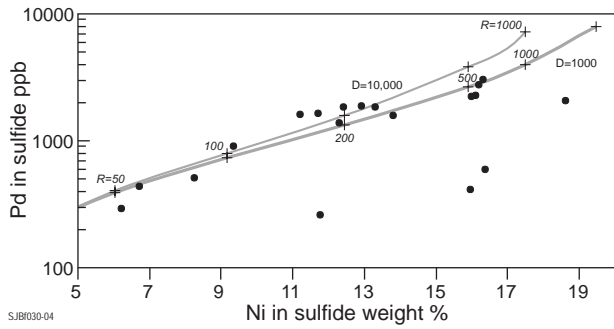
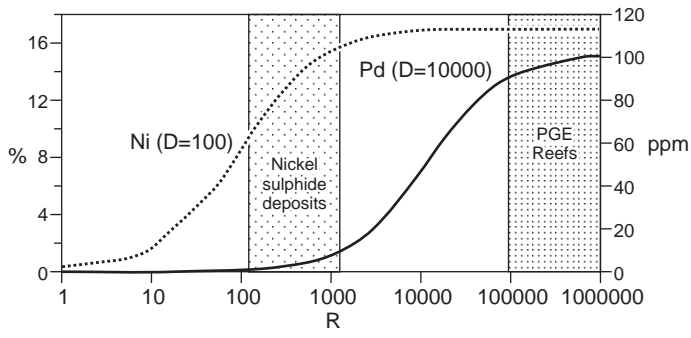
Figure(s) 4



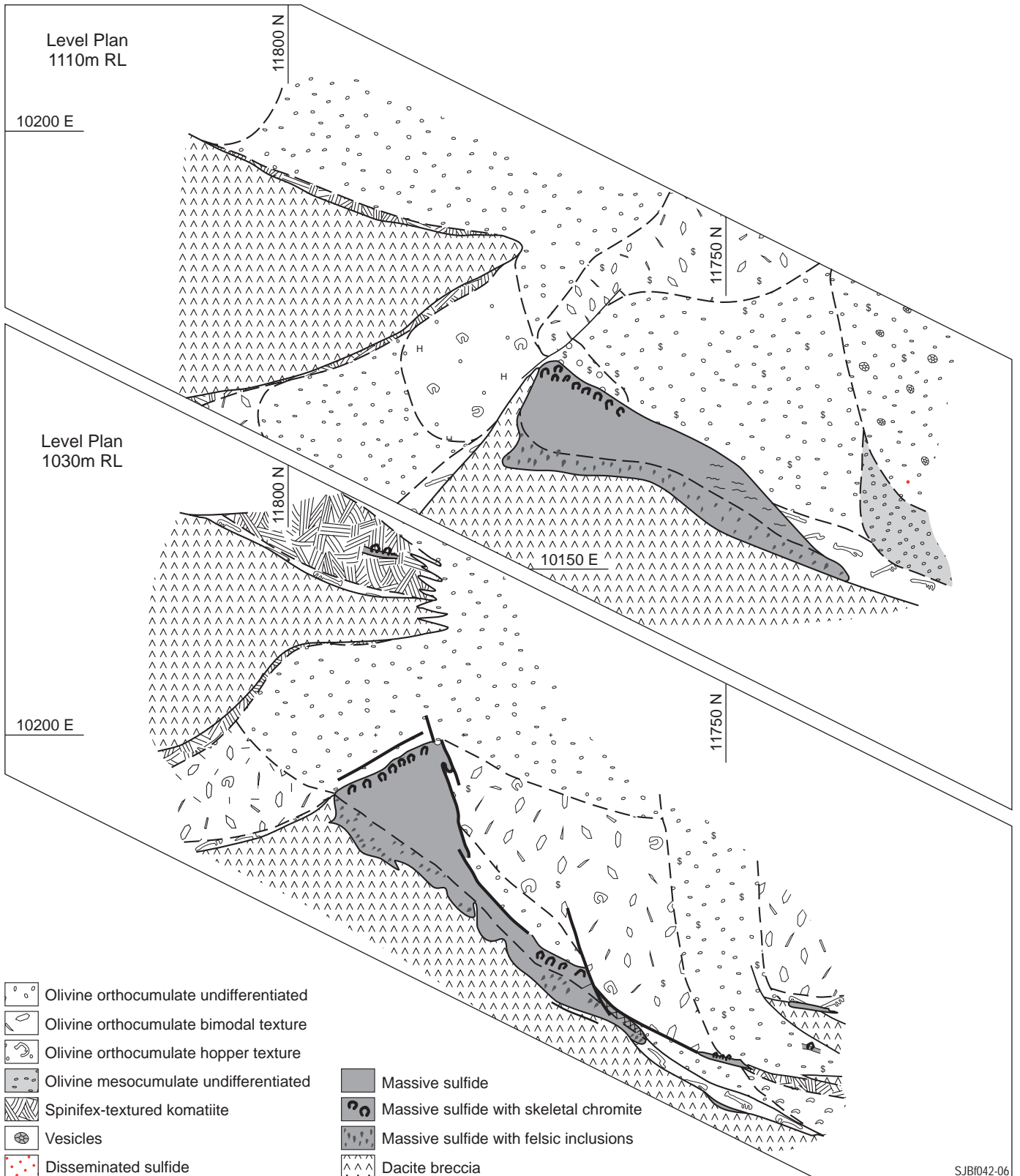
Figure(s) 5,6,7



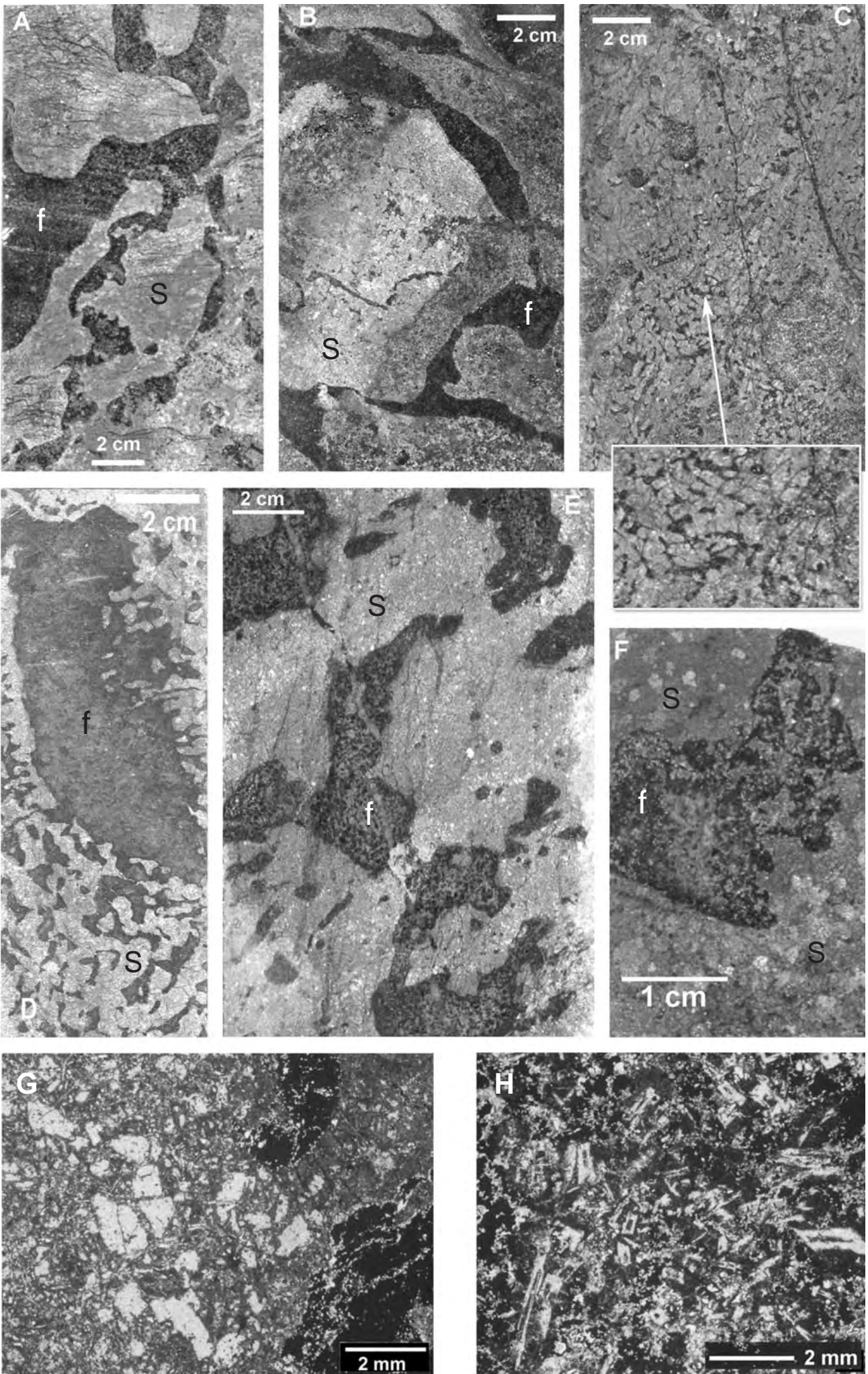
Figure(s) 8,9



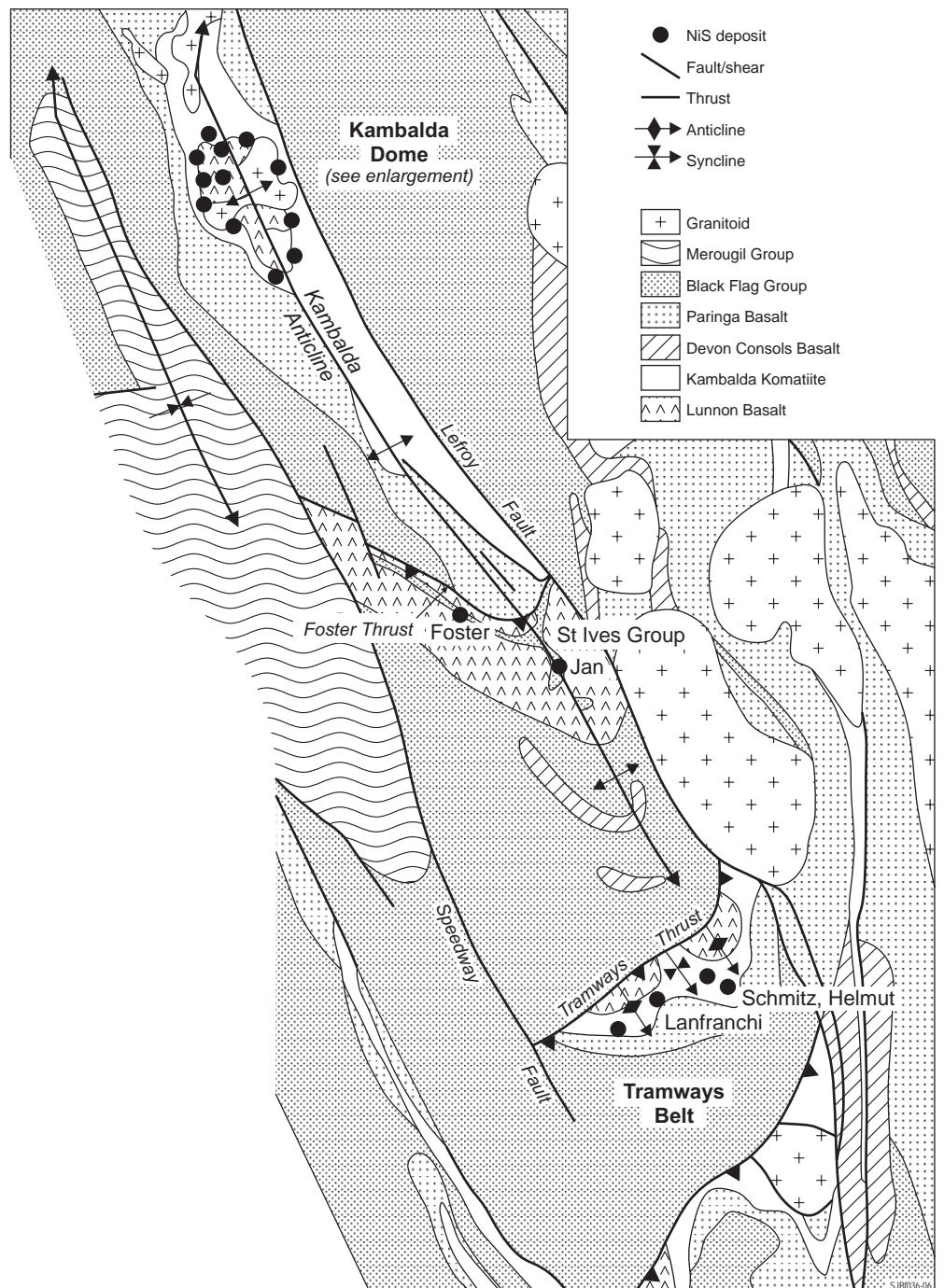
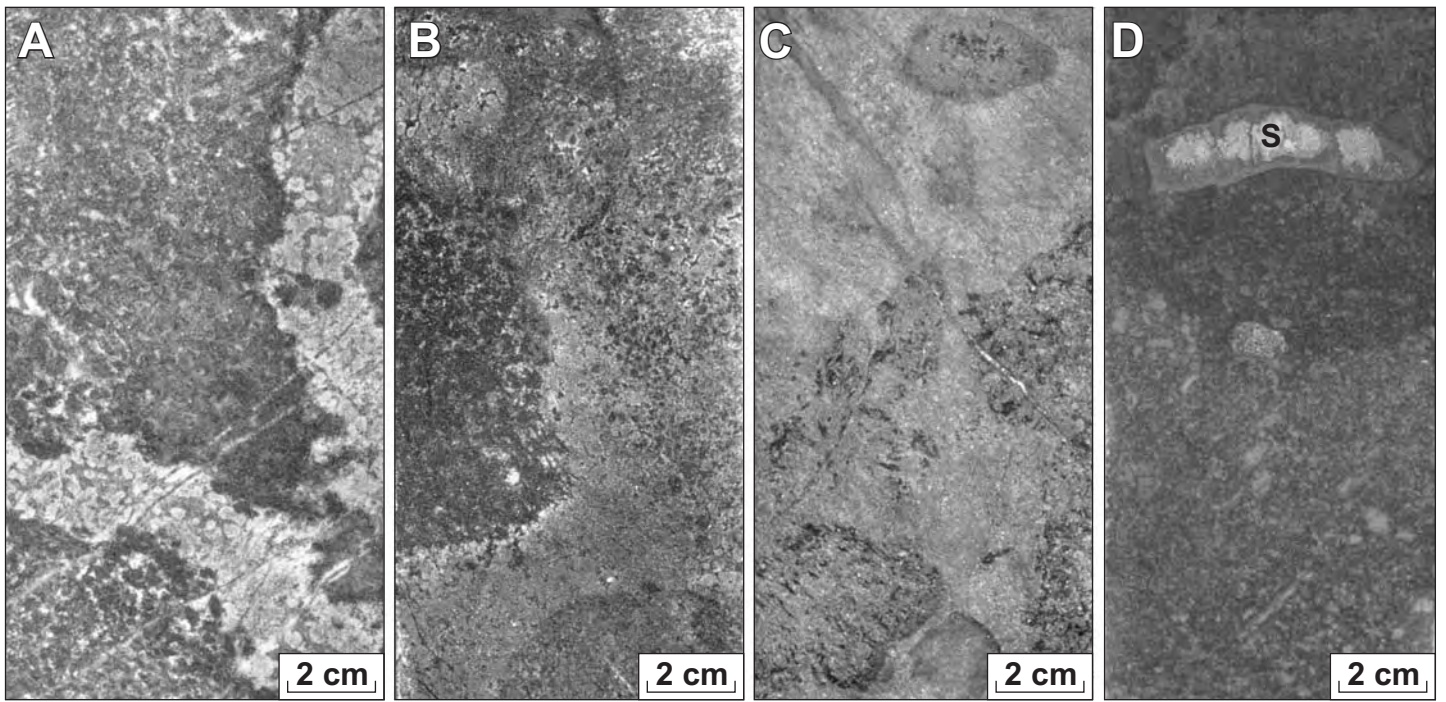
Figure(s) 10, 11



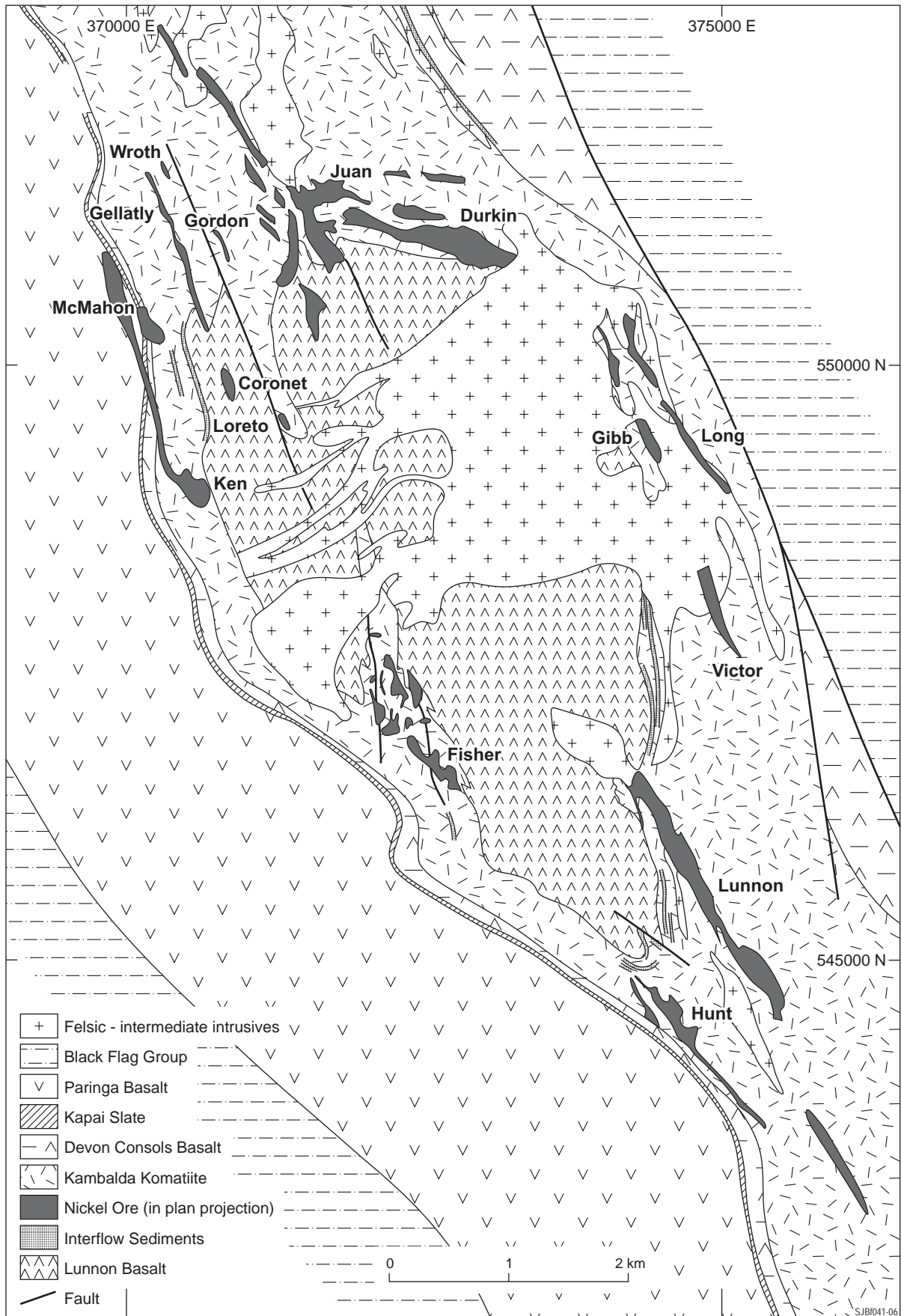
Figure(s) 12



Figure(s) 13

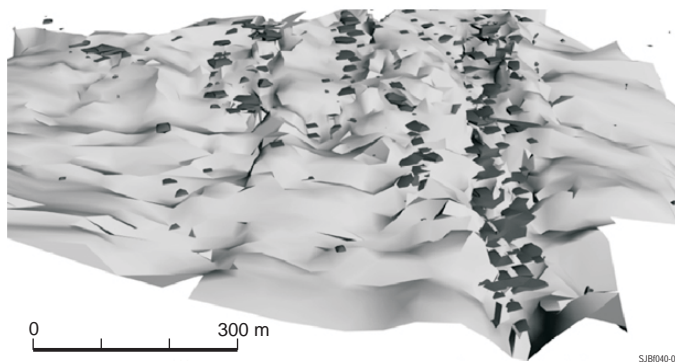
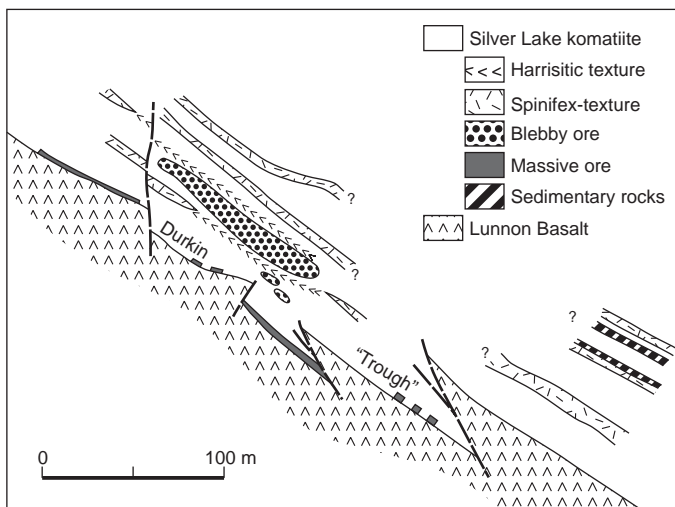
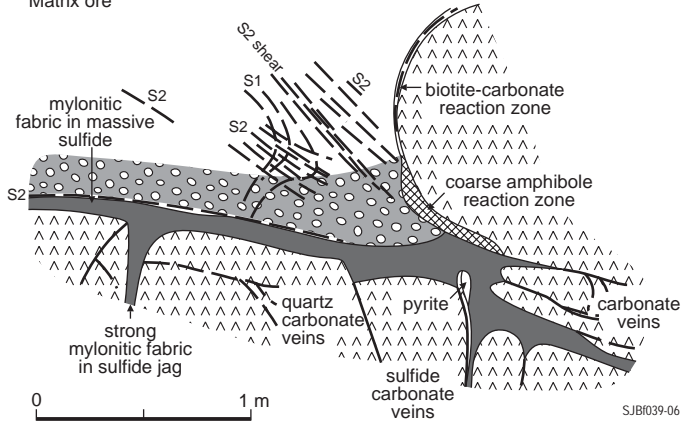
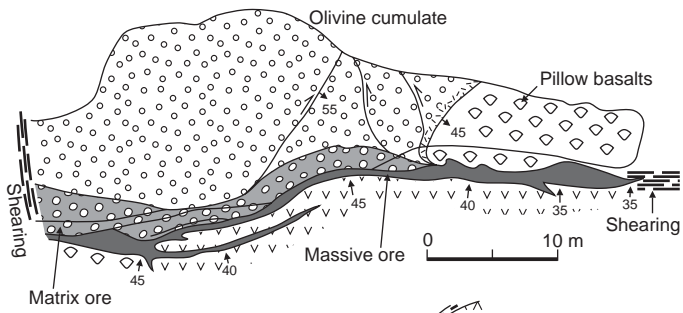


Figure(s) 14, 15

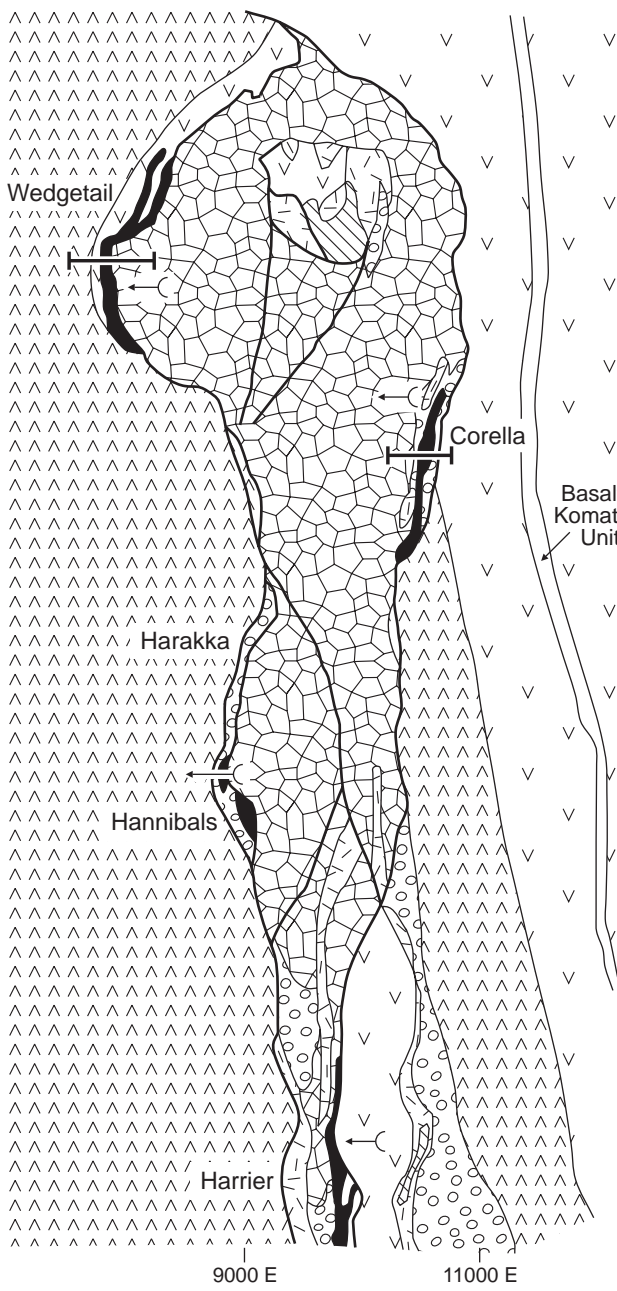


Figure(s) 16

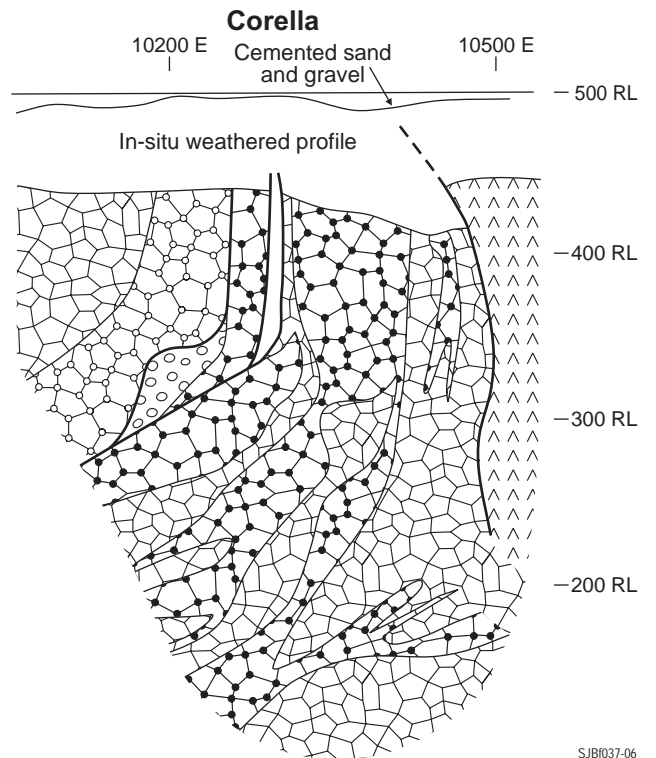
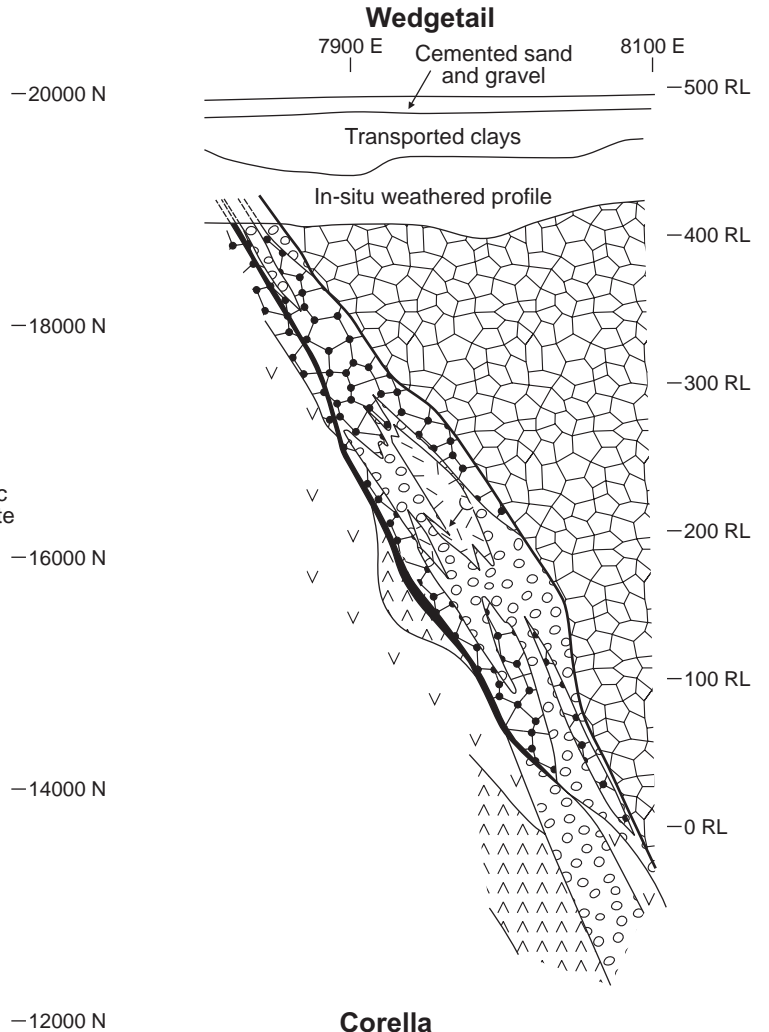




Figure(s) 19, 20



-  Massive / heavily disseminated sulfide
-  Pyroxene cumulate
-  Thin, differentiated komatiite flow units
-  Olivine orthocumulate
-  Olivine adcumulate
-  Olivine mesocumulate and adcumulate
-  Olivine-sulfide orthocumulate to adcumulate
-  Felsic volcanic and volcanoclastic rocks
-  Basalt



SJB037-06

Figure(s) 21



Figure(s) 22

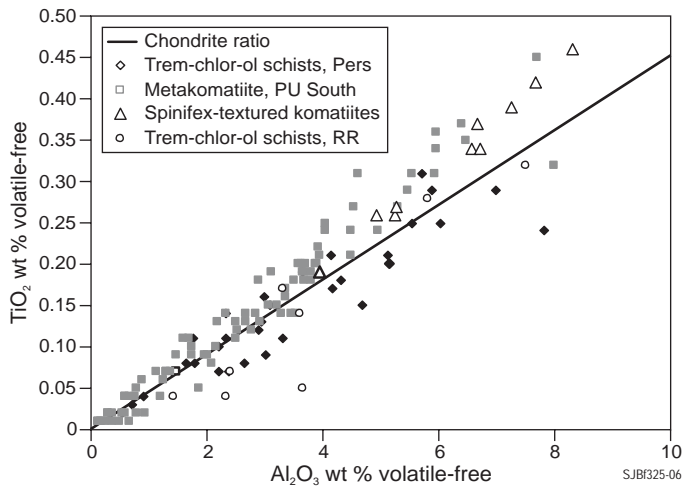


Fig 23

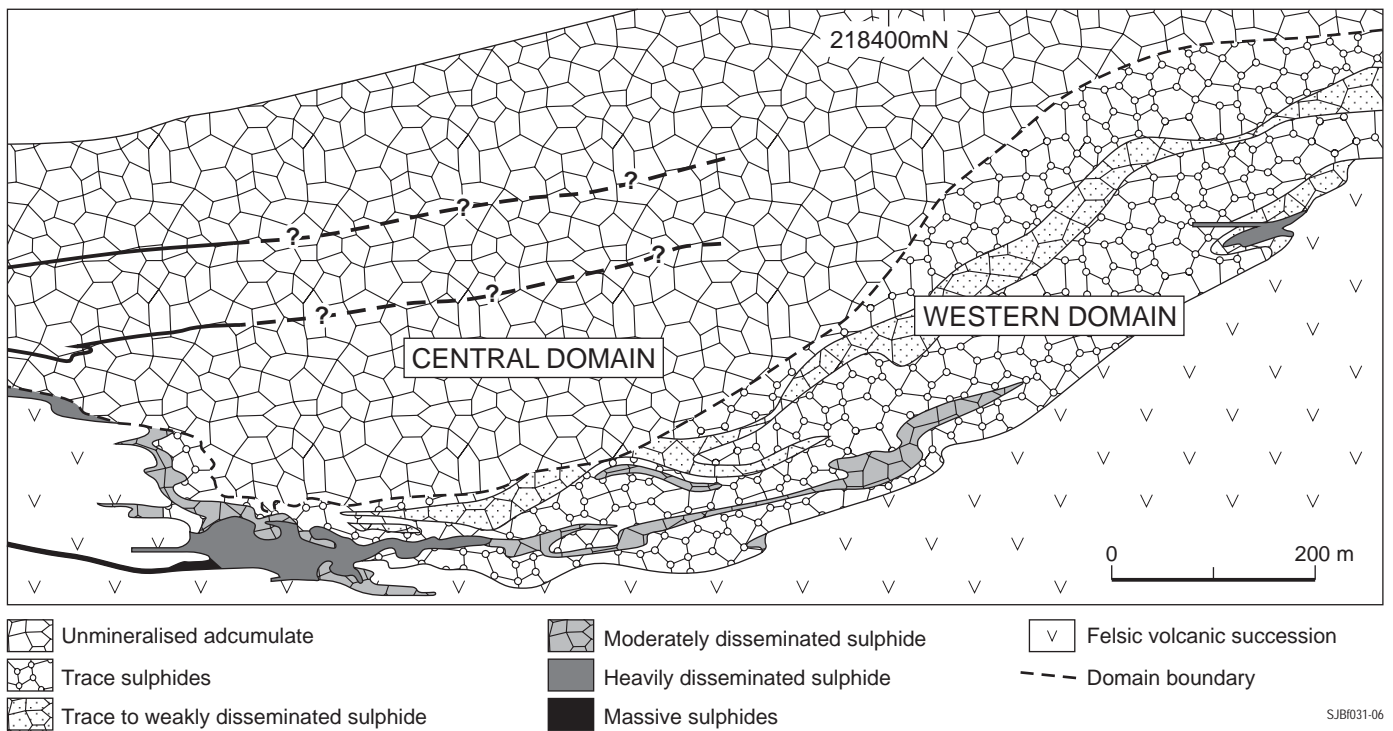
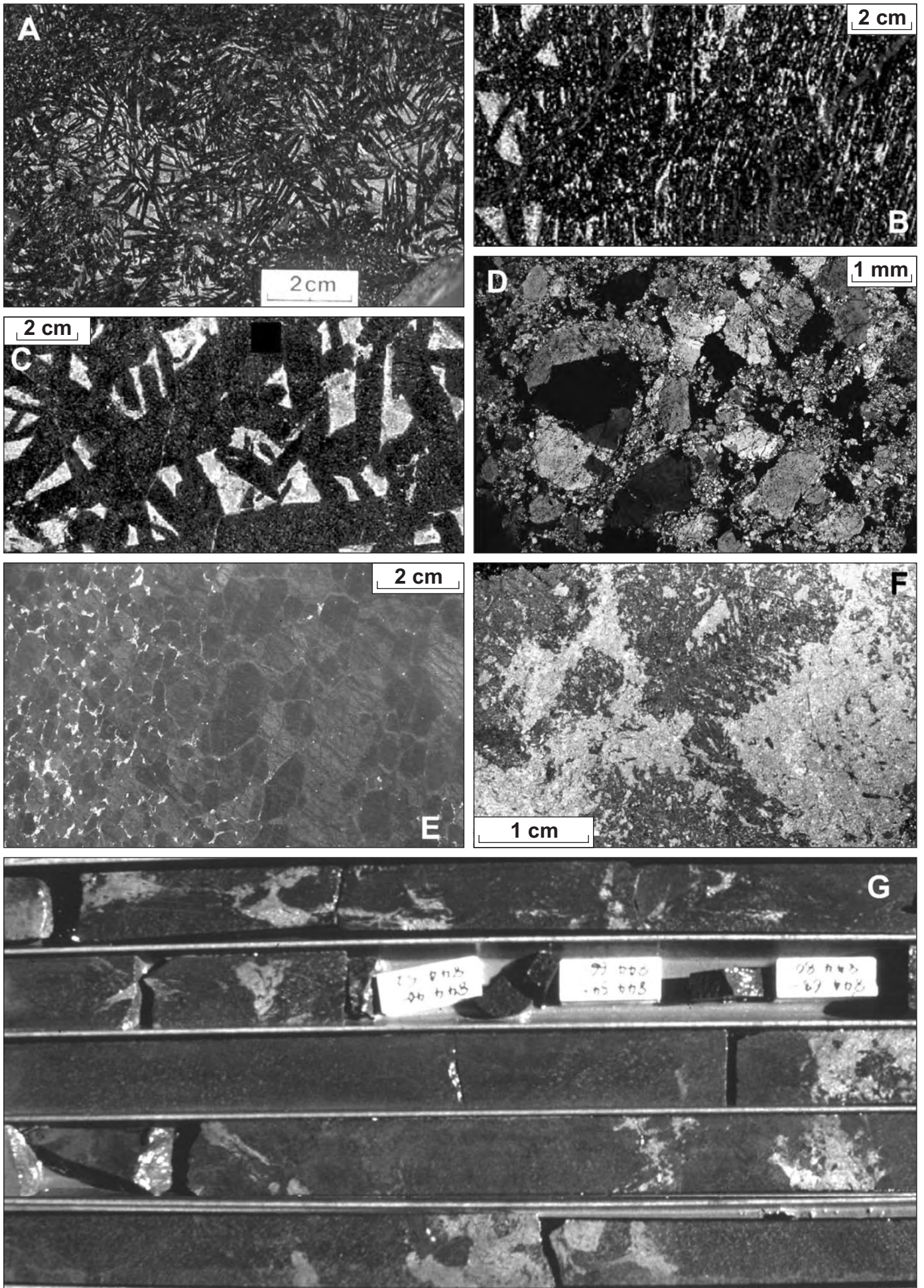
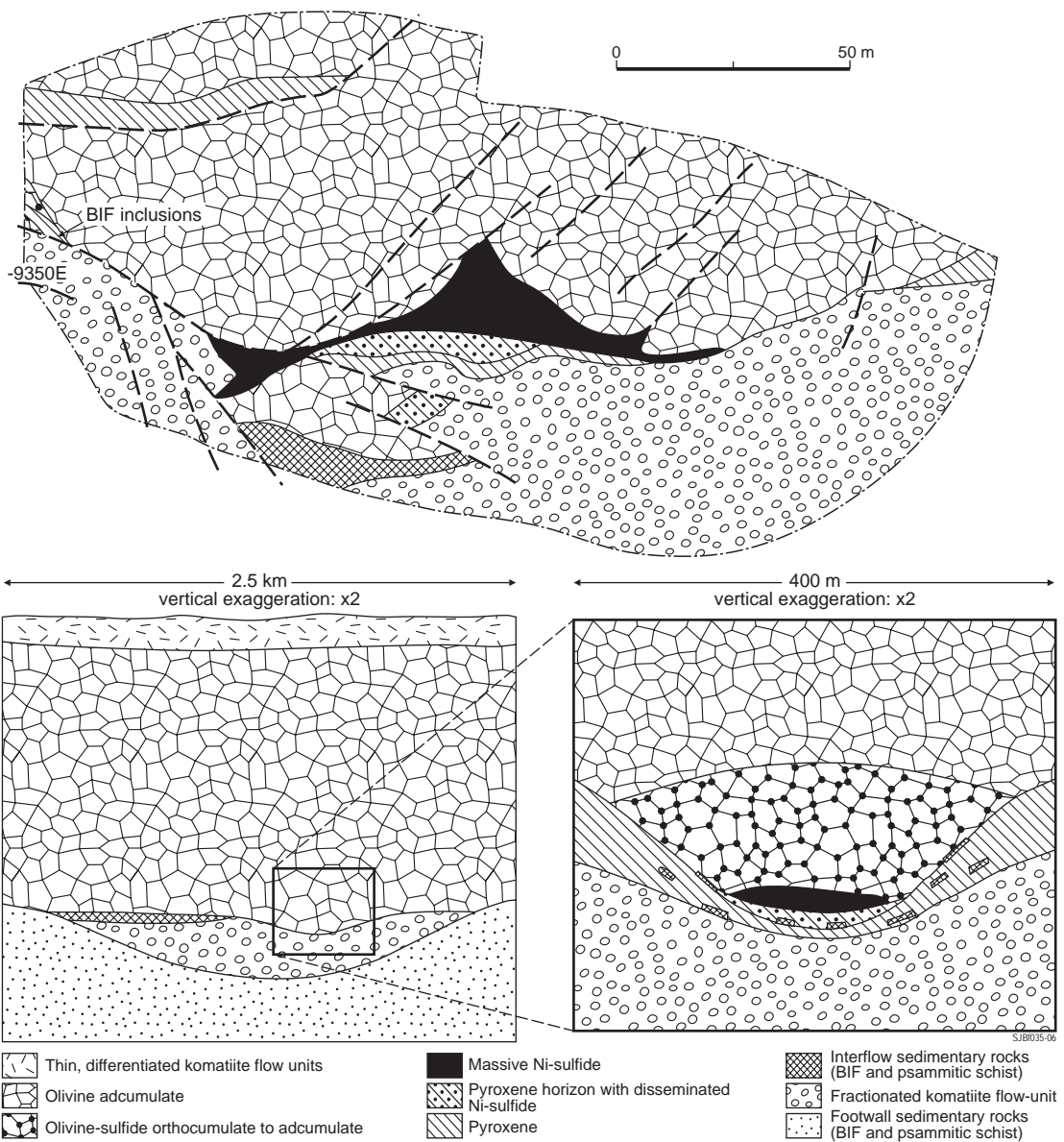
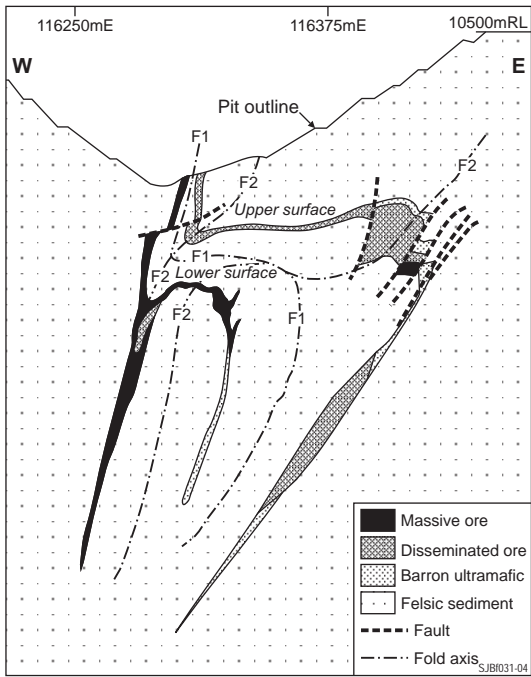


Fig 25



Figure(s) 24



Figure(s) 26, 27

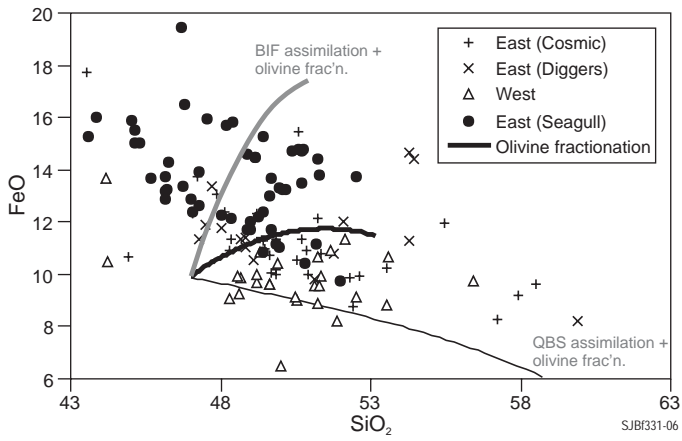


Fig 28

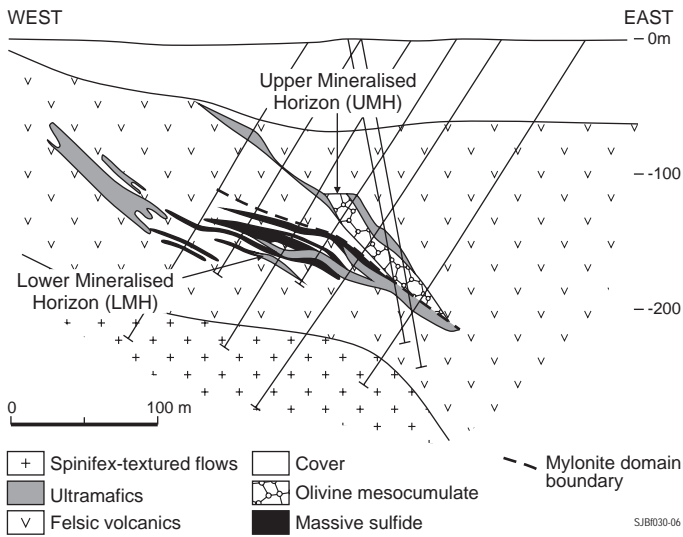


Fig 30

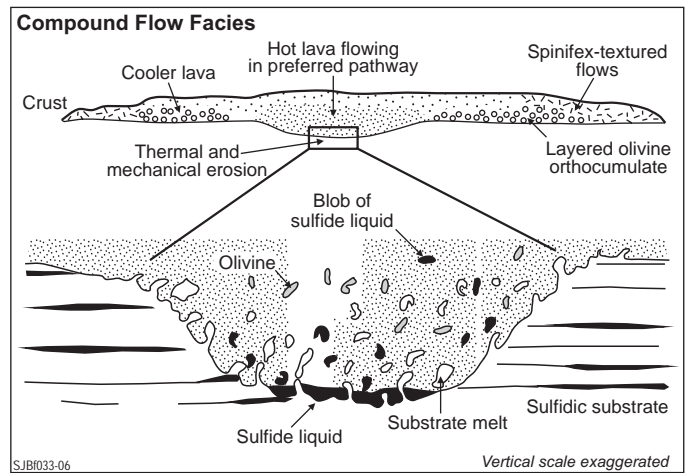


Fig 31

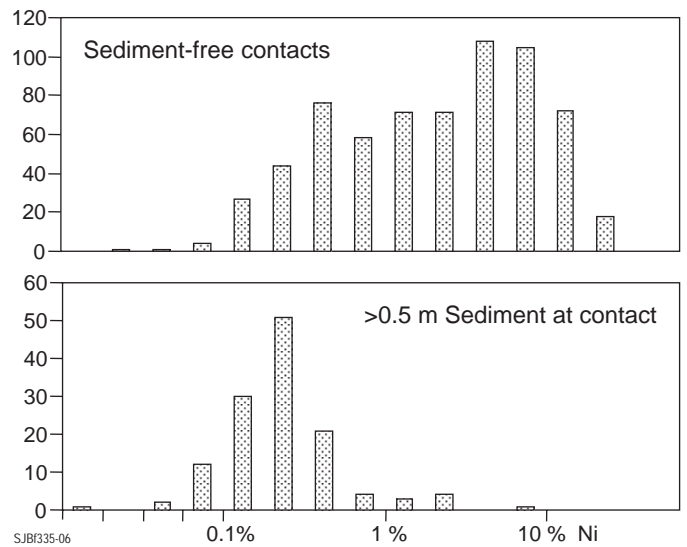
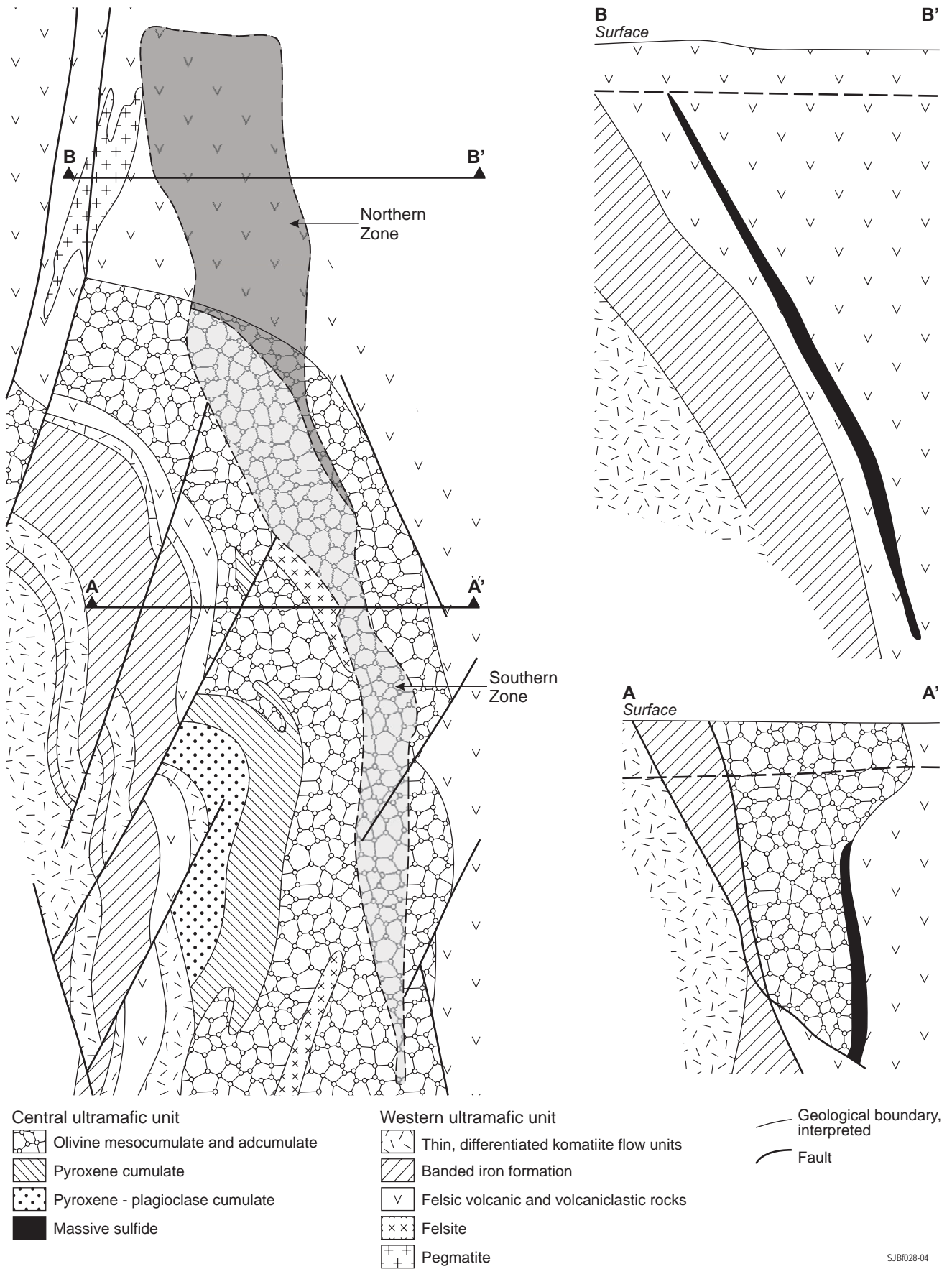


Fig 32

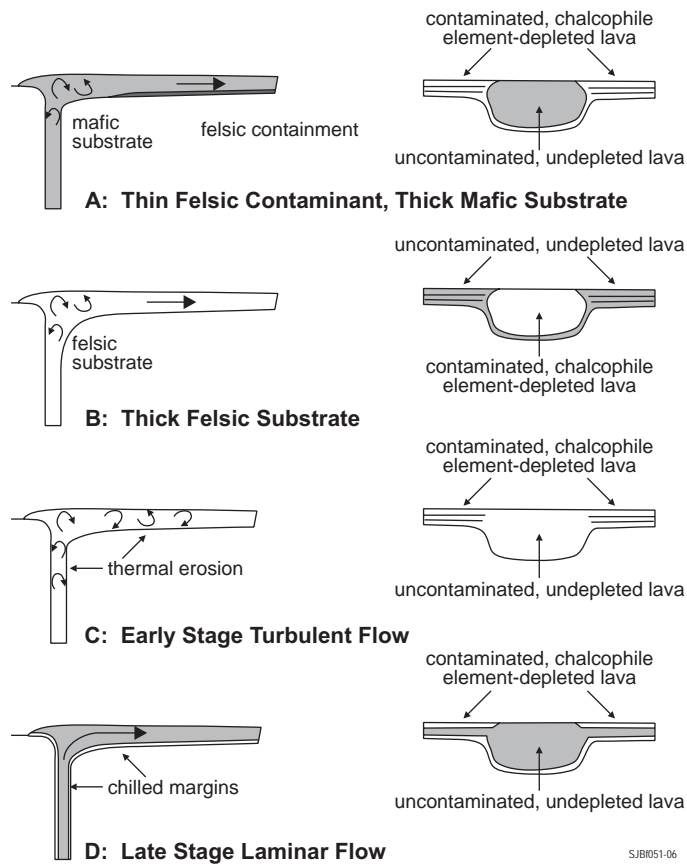
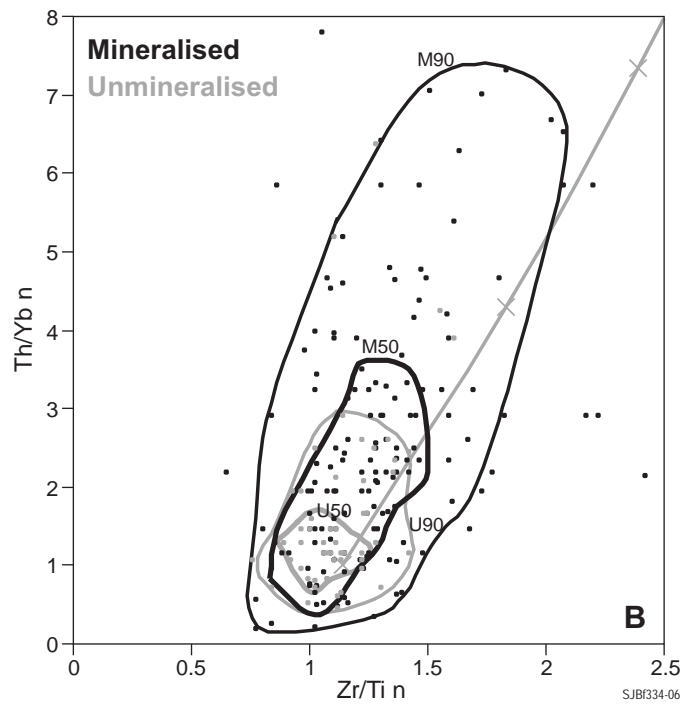
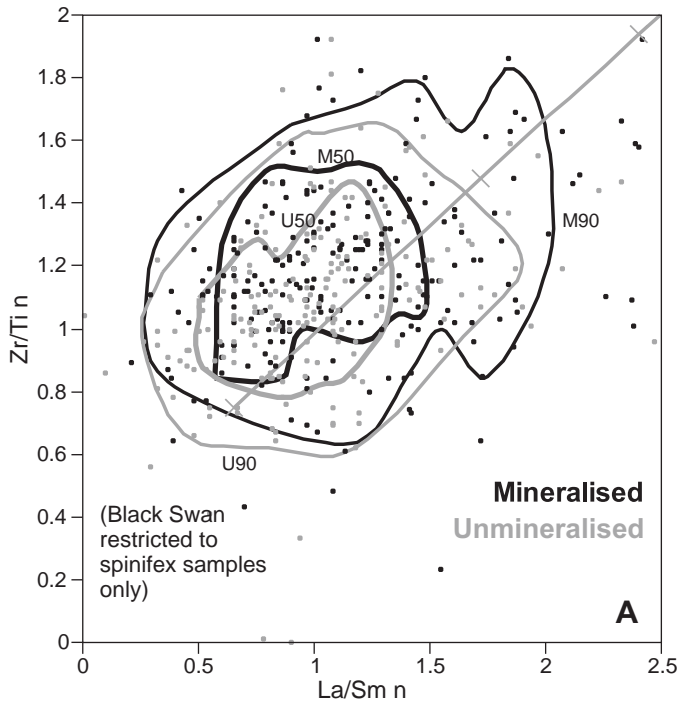


SJB028-04

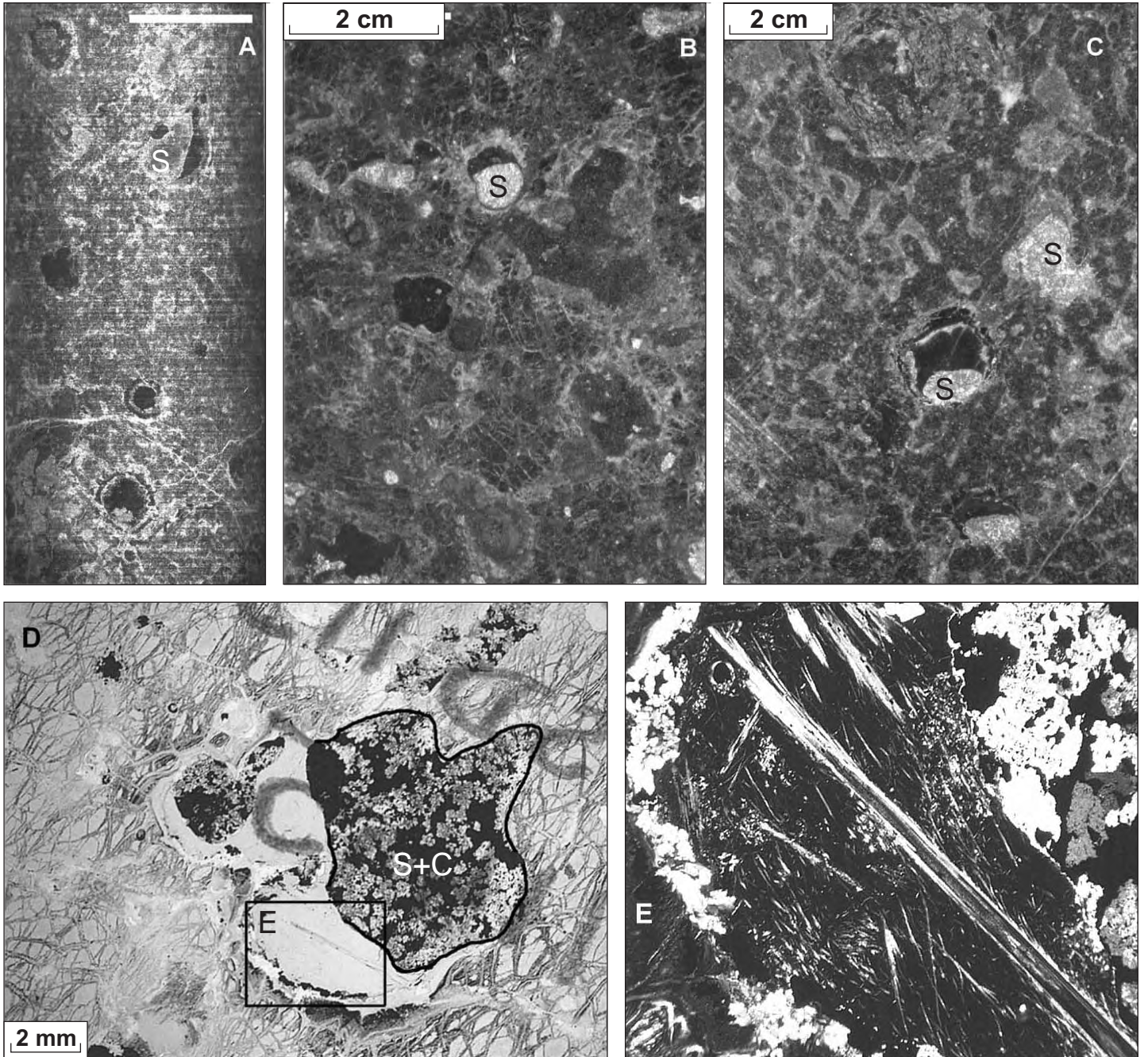
Figure(s) 29



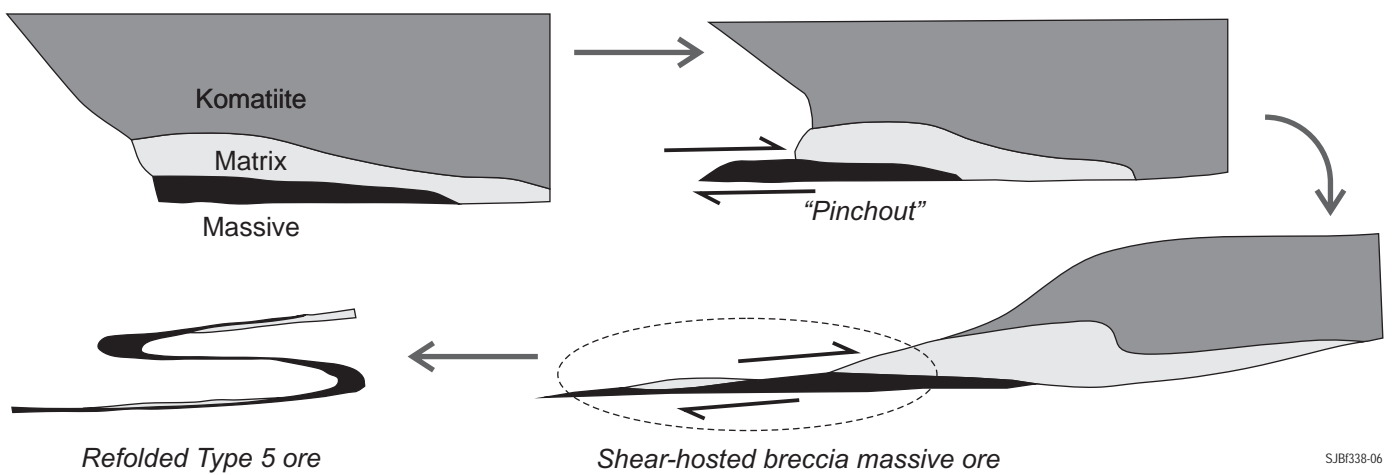
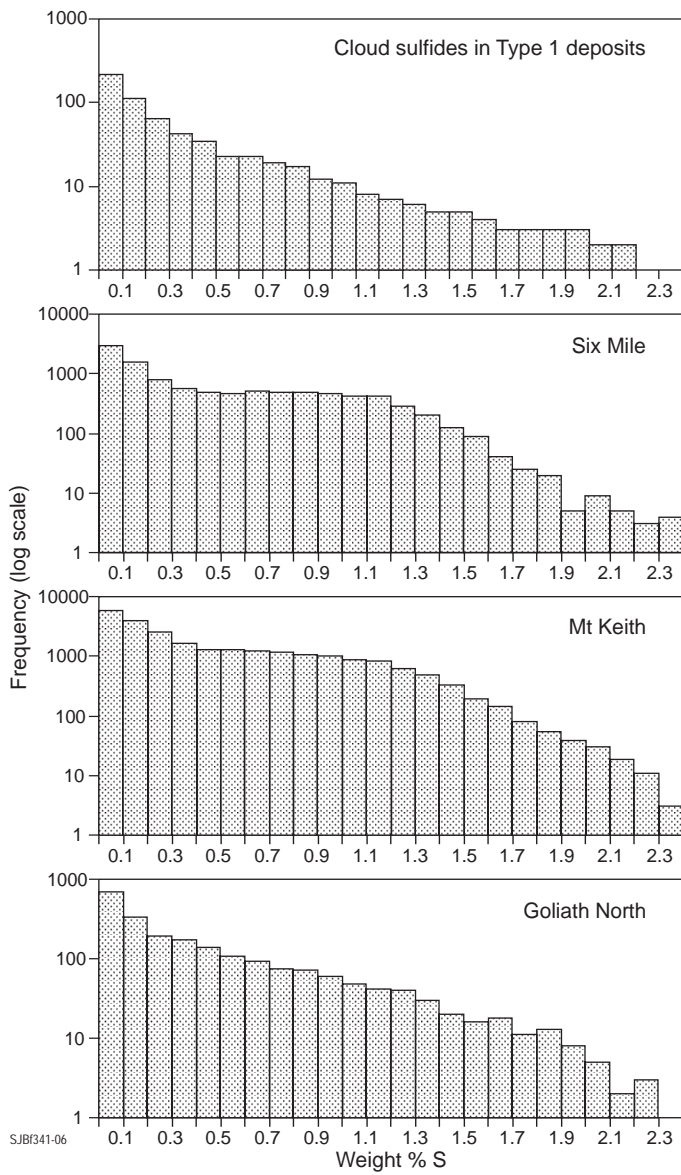
Figure(s) 33



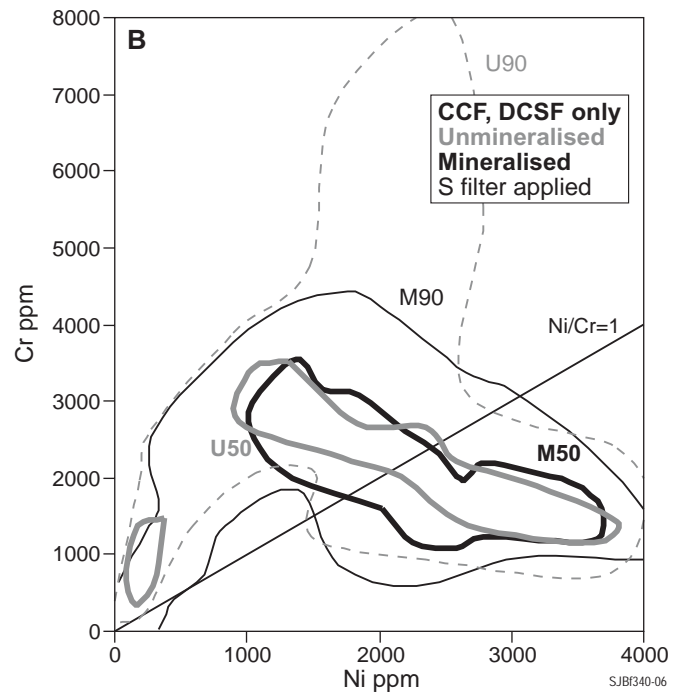
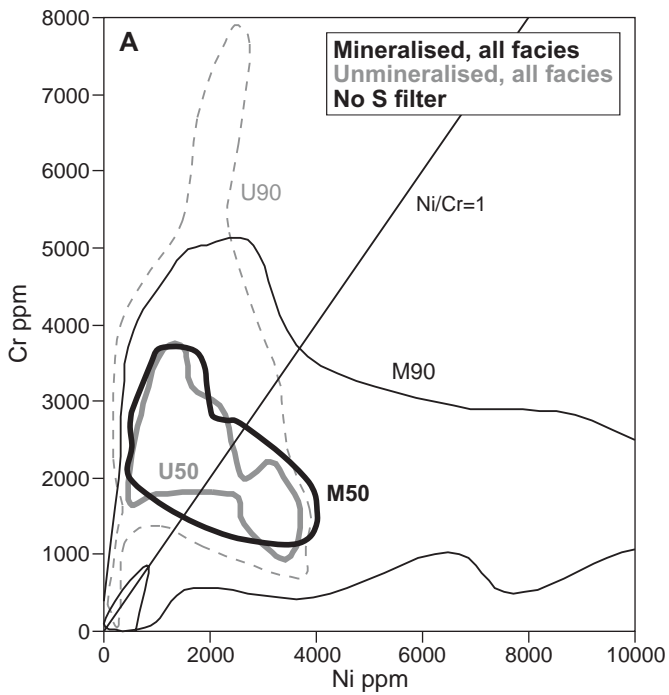
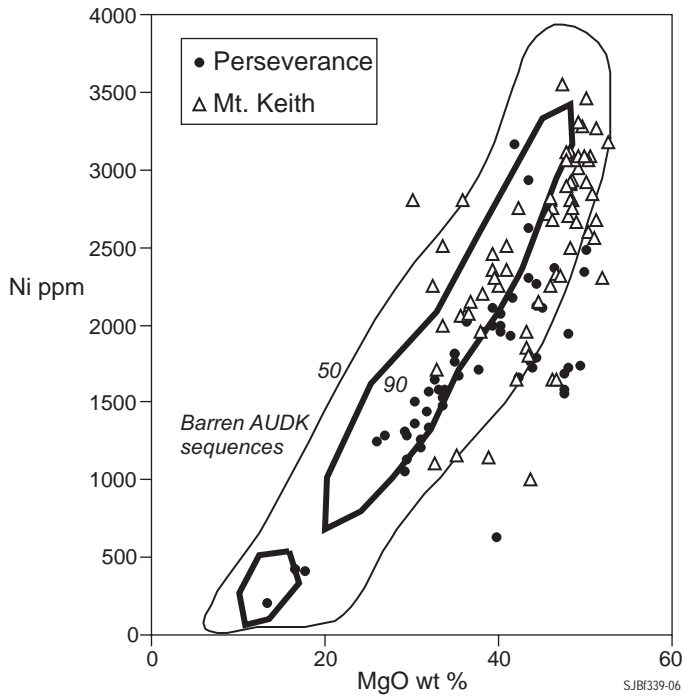
Figure(s) 34, 35



Figure(s) 36



Figure(s) 37, 38



Figure(s) 39, 40